**PHD DISSERTATION**

# PHYTOCHEMICAL ANALYSIS OF JAPANESE PLANT *(LASIANTHUS VERTICILLATUS)* AND SAUDI PLANT *(CADABA ROTUNDIFOLIA)*

HIROSHIMA UNIVERSITY

**2019**

**GADAH ABDULAZIZ AL-HAMOUD**

**GRADUATE SCHOOL OF BIOMEDICAL AND HEALTH SCIENCES**
**HIROSHIMA UNIVERSITY**
**JAPAN**

**INDEX**

# CHAPTER 1

## *Lasianthus verticillatus*

## (Japanese plant)

## 1.1. Introduction

Rubiaceae is the fourth-largest angiosperm family, comprising approximately 660 genera and 11,500 species and classified into 42 tribes [1]. Rubiaceae has a long history of investigation on the distribution of iridoid glycoside through its species. These investigations were started by isolation of asperuloside, characteristic iridoid for Rubiaceae, from six plants belonging to family Rubiaceae [2]. The classification of occurrence of iridoid glycoside in Rubiaceae subfamilies was initiated by Kooiman in 1969 [3]. Later, this classification was approved by investigation of 35 selected Rubiaceae plants by TLC, GC and GC-MS. The result revealed that the asperuloside and deacetylasperulosidic acid occurred in most plants of Rubioideae subfamily, especially in *Lasianthus* species [4].

The genus *Lasianthus* contains approximately 180 species distributed in Asia, Africa, America and Australia. Most species are found in tropical Asia, while only one species exists in Australia [5, 6]. Some species have been used in traditional medicine to treat tinnitus, arthritis, fever and bleeding [7-10].

**Figure 1.** *Lasianthus verticillatus*

Previous phytochemical studies on some *Lasianthus* species revealed the presence of iridoids, iridoid glucosides, bis-iridoid glucosides, together with anthraquinones, megastigmane glucosides and terpenes [9, 11-17].

*Lasianthus verticillatus* (Lour.) Merr. (Syn. *Lasianthus trichophlebus* auct. non Hemsl.) (Fig.1) is a shrub, branchlets terete with about 1.5-3 m in height. The leaves are coriaceous, blades oblong to oblong-lanceolate, 9-18 x 1.5-7 cm, apex is cuspidate-acute, acute or cuspidate-acuminate, base is acute, midrib and nerves are flat, slightly prominent above, conspicuously prominent beneath, nerves are 5-9 pairs. The flowers are sessile, calyx cupular, 3-5 mm long, subglabrous or puberulous, tube short about 1-2 mm long, limb is 2-3 mm long, puberulous, truncate or minutely dentate at apex. Their corolla is ovate with 5 lobes, up to 10-12 mm long, hirsute outside, villous inside. The fruits are blue, smooth, oval, 10 mm or less in diameter, their season is from October to November [18, 19].

On our previous investigation of 1-BuOH fraction of *L. verticillatus* leaves, eleven new compounds including (iridoids, iridoid glucosides, bis-iridoid glucosides and phenolic compound) together with seven known compounds have been isolated. It is worth to mention that none of these compounds have been published as a chemical constituent from *L. verticillatus*. In other hand, two of the known compounds from *L. verticillatus* (non glucosidic iridoid and bis-iridoid glucoside) have been published as new constituents from methanolic extract of *L. wallichii* leaves [12].

As a part of our ongoing search for new bioactive compounds from Japanese plants, the chemical constituents of EtOAc and 1-BuOH fractions of the methanolic extract of *L. verticillatus* leaves were subjected to further investigation, leading to isolation of two new iridoids (**1** – **2**), three new iridoid glucosides (**3**, **4** and **8**), four new acylated iridoid glucosides (**5** – **7** and **9**), three new bis-iridoid glucosides (**10** – **12**) and new tetrahydrofuran lignan glucoside (**13**) together with twelve known compounds; lasianol (**14**), bis-iridoid glucoside (**15**), asperuloside (**16**), Deacetyl asperuloside (**17**), besperuloside (**18**), deacetyl daphylloside (**19**), daphylloside (**20**), grasshopper ketone (**21**), lauroside A (**22**), secoisolariciresinol diglucoside (**23**), 8,8′-bisdihydrosiringenin glucoside (**24**) and huazhongilexin (**25**) (Fig. 2). The isolation processes were carried out by various chromatographic techniques, while the structures of these compounds were characterized by physical and spectroscopic data analyses including 1D and 2D NMR, IR, UV, HR-ESI-MS, and electronic circular dichroism (ECD). All the obtained compounds were evaluated for their free radical scavenging properties by DPPH radical scavenging assay.

1.2. **Extraction and Isolation of Chemical Constituents**

The air-dried and powdered leaves (7.0 kg) of *Lasianthus verticillatus* (Lour.) Merr. were extracted by maceration with MeOH (98 L x 2) and concentrated to 90% MeOH solution, then defatted with 3 L of *n*-hexane. The remaining solution was evaporated and re-suspended in 1 L $H_2O$ and extracted by EtOAc (1 L x 3, 46.5 g) and 1-BuOH (1 L x 3, 178.5 g), successively.

A portion of EtOAc fraction (42.8 g) was chromatographed on silica gel column chromatography (Φ = 6 cm, *L* = 40 cm, 400 g), using stepwise gradient elution with increasing amount of MeOH in $CHCl_3$ ($CHCl_3$ 1 L, $CHCl_3$–MeOH 2, 5, 7, 10, 15, 20, 50, 100% MeOH 1 L), to give 10 fractions (Frs. LtE1–LtE10).

Each fraction LtE4 (21.9 g) and LtE6 (22.0 g) were subjected to open reversed phase (ODS) column chromatography with 10% aq. methanol (400 ml) – 100% methanol (400 ml), linear gradient, lead 8 fractions (Frs. LtE4.1 – LtE4.8 and Frs. LtE6.1 – LtE6.8). Fraction LtE4.1 (547 mg) was purified by HPLC (ODS) with 15% aq. acetone to give **1** (LtE4.1.1, 1-acetyl lasianol, 21.7 mg), **2** (LtE4.1.2, 10-acetyl lasianol, 32.7 mg), **25** (huazhongilexin, 10.2 mg) and **21** (grasshopper ketone, 5.2 mg). The residue LtE6.2 (199 mg) was purified by preparative HPLC (ODS) with 20% aq. acetone to obtain **16** (asperuloside, 7.6 mg) and **22** (lauroside A, 4.7 mg). The other residue LtE6.4 (262 mg) was purified by HPLC (ODS) with 35% aq. acetone to give **9** (LtE6.4.1, 6′-*O*-*trans*-caffeoyl asperuloside, 3.4 mg) and **18** (besperuloside, 5.6 mg).

Part of 1-BuOH fraction (124 g) was fractionated by column chromatography on a highly porous synthetic resin, Diaion HP 20 column (Φ = 10 cm, *L* = 60 cm, 2.5kg). The column was eluted initially with $H_2O$, then with MeOH / $H_2O$ stepwise gradient with increasing MeOH content using (10, 20, 30, 40, 60% MeOH), then 100% MeOH, 15 L each. Similar fractions were grouped together according to their TLC profiles to give 20 fractions (Frs. LtB1 – LtB20).

Fraction LtB8 (18.8 g) was proceeded on silica gel column chromatography (Φ = 4.5 cm, *L* = 50 cm, 400 g), started with $CHCl_3$ (2.5 L), followed by $CHCl_3$ / MeOH developing solvent systems (7, 10, 15, 20, 30, 100% MeOH, 2.5 L each), to obtain 16 fractions (Frs. LtB8.1–LtB8.16). Each fraction of LtB8.12 (681 mg) and LtB8.13 (240 mg) was subjected to open reversed phase (ODS) column chromatography with 10% aq. methanol (400 mL) to 100% methanol (400 mL), linear gradient, to give (Frs. LtB8.12.1–LtB8.12.6 and Frs. LtB8.13.1–LtB8.13.6, respectively).

The residue LtB8.12.2 (131 mg) was purified by HPLC (ODS) with 5% aq. methanol to give **3** (LtB8.12.2.1, Lasianoside A, 4.0 mg), while residue LtB8.13.2 (174 mg) was purified by HPLC (ODS) with 5% aq. methanol to give **14** (lasianol, 10.4 mg), **4** (LtB8.12.2.2, Lasianoside B, 13.6 mg) and **17** (Deacetyl asperuloside, 30.5 mg). Fraction LtB13 (4.3 g) was proceeded on silica gel column chromatography (Φ = 4 cm, *L* = 40 cm, 230 g), started with $CHCl_3$ (1.5 L), followed by $CHCl_3$ / MeOH developing solvent systems (5, 7, 10, 15, 20, 30, 40, 100% MeOH, 1.5 L each) to give 14 fractions (Frs. LtB13.1–LtB13.14). The residue LtB13.5 (455 mg) was purified by preparative HPLC (ODS) with 15% aq. acetone to give **19** (deacetyl daphylloside, 5.8 mg) and **20** (daphylloside, 23.4 mg). The other residue LtB13.10 (215 mg) was purified by preparative HPLC (ODS) with 30% aq. methanol to give **5** (LtB13.10.1, Lasianoside C, 6.0 mg).

Fraction LtB15 (7.2 g) was chromatographed on silica gel column chromatography (Φ = 5.2 cm, *L* = 38 cm, 350 g), started with $CHCl_3$ (2.5 L), followed by $CHCl_3$ / MeOH developing solvent systems (5, 10, 12, 15, 20, 30, 100% MeOH, 2.5L each) to obtain 12 fractions (Frs. LtB15.1–LtB15.12). Fraction LtB15.5 (656 mg) was re-chromatographed on silica gel CC (Φ = 2.5 cm, *L* = 50 cm, 120 g), started with $CHCl_3$ (500 ml), followed by $CHCl_3$ / MeOH developing solvent systems (5, 7, 10, 12, 100% MeOH, 500 ml each), to give 11 fractions (Frs. LtB15.5.1–LtB15.5.11). The residue LtB15.5.8 (194 mg) was separated by HPLC (ODS) with 40% aq. methanol to give LtB15.5.8.5 (24.0 mg) and subjected to further purification by HPLC (ODS) with 38% aq. methanol to give **13** (LtB15.5.8.5.1, tripterygiol 7'-*O*-*β*-D-glucopyranoside, 4.6 mg). The other fraction LtB15.5.9 (88.0 mg) was purified by HPLC (ODS) with 30% aq. methanol to give **23** (secoisolariciresinol diglucoside, 8.9 mg), while fraction LtB15.6 (895 mg) was purified by HPLC (ODS) with 35% aq. methanol to give **24** (8,8′-bisdihydrosiringenin glucoside, 2.5 mg).

Fraction LtB15.7 (577 mg) was separated by HPLC (ODS) with 28% aq. acetone to give **6** (LtB15.7.1, Lasianoside D, 3.0 mg). The residue LtB15.8 (1.8 g) was separated by HPLC, 40% aq. methanol to provide compounds **15** (bis-iridoid glucoside, 42.0 mg) and **10** (LtB15.8.1, Lasianoside G, 3.0 mg).

The fraction LtB17 (6.1 g) was further purified by silica gel column chromatography (Φ = 5 cm, *L* = 40 cm, 380 g), eluting with stepwise $CHCl_3$ / MeOH gradient (100:0 to 70:30, 2.4 L each), to obtain 11 fractions (Frs. LtB17.1–LtB17.11). The residue LtB17.5 (282 mg) was further purified by HPLC, 25% aq. acetone to give compound **8** (LtB17.5.1, Lasianoside F, 13.4 mg),

while the other residue LtB17.7 (839 mg) was separated by HPLC, 28% aq. acetone to obtain compounds **11** (LtB17.7.1, Lasianoside H, 25.0 mg), **12** (LtB17.7.2, Lasianoside I, 13.0) and **7** (LtB17.7.3, Lasianoside E, 7.0 mg). The isolation procedures are presented in (Charts. 1 and 2).

**CHART 1.** Extraction and isolation

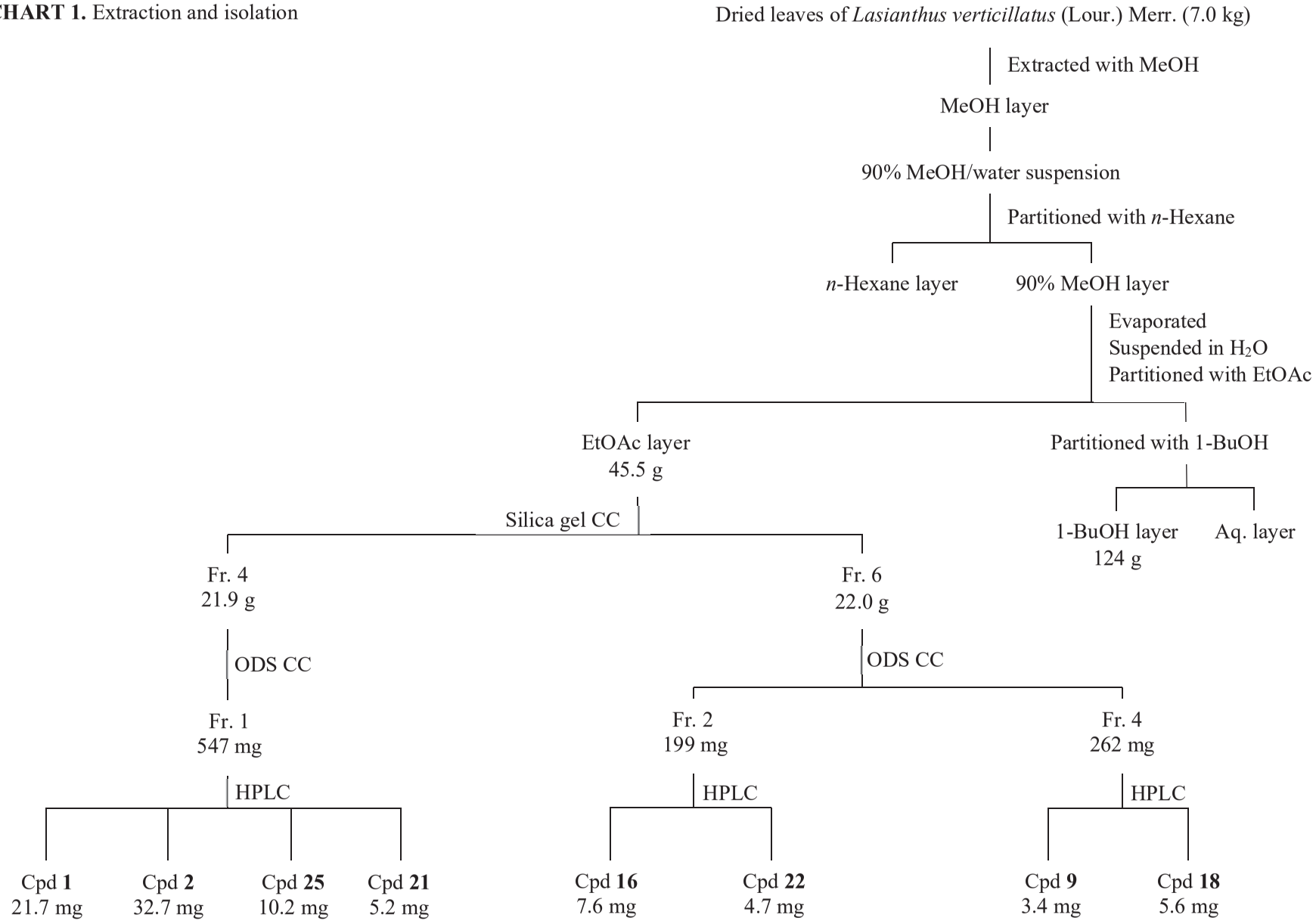

**CHART 2.** Extraction and isolation

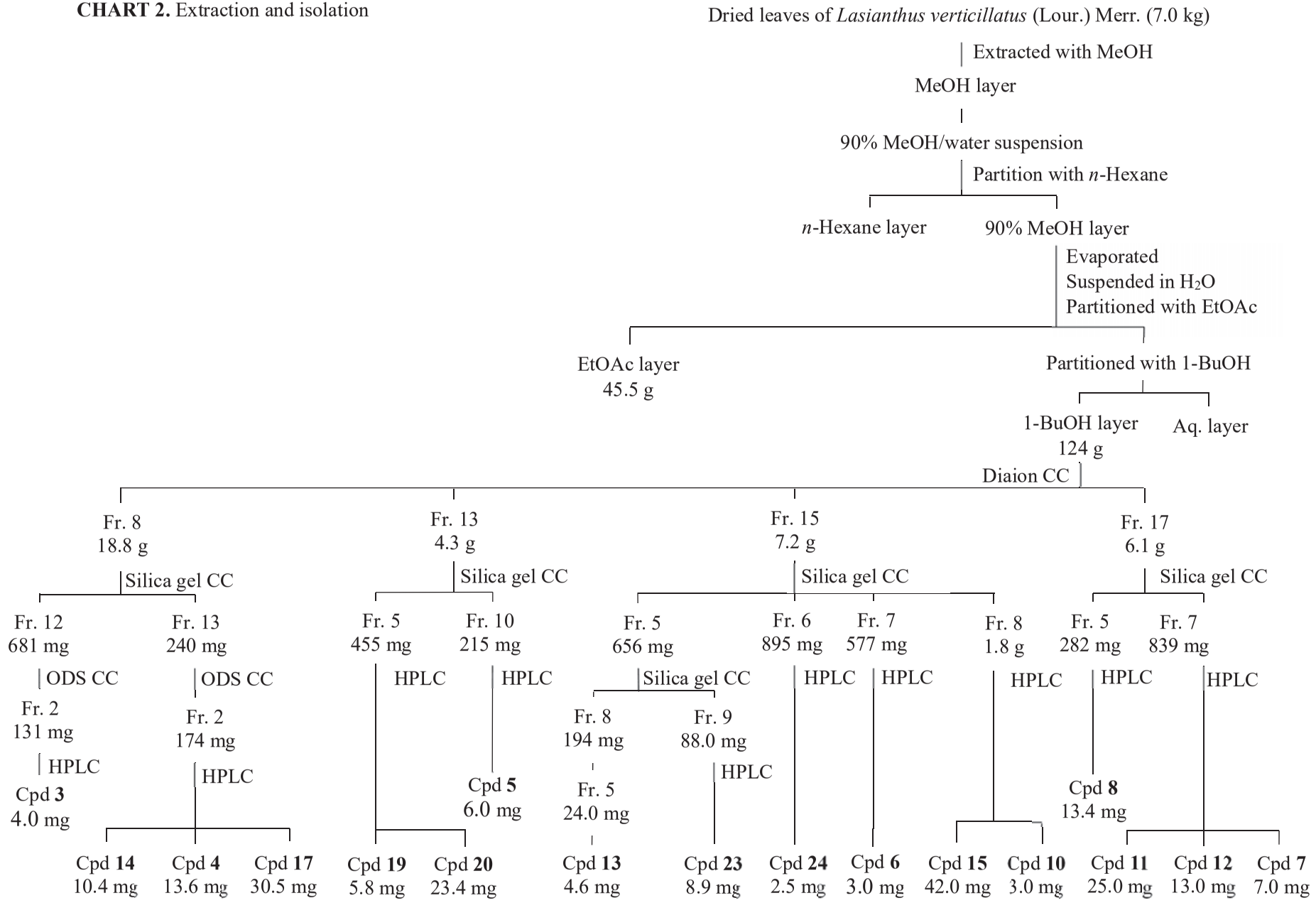

### 1.3. Structural Elucidations of Chemical Constituents

The EtOAc and 1-BuOH fractions of methanolic extract of *Lasianthus verticillatus* (Lour.) Merr. leaves were subjected to fractionation by silica gel and Diaion HP-20 columns, respectively. The resulting fractions were separated on silica gel or octadecylsilane (ODS) column chromatography, then purified by preparative high-performance liquid chromatography (HPLC) to obtain (**1** – **25**) (Fig. 2).

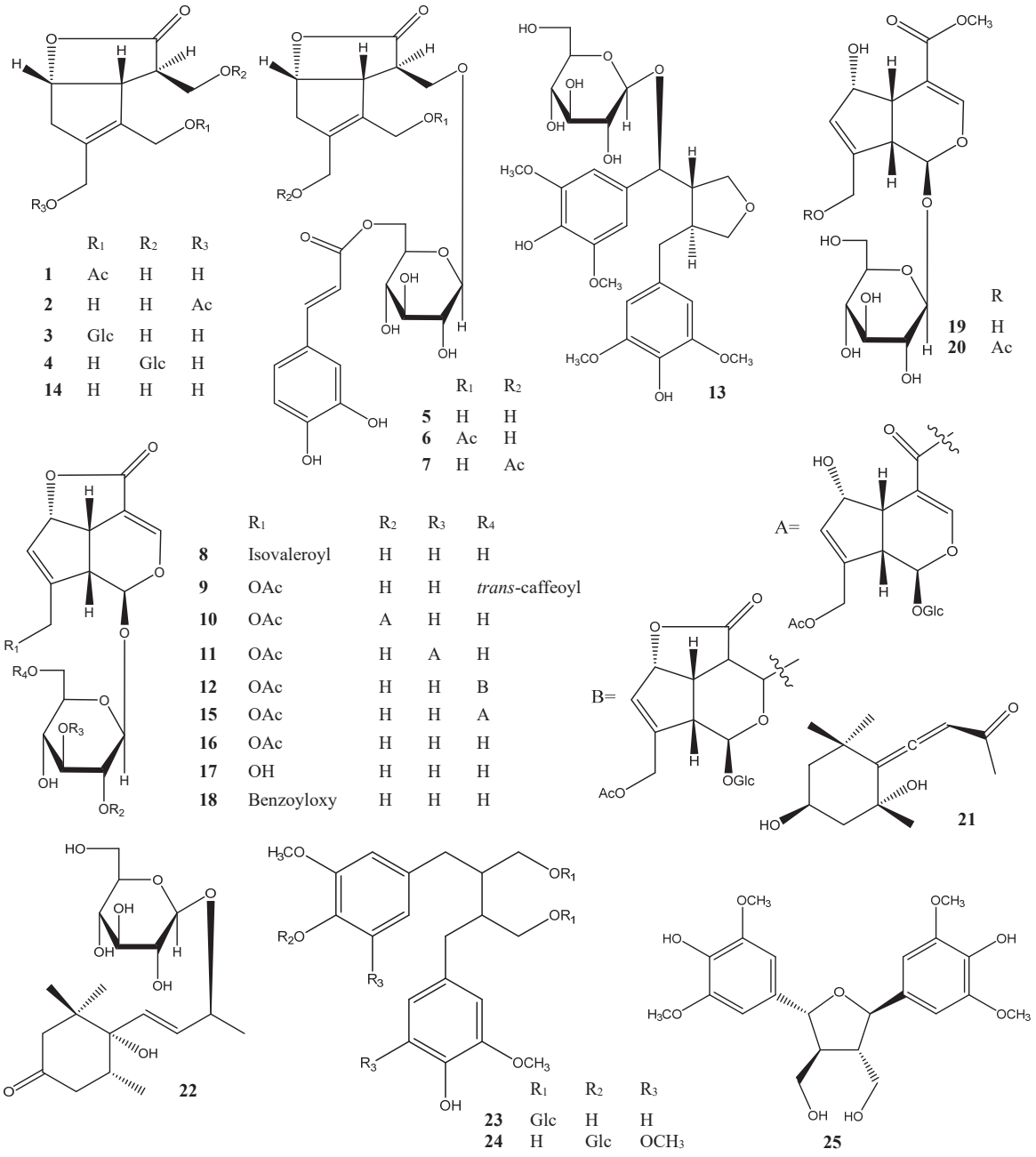


**Figure 2.** Isolated compounds from *Lasianthus verticillatus* (**1** – **25**)

1-Acetyl lasianol (**1**) was isolated as a viscous colorless syrup with $[\alpha]_D^{22}$ –32.4 (*c* 1.02, MeOH). Its molecular formula, $C_{12}H_{16}O_6$, was determined by the $^{13}C$ NMR data and the molecular ion $[M + Na]^+$ at *m/z* 279.0841 (calcd for $C_{12}H_{16}O_6$ Na 279.0839) in the positive-ion HR-ESI-MS, indicating five degrees of unsaturation. Its IR spectrum revealed the presence of a hydroxy (3418 $cm^{-1}$), γ-lactone (1747 $cm^{-1}$) and carbonyl ester (1731 $cm^{-1}$). The $^1H$ NMR spectrum of **1** (Table. 1) displayed resonances of a methylene at $\delta_H$ 2.76 (1H, br d, *J* = 18.1 Hz) and 2.94 (1H, dd, *J* = 18.1, 6.3 Hz), three oxygenated methylenes at $\delta_H$ 3.83 (1H, dd, *J* = 10.7, 3.5 Hz), 3.94 (1H, dd, *J* = 10.7, 4.1 Hz), 4.24 (2H, br s), 4.75 (1H, br d, *J* = 13.0 Hz), 4.82 (1H, br d, *J* = 13.0 Hz), an oxygenated methine at $\delta_H$ 5.14 (1H, t, *J* = 6.3Hz), two methines at $\delta_H$ 2.80 (1H, m), 3.62 (1H, d, *J* = 6.3 Hz), and an acetyl methyl proton at $\delta_H$ 2.06 (3H, s). The $^{13}C$ NMR spectrum (Table. 1) of **1** showed twelve carbon resonances that were classified by chemical shift values and HSQC as; an acetyl group ($\delta_c$ 20.7 and 172.5), a methylene carbon ($\delta_c$ 41.7), three oxygenated methylene carbons ($\delta_c$ 58.5, 59.3 and 63.3), two methine carbons ($\delta_c$ 48.6 and 53.1), an oxygenated methine carbon ($\delta_c$ 83.0), two $sp^2$ quaternary carbons ($\delta_c$ 132.5 and 142.0) and a carbonyl carbon ($\delta_c$ 180.5).

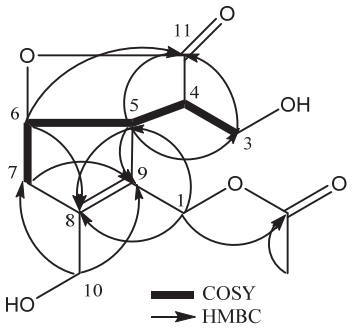


**Figure 3.** HMBC and COSY correlations of **1**

The HMBC (Fig. 3) revealed correlations from H-5 ($\delta_H$ 3.62) to C-11 ($\delta_c$ 180.5), C-3 ($\delta_c$ 63.3), C-8 ($\delta_c$ 142.0) and C-9 ($\delta_c$ 132.5) and from H-6 ($\delta_H$ 5.14) to C-11 ($\delta_c$ 180.5), while COSY (Correlation Spectroscopy) (Fig. 3) displayed correlations between $H_2$-3/H-4 /H-5/H-6/$H_2$-7. Comparison of the 1D and 2D spectroscopic data of **1** with those of lasianol

(**14**) [12] revealed that **1** carried an additional acetyl group. In HMBC spectrum (Fig. 3), the correlations from downfield shifted protons $H_2$-1 ($\delta_H$ 4.75 and 4.82) to acetyl carbonyl carbon ($\delta_c$ 172.5), indicating the position of acetyl group at C-1. The relative configuration was established by NOESY analysis (Fig. 4). The correlation between H-3/H-5, H-5/H-6, and H-6/H-7 suggested as $\beta$-orientation, while no correlation between H-4 and H-6 suggested as $\alpha$-orientation. The chemical shift values and the coupling patterns of aglycone moiety were essentially superimposable to lasianol (**14**) except for the acylation position C-1, which supported the relative stereochemistry of **1** as shown in (Fig. 1).

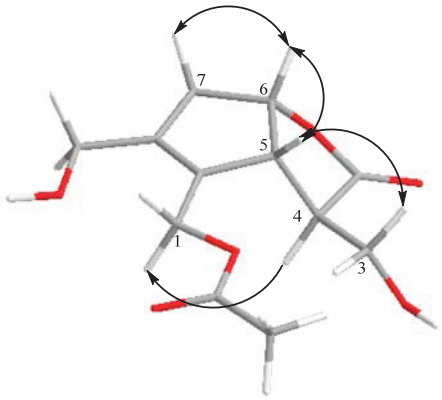


**Figure 4.** Key NOESY correlations of **1**

The absolute stereochemistry of **1** was elucidated by comparison of the circular dichroism (CD) spectrum. The positive cotton effect at 215 nm ($\Delta\varepsilon$ = + 1.290) showed the same absolute stereochemistry with lasianol (**14**) [12], and consequently the structure of **1** was determined to be (4*R*,5*R*,6*S*) configuration. From these data, the structure of **1** was established to be 1-acetyl derivative of **14**.

**Table 1** $^{1}H$ and $^{13}C$ NMR spectroscopic data for **1** and **2**

| Position | **1** | | **2** | |
|---|---|---|---|---|
| | $\delta_c$ | $\delta_H$ Multi (*J* in Hz) | $\delta_c$ | $\delta_H$ Multi (*J* in Hz) |
| 1 | 59.3 | 4.75 br d (13.0)<br>4.82 br d (13.0) | 57.1 | 4.19 br d (13.4)<br>4.34 br d (13.4) |
| 3 | 63.3 | 3.83 dd (10.7, 3.5)<br>3.94 dd (10.7, 4.1) | 63.4 | 3.88 dd (10.7, 3.5)<br>3.95 dd (10.7, 4.1) |
| 4 | 48.6 | 2.80 m | 48.4 | 2.86 m |
| 5 | 53.1 | 3.62 d (6.3) | 53.0 | 3.70 d (6.3) |
| 6 | 83.0 | 5.14 t (6.3) | 83.0 | 5.13 t (6.3) |
| 7 | 41.7 | 2.76 br d (18.1)<br>2.94 dd (18.1, 6.3) | 42.0 | 2.68 br d (18.0)<br>2.91 dd (18.0, 6.3) |
| 8 | 142.0 | - | 133.3 | - |
| 9 | 132.5 | - | 140.5 | - |
| 10 | 58.5 | 4.24 2H br s | 60.9 | 4.73 br d (12.8)<br>4.78 br d (12.8) |
| 11 | 180.5 | - | 180.6 | - |
| *CO*$CH_3$ | 172.5 | - | 172.6 | - |
| CO*$CH_3$* | 20.7 | 2.06 3H s | 20.7 | 2.06 3H s |

Recorded at 500 and 175 MHz in $CD_3OD$. Chemical shifts ($\delta$) are expressed in ppm and *J* values are presented in Hz in parenthesis. m: multiplet or overlapped signals.

10-acetyl lasianol (**2**) was obtained as a viscous colorless syrup with $[\alpha]_D^{22}$ –63.38 (*c* 0.68, MeOH). It gave a molecular formula of $C_{12}H_{16}O_6$ by HR-ESI-MS at *m/z*: 279.0841 $[M+Na]^+$ (calcd for $C_{12}H_{16}O_6$ Na: 279.0839), which was the same to that of **1**. Further comparison of $^1H$ and $^{13}C$ spectra (Table. 1) revealed that compound **2** and **1** shared the same functional group. The major change was that the upfield shift of $H_2$-1 to $\delta_H$ 4.19, 4.34 and the downfield shift of $H_2$-10 to $\delta_H$ 4.73, 4.78, which suggested that the acetyl group was linked to C-10 in **2**. This was verified by correlations from $H_2$-10 to acetyl carbonyl carbon ($\delta_c$ 172.6), C-7 ($\delta_c$ 42.0) and C-9 ($\delta_c$ 140.5) in the HMBC spectrum (Fig. 5).

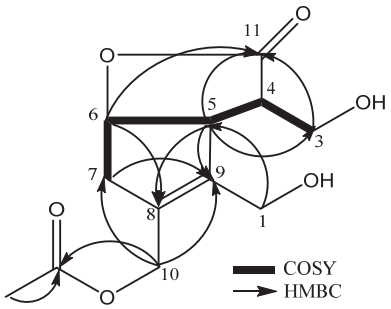


**Figure 5.** HMBC and COSY correlations of **2**

Detailed analysis of COSY, HSQC and HMBC suggested that other parts of **2** were the same to those of **1**. The relative and absolute configurations of **2** were assigned to be the same as that of **1**, based on coupling constant, NOESY experiment (Fig. 6) and CD data. Therefore, the structure of compound **2** was characterized as 10-acetyl derivative of **14**.

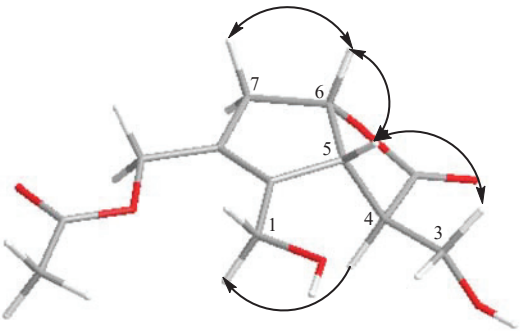


**Figure 6.** Key NOESY correlations of **2**

Lasianoside A (**3**) $[\alpha]^{22}_{D}$ –20.6, was obtained as a viscous colorless syrup. Its molecular formula was determined as $C_{16}H_{24}O_{10}$ based on sodium adduct ion at *m/z* 399.1263 $[M + Na]^+$ (calcd for $C_{16}H_{24}O_{10}Na$ 399.1262) in HR-ESI-MS, which suggests five degrees of unsaturation. The IR spectrum exhibited absorption bands at 3390 and 1748 $cm^{-1}$ indicated the presence of hydroxy and γ-lactone ring, respectively. $^1$H NMR spectrum displayed signals of four methylenes, including a methylene at $\delta_H$ 2.75 (1H, br d, $J$ = 18.1Hz) and 2.95 (1H, dd, $J$ = 18.1, 6.3 Hz), and three methylenes attached to oxygen at $\delta_H$ 3.91 (2H, d, $J$ = 3.9 Hz), 4.20 (1H, br d, $J$ = 13.4 Hz), 4.24 (1H, br d, $J$ = 13.4 Hz), 4.28 (1H, br d, $J$ = 12.0 Hz), 4.61 (1H, br d, $J$ = 12.0 Hz) (Table 2). Furthermore, the $^1$H NMR data supported the existence of three methines, two of them showed signals at $\delta_H$ 2.99 (1H, m), 3.73 (1H, br d, $J$ = 6.3 Hz), and an oxygenated methine proton at $\delta_H$ 5.14 (1H, t, $J$ = 6.3 Hz).

Taking into consideration of the above-mentioned molecular formula and degree of unsaturation, the sixteen carbon signals in the $^{13}$C NMR spectrum are thus ascribable to the presence of three oxymethylenes ($\delta_c$ 58.4, 63.3, 64.4), an oxymethine ($\delta_c$ 83.2), as well as two unsaturated quaternary carbons ($\delta_c$ 134.4, 140.2) and carbonyl carbon ($\delta_c$ 180.9) (Table 3). The COSY (Fig. 7) correlations between $H_2$-3/H-4 and H-4/H-5 together with the HMBC (Fig. 7) correlations from H-5 to C-11 ($\delta_c$ 180.9), C-3 ($\delta_c$ 63.3), C-8 ($\delta_c$ 140.2) and C-9 ($\delta_c$ 134.4) and from H-6 to C-11 ($\delta_c$ 180.9) indicated that **3** shared the same core structure as lasianol (**14**) [12].

Moreover, 1D NMR data of **3** were also gave an anomeric proton signal at $\delta_H$ 4.30 (d, $J$ = 7.9 Hz), in addition to six carbon signals at $\delta_c$ 103.8, 78.0, 78.0, 75.1, 71.6, 62.8 that belong to glucose moiety, which means **3** was the glucoside of lasianol (**14**) as aglycone moiety. The HMBC correlation (Fig. 7) from the anomeric proton of glucose H-1′ ($\delta_H$ 4.30) to C-1 ($\delta_H$ 64.4) of the aglycone moiety, indicated the glucosidation position on C-1. The presence of D-glucose moiety was confirmed by acid hydrolysis of **3** followed by HPLC analysis with a chiral detector (Fig. 17).

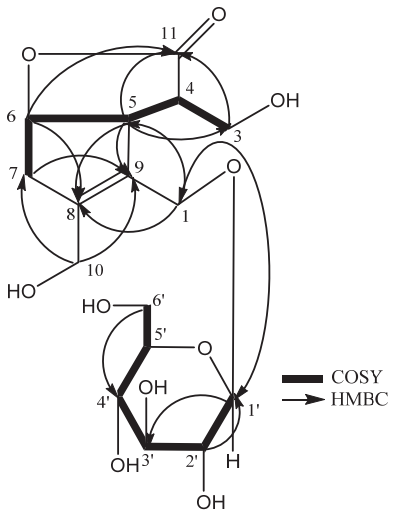


**Figure 7.** HMBC and COSY correlations of **3**

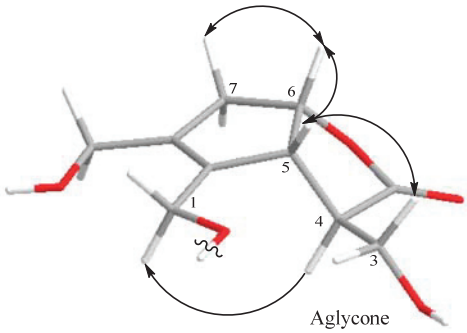


**Figure 8.** Key NOESY correlations of **3**

The coupling constant ($J$ = 7.9 Hz) of H-1′ indicated $\beta$ linkage for glucose moiety. The relative and absolute configurations of **3** were assigned to be the same as that of **14**, based on coupling constant, NOESY experiment (Fig. 8) and CD data. Thus, based on above analysis, the structure was determined as 1-*O*-$\beta$-D-glucopyranoside of **14**, designated as lasianoside A.

**Table 2** $^{1}$H NMR spectroscopic data for **3**–**7**

| Position | **3** | **4** | **5** | **6** | **7** |
|---|---|---|---|---|---|
| 1 | 4.28 br d (12.0)<br>4.61 br d (12.0) | 4.16 br d (13.0)<br>4.33 br d (13.0) | 4.16 br d (13.0)<br>4.27 br d (13.0) | 4.75 br s | 4.18 br d (13.4)<br>4.28 br d (13.4) |
| 3 | 3.91 2H d (3.9) | 3.93 dd (9.7, 5.5)<br>4.23 dd (9.7, 4.0) | 4.02 dd (10.0, 5.0)<br>4.13 m | 4.04 dd (10.1, 3.5)<br>4.09 dd (10.1, 4.4) | 4.04 dd (10.0, 5.0)<br>4.13 dd (10.0, 3.4) |
| 4 | 2.99 m | 3.00 m | 2.98 m | 2.94 m | 2.99 m |
| 5 | 3.73 br d (6.3) | 3.78 br d (6.3) | 3.75 m | 3.68 br d (6.3) | 3.76 m |
| 6 | 5.14 t (6.3) | 5.21 td (6.3, 1.0) | 5.16 t (6.4) | 5.13 t (6.3) | 5.15 t (6.4) |
| 7 | 2.75 br d (18.1)<br>2.95 dd (18.1, 6.3) | 2.73 br d (18.1)<br>2.94 dd (18.1, 6.3) | 2.69 br d (18.0)<br>2.85 dd (18.0, 6.4) | 2.69 br d (18.3)<br>2.82 dd (18.3, 6.3) | 2.62 br d (18.0)<br>2.82 dd (18.0, 6.4) |
| 8 | - | - | - | - | - |
| 9 | - | - | - | - | - |
| 10 | 4.20 br d (13.4)<br>4.24 br d (13.4) | 4.20 2H, br s | 4.13 2H, br s | 4.11 br d (13.7)<br>4.19 br d (13.7) | 4.67 2H, br s |
| 11 | - | - | - | - | - |
| 12 | | | | - | - |
| 13 | | | | 2.04 3H, s | 2.03 3H, s |
| 1′ | 4.30 d (7.9) | 4.33 d (7.9) | 4.37 d (8.0) | 4.36 d (8.0) | 4.63 d (7.9) |
| 2′ | 3.18 dd (9.0, 7.9) | 3.21 dd (9.1, 7.9) | 3.23 t (8.0) | 3.24 dd (9.1, 8.0) | 3.23 dd (9.0, 7.9) |
| 3′ | 3.37 t (9.0) | 3.38 t (9.1) | 3.40 m | 3.40 m | 3.40 m |
| 4′ | 3.28 m | 3.30 m | 3.39 m | 3.39 m | 3.39 m |
| 5′ | 3.29 m | 3.31 m | 3.56 m | 3.56 m | 3.56 m |
| 6′ | 3.68 dd (12, 5.5)<br>3.90 dd (12, 1.8) | 3.72 dd (12, 5.2)<br>3.89 dd (12, 1.3) | 4.34 dd (12.0, 5.7)<br>4.57 dd (12.0, 1.8) | 4.43 dd (12.0, 5.7)<br>4.59 dd (12.0, 2.0) | 4.35 dd (11.9, 6.0)<br>4.56 dd (11.9, 2.0) |
| 1″ | | | - | - | - |
| 2″ | | | 7.07 d (1.7) | 7.05 d (2.0) | 7.06 d (2.0) |
| 3″ | | | - | - | - |
| 4″ | | | - | - | - |
| 5″ | | | 6.80 d (8.2) | 6.80 d (8.2) | 6.80 d (8.2) |
| 6″ | | | 6.98 dd (8.2, 1.7) | 6.97 dd (8.2, 2.0) | 6.97 dd (8.2, 2.0) |
| 7″ | | | 7.57 br d (15.9) | 7.56 br d (15.9) | 7.56 br d (15.9) |
| 8″ | | | 6.30 br d (15.9) | 6.28 br d (15.9) | 6.30 br d (15.9) |
| 9″ | | | - | - | - |

Recorded at 500 MHz in $CD_3OD$. Chemical shifts ($\delta$) are expressed in ppm and $J$ values are presented in Hz in parenthesis. m: multiplet or overlapped signals.

**Table 3** $^{13}$C NMR spectroscopic data for **3–7**

| Position | 3 | 4 | 5 | 6 | 7 |
|---|---|---|---|---|---|
| 1 | 64.4 | 56.8 | 58.4 | 59.4 | 57.1 |
| 3 | 63.3 | 70.5 | 71.2 | 71.2 | 71.3 |
| 4 | 48.4 | 46.8 | 46.9 | 47.0 | 46.8 |
| 5 | 53.4 | 53.0 | 53.4 | 53.4 | 53.3 |
| 6 | 83.2 | 83.3 | 83.4 | 83.3 | 83.2 |
| 7 | 41.8 | 41.7 | 41.6 | 41.5 | 41.7 |
| 8 | 140.2 | 138.5 | 138.5 | 142.0 | 133.4 |
| 9 | 134.4 | 137.4 | 137.4 | 132.5 | 140.5 |
| 10 | 58.4 | 58.4 | 57.0 | 58.5 | 60.9 |
| 11 | 180.9 | 180.2 | 180.2 | 180.0 | 180.0 |
| 12 | | | | 172.6 | 172.6 |
| 13 | | | | 20.8 | 20.7 |
| | | | | | |
| 1′ | 103.8 | 104.6 | 104.8 | 104.8 | 104.9 |
| 2′ | 75.1 | 75.0 | 75.0 | 75.0 | 75.0 |
| 3′ | 78.0 | 77.9 | 77.7 | 77.8 | 77.7 |
| 4′ | 71.6 | 71.5 | 71.6 | 71.6 | 71.6 |
| 5′ | 78.0 | 78.1 | 75.5 | 75.5 | 75.5 |
| 6′ | 62.8 | 62.7 | 64.3 | 64.2 | 64.3 |
| | | | | | |
| 1″ | | | 127.6 | 127.6 | 127.6 |
| 2″ | | | 115.2 | 115.2 | 115.2 |
| 3″ | | | 146.8 | 146.9 | 146.9 |
| 4″ | | | 149.7 | 149.8 | 149.7 |
| 5″ | | | 116.5 | 116.5 | 116.5 |
| 6″ | | | 123.1 | 123.1 | 123.1 |
| 7″ | | | 147.3 | 147.3 | 147.3 |
| 8″ | | | 114.8 | 114.8 | 114.8 |
| 9″ | | | 169.1 | 169.0 | 169.1 |

Recorded at 175 MHz in $CD_3OD$. Chemical shifts ($\delta$) are expressed in ppm.

Lasianoside B (**4**), $[\alpha]_D^{22}$ –26.6, was isolated as viscous colorless syrup and displayed the same molecular formula $C_{16}H_{24}O_{10}$ of **3** in HR-ESI-MS at *m/z* 399.1265 $[M + Na]^+$ (calcd for $C_{16}H_{24}O_{10}Na$ 399.1262). Analysis of 1D and 2D NMR data revealed that the data of **4** were very similar to those of **3** except for apparent differences for the signals of $H_2$-1 [$\delta_H$ 4.16 (1H, br d, $J$ = 13.0 Hz), 4.33 (1H, br d, $J$ = 13.0 Hz)], and $H_2$-3 [$\delta_H$ 3.93

(1H, dd, $J$ = 9.7, 5.5 Hz) and 4.23 (1H, dd, $J$ = 9.7, 4.0 Hz)] in **4** compared to the corresponding signals of $H_2$-1 and $H_2$-3 in **3** (Tables. 2 and 3). The downfield shift of $H_2$-3 ($\delta_H$ 3.93 and 4.23) suggested that the glucose moiety in **4** was linked at C-3 instead of C-1 as **3**. This assumption was confirmed by HMBC correlation from anomeric proton H-1′ ($\delta_H$ 4.33) to C-3 ($\delta_c$ 70.5) (Fig. 9). The relative and absolute configurations of **4** were determined to be the same as **14** by NOESY (Fig. 10) and CD spectral data, thus the structure of **4** was deduced to be 3-*O*-*β*-D-glucopyranoside of **14**, designated as lasianoside B.

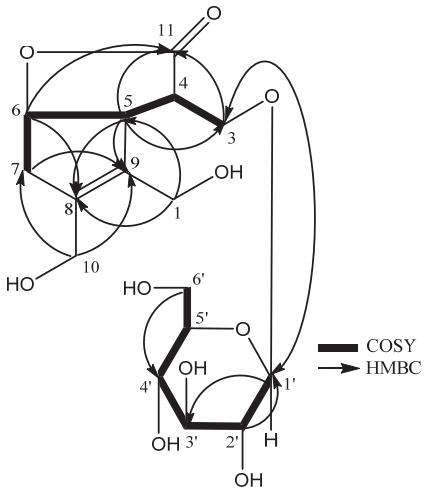


**Figure 9.** HMBC and COSY correlations of **4**

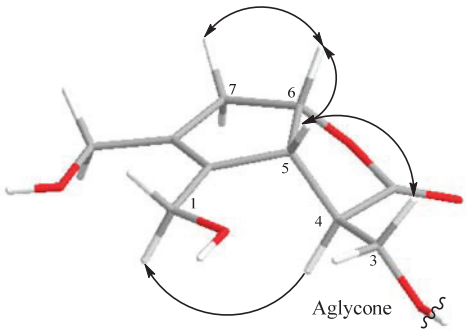


**Figure 10.** Key NOESY correlations of **4**

Lasianoside C (**5**), $[\alpha]^{22}_{D}$ –10.2, was obtained as a viscous pale-yellow syrup, it had a molecular formula of $C_{25}H_{30}O_{13}$ with 11 degrees of unsaturation as determined by HR-ESI-MS (measured at *m/z*: 561.1572 $[M+Na]^+$, calcd for $C_{25}H_{30}O_{13}Na$: 561.1579). The

UV spectrum showed absorption maxima at 329, 300 and 245 nm suggested the presence of aromatic ring. In the same way, the IR spectrum of **5** exhibited absorption bands at 3356, 1745, 1712, 1623, 1600, 1512 $cm^{-1}$ suggested the presence of hydroxy, γ-lactone ring, conjugated ester carbonyl, *α,β*-unsaturated olefinic carbons and aromatic ring, respectively. The $^{13}C$ NMR spectrum was closely resemble to that of **4**, except for the presence of additional eight $sp^2$ signals ($\delta_c$ 114.8, 115.2, 116.5, 123.1, 127.6, 146.8, 147.3, 149.7) together with a carboxyl carbon signal ($\delta_c$ 169.1) (Table. 3). Thus, compound **5** was expected to be an acylated derivative of **4**. Moreover, the $^1H$ NMR spectrum of **5** showed three ABX-coupled aromatic protons, H-2″ at $\delta_H$ 7.07 (1H, d, $J$ = 1.7 Hz), H-5″ at $\delta_H$ 6.80 (1H, d, $J$ = 8.2 Hz) and H-6″ at $\delta_H$ 6.98 (1H, dd, $J$ = 8.2, 1.7 Hz), and two *trans*-olefinic protons, H-7″ at $\delta_H$ 7.57 (1H, br d, $J$ = 15.9 Hz) and H-8″ at $\delta_H$ 6.30 (1H, br d, $J$ = 15.9 Hz) (Table. 2). This data implied the acyl portion is a *trans*-caffeoyl group.

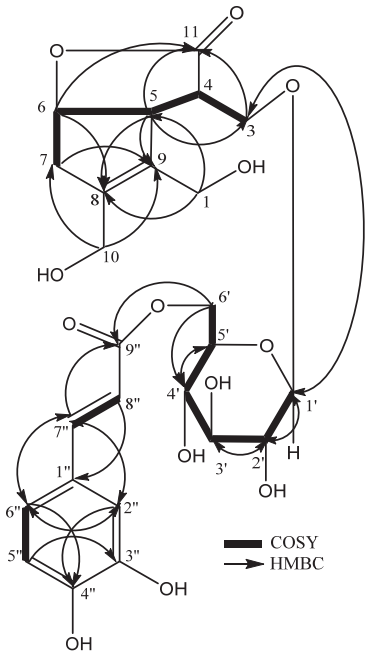


**Figure 11.** HMBC and COSY correlations of **5**

The esterification position was indicated to be at C-6′ of glucose moiety, due to downfield shift of $H_2$-6′ to $\delta_H$ 4.34 (1H, dd, $J$ = 12.0, 5.7 Hz) and 4.57 (1H, dd, $J$ = 12.0, 1.8 Hz). This suggestion was confirmed by HMBC correlation (Fig. 11) from $H_2$-6′ ($\delta_H$ 4.34 and 4.57) to carbonyl carbon C-9″ ($\delta_c$ 169.1), while the glucosylation position was indicated to be at C-3 due to HMBC correlation from anomeric proton H-1′ ($\delta_H$ 4.37) to C-

3 ($\delta_c$ 71.2). Acid hydrolysis of **5** released D-glucose, while alkaline hydrolysis afforded caffeic acid, these results were identified by HPLC comparing with authentic samples (Fig. 17). The configuration of glucopyranose was assigned to be $\beta$ according to coupling constant of anomeric proton H-1′ at $\delta_H$ 4.37 ($J$ = 8.0 Hz), while the caffeoyl configuration was determined as *E* configuration according to the coupling constant of olefinic protons H-7″ and H-8″ ($J$ = 15.9 Hz).

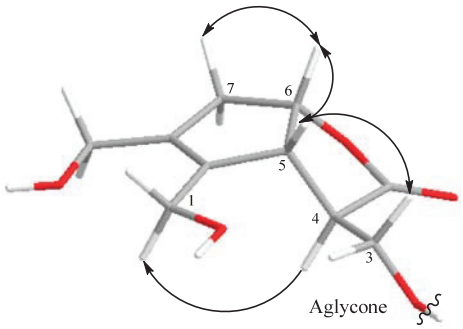


**Figure 12.** Key NOESY correlations of **5**

The relative and absolute configurations of **5** were determined by comparing its NOESY correlation (Fig. 12) and CD spectrum to those of **14**. Therefore, the structure of **5** was established to be 6'-caffeoyl-3-*O*-$\beta$-D-glucopyranoside of **14**, designated as lasianoside C.

Lasianoside D (**6**), $[\alpha]^{22}_{D}$ –22.9, was also obtained as a viscous pale-yellow syrup with a molecular formula $C_{27}H_{32}O_{14}$ with 12 degrees of unsaturation, deduced by the molecular ion peak $[M+Na]^+$ at *m/z*: 603.1681 (calcd for $C_{27}H_{32}O_{14}Na$: 603.1684) in HR-ESI-MS. Analysis of $^1H$ and $^{13}C$ NMR (Table 2 and 3), together with the molecular formula revealed that compound **6** was acetyl derivative of **5**. In the HMBC spectrum (Fig. 13), downfield shifted $H_2$-1 ($\delta_H$ 4.75) showed correlation to the acetyl carbonyl carbon at $\delta_c$ 172.6, indicated that **6** should be 1-acetyl derivative of **5**. Further analyses of NMR data suggested that the other part of **6** were same to those of **5**.

The relative and absolute configurations of **6** were also identified to be the same as **5** by comparing NOESY (Fig. 14) and CD spectral data with those of **5**, thus the structure

of **6** was elucidated to be 1-acetyl-6'-caffeoyl-3-*O*-*β*-D-glucopyranoside of **14**, and designated as lasianoside D.

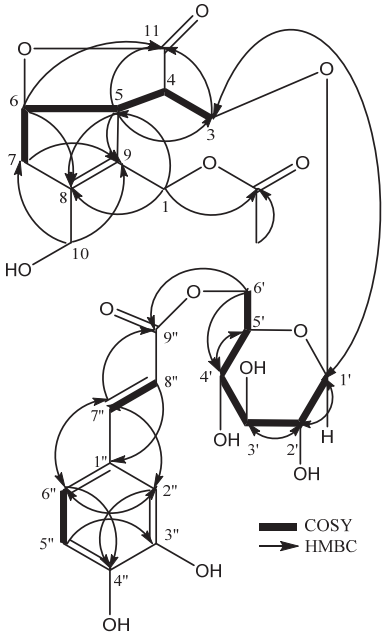


**Figure 13.** HMBC and COSY correlations of **6**

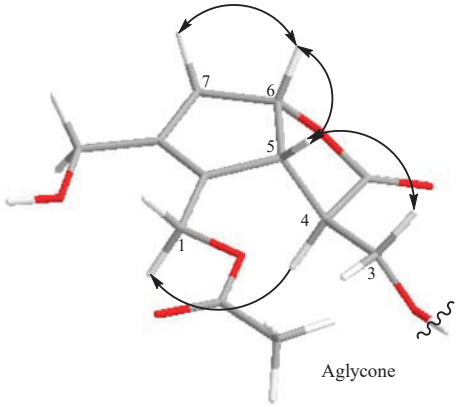


**Figure 14.** Key NOESY correlations of **6**

Lasianoside E (**7**), $[\alpha]_D^{22}$ –24.5, has the same molecular formula as that of **6** by HR-ESI-MS (*m/z*: 603.1682 $[M+Na]^+$ (calcd for $C_{27}H_{32}O_{14}Na$: 603.1684). Further comparison of NMR data (Table 2 and 3) displayed that compounds **7** and **6** shared same functional group. In HMBC spectrum (Fig. 15), significant downfield shift of $H_2$-10 ($\delta_H$

4.67) showed correlation to acetyl carbonyl carbon at $\delta_c$ 172.6. Detailed analyses of 2D NMR data indicated that the other part of **7** were the same of that of **6**. The relative and absolute configurations of **7** were determined by comparison of NOESY experiment (Fig. 16) and CD data with that of **5**.

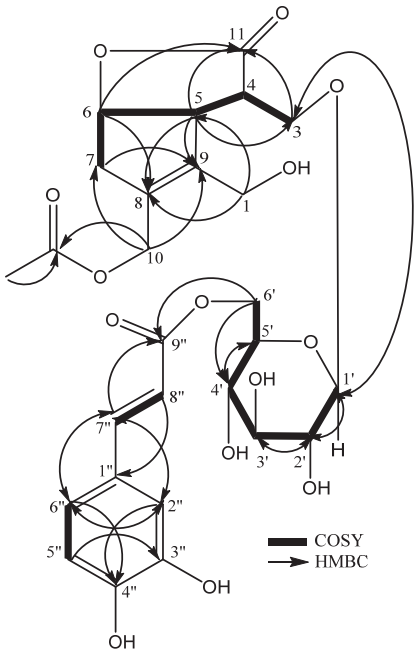


**Figure 15.** HMBC and COSY correlations of **7**

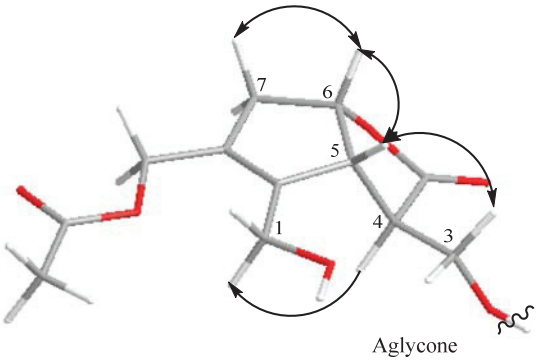


**Figure 16.** Key NOESY correlations of **7**

Therefore, the structure of **7** was elucidated to be 10-acetyl-6'-caffeoyl-3-*O*-*β*-D-glucopyranoside of **14**, and designated as lasianoside E. The plausible biosynthetic pathways of compounds **1** – **7** and **16** were illustrated in Fig. 18.

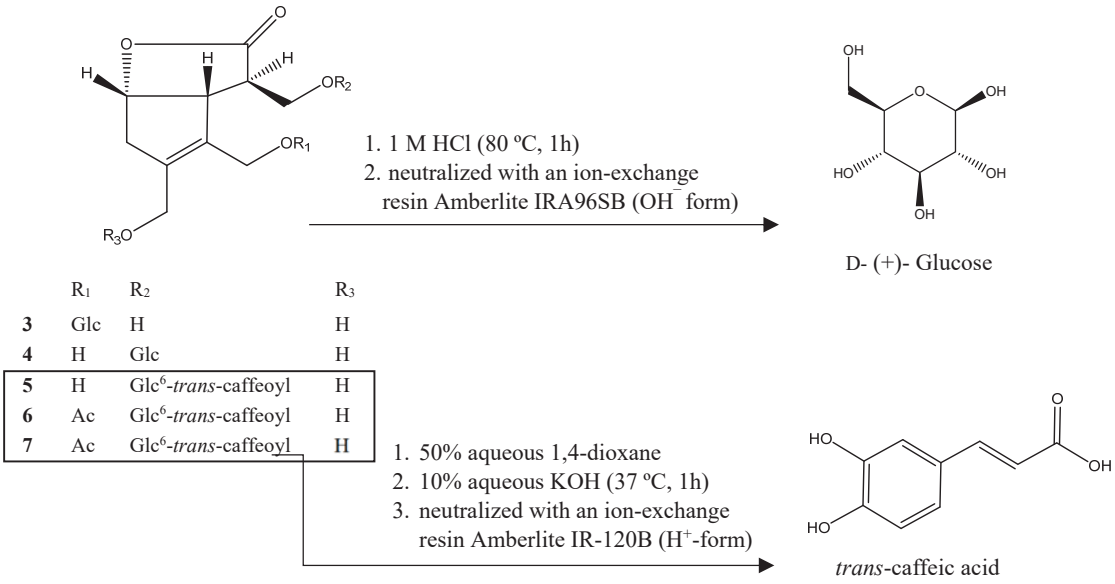


| | $R_1$ | $R_2$ | $R_3$ |
|---|---|---|---|
| **3** | Glc | H | H |
| **4** | H | Glc | H |
| **5** | H | Glc$^6$-*trans*-caffeoyl | H |
| **6** | Ac | Glc$^6$-*trans*-caffeoyl | H |
| **7** | Ac | Glc$^6$-*trans*-caffeoyl | H |

**Figure 17.** Acid hydrolysis of (**3** – **7**) and alkaline hydrolysis of (**5 – 7**)

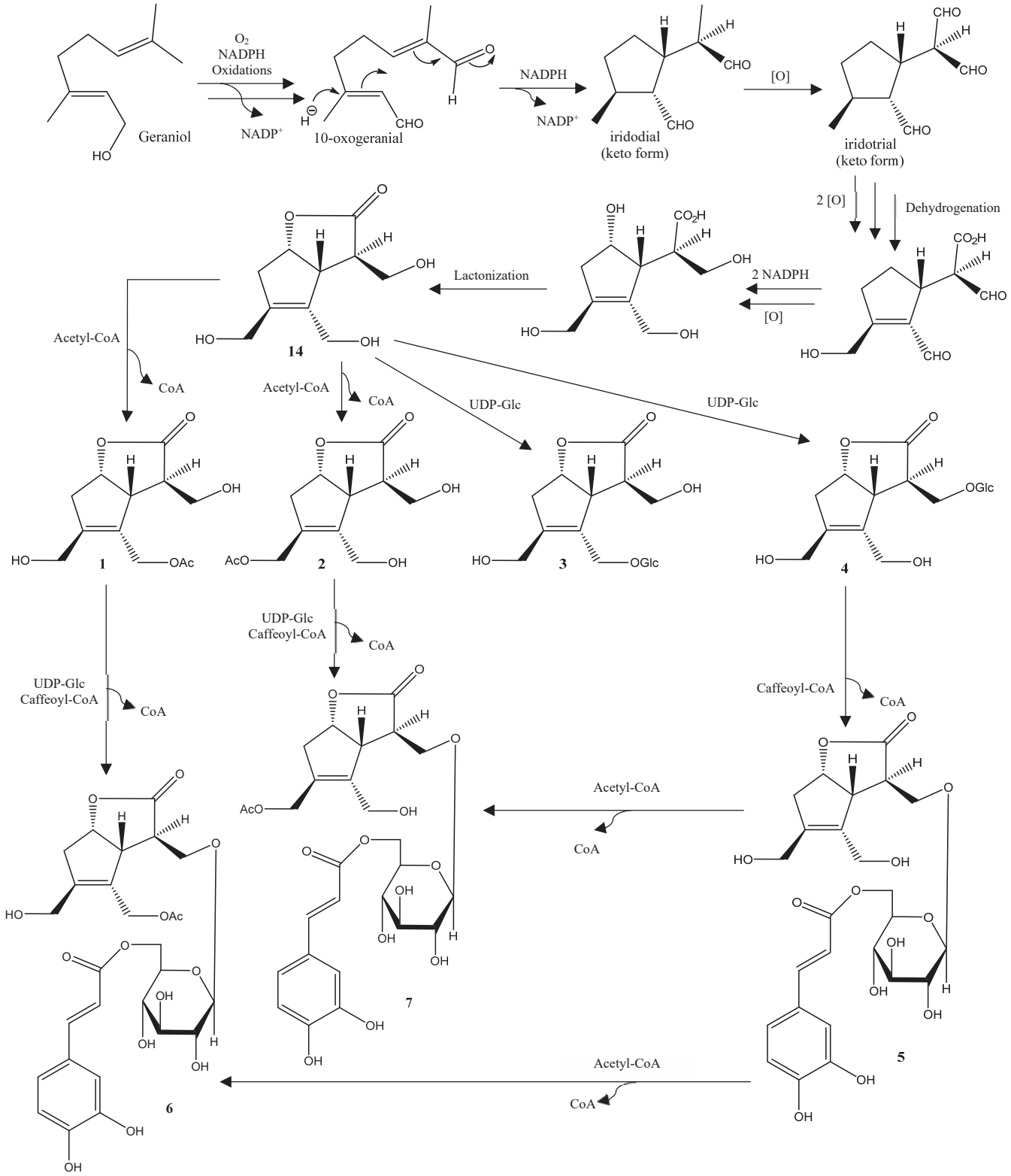


**Figure 18.** Plausible biosynthetic pathways of compounds **1** – **7** and **14**.

Lasianoside F (**8**), was obtained as a viscous colorless syrup with a specific optical rotation of $[\alpha]_D^{22}$ –65.5. A $C_{21}H_{28}O_{11}$ molecular formula was deduced from HR-ESI-MS (*m/z* 479.1521 $[M+Na]^+$, calcd for $C_{21}H_{28}O_{11}Na$, 479.1524), which suggests eight degrees of unsaturation. The UV spectrum showed absorption maxima at 234 nm indicated presence of enone system and IR absorption bands at 3405, 1732, 1658 and 1634 $cm^{-1}$ that corresponding to hydroxy, carbonyl and olefinic groups. The $^1H$ NMR spectrum of **8** (Table. 4) showed one oxymethylene at $\delta_H$ 4.69 (1H, dd, $J$ = 14.5, 1.0 Hz) and 4.81 (1H, dd, $J$ = 14.5, 1.0 Hz), two olefinic protons; one at $\delta_H$ 7.32 (1H, d, $J$ = 2.0 Hz) assigned to conjugated enol ether and the other at $\delta_H$ 5.75 (1H, t, $J$ = 2.0 Hz), two methines at 3.70 (1H, ddd, $J$ = 6.5, 6.5, 2.0 Hz) and 3.31 (1H, m), two oxymethines at $\delta_H$ 5.59 (1H, dt, $J$ = 6.5, 2.0 Hz) and $\delta_H$ 5.98 (1H, d, $J$ = 1.0 Hz), one anomeric proton at $\delta_H$ 4.70 (1H, d, $J$ = 8.0 Hz), together with signals of isovaleroyl unit [one methylene at $\delta_H$ 2.27 (2H, d, $J$ = 7.0 Hz), one methine at $\delta_H$ 2.09 (1H, m) and two equivalent methyl signals at $\delta_H$ 0.98 (6H, d, $J$ = 6.7 Hz)]. The $^{13}C$ NMR spectrum (Table. 4) of **8** showed 21 signals, of which 6 signals could be attributed to a glucopyranosyl unit ($\delta_c$ 100.0, 78.4, 77.9, 74.6, 71.6, 62.8), 10 signals for an iridoid skeleton ($\delta_c$ 37.5, 45.3, 61.7, 86.3, 93.3, 106.2, 129.0, 144.4, 150.3, 172.6) which were similar to those reported for asperuloside (**16**) [20], and other five signals that contributed to isovaleroyl unit ($\delta_c$ 22.7, 22.7, 26.8, 43.9, 174.1).

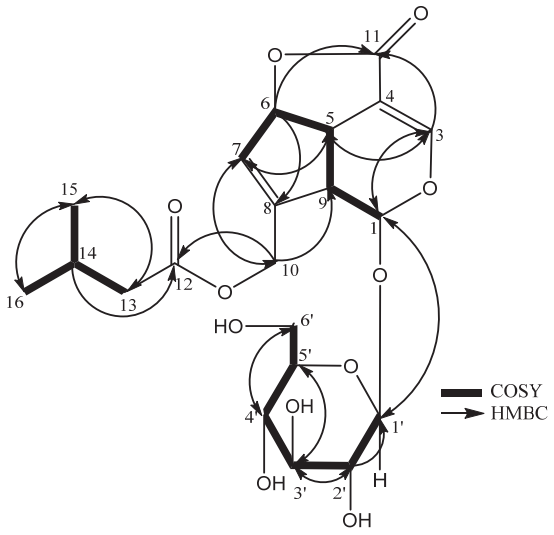


**Figure 19.** HMBC and COSY correlations of **8**

The HMBC correlations (Fig. 19) from $H_2$-10 ($\delta_H$ 4.69 and 4.81) to C-12 ($\delta_c$ 174.1), and from anomeric proton H-1′ ($\delta_H$ 4.70) to C-1 ($\delta_c$ 93.3) ascertained the presence of isovaleroyl moiety on C-10 and clarified connection of glucosyl moiety to C-1, respectively. The coupling constant of anomeric proton H-1' ($J$ = 8.0 Hz) indicated $\beta$ linkage for glucose moiety, while acid hydrolysis of **8** yielded D-glucose that identified by HPLC analysis with a chiral detector in comparison of authentic D-glucose (Fig. 23). The relative configuration of **8** was assigned based on NOESY experiment (Fig. 20). The correlations observed between H-5/H-6 and H-9 suggested $\beta$-orientation of H-5, H-6 and H-9. The chemical shift values and the coupling patterns of **8** were similar to those of asperuloside (**16**) [20, 21]. The CD spectrum data ($\Delta\varepsilon$ = –4.11 at 245 nm) had used to confirm the absolute configuration. Thus, compound **8** was identified as isovalerate of deacetyl asperuloside, designated as lasianoside F.

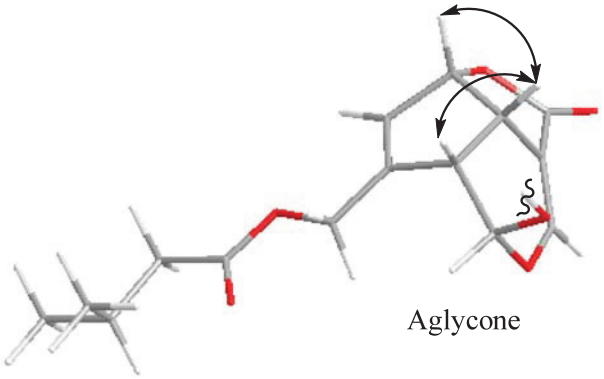


**Figure 20.** Key NOESY correlations of **8**

6'-*O*-*trans*-caffeoyl asperuloside (**9**), $[\alpha]^{22}_D$ –62.5, was isolated as a colorless syrup and determined to have the molecular formula $C_{27}H_{28}O_{14}$ from HR-ESI-MS (*m/z* 599.1370 $[M+Na]^+$, calcd for $C_{27}H_{28}O_{14}Na$, 599.1371), which suggested 14 degrees of unsaturation. UV spectrum revealed absorption maxima at 331, 297, and 241, while IR spectrum showed absorption bands at 3389, 1725, 1658, 1604 and 1515 $cm^{-1}$ indicating the presence of hydroxy group, conjugated carbonyl carbons and olefinic carbons, respectively. Beside the signals assignable for asperuloside (**16**) [20, 21], the $^1H$ NMR spectrum (Table. 4) of **9** revealed five new protons at $\delta_H$ 6.06 (1H, d, $J$ = 1.8 Hz), 6.79 (1H, d, $J$ = 8.2 Hz) and 6.97

**Table 4.** $^{1}H$ and $^{13}C$ NMR spectroscopic data for **8** and **9**

| Position | **8** | | **9** | |
|---|---|---|---|---|
| | $\delta_c$ | $\delta_H$ Multi (*J* in Hz) | $\delta_c$ | $\delta_H$ Multi (*J* in Hz) |
| 1 | 93.3 | 5.98 d (1.0) | 93.3 | 5.83 d (1.0) |
| 3 | 150.3 | 7.32 d (2.0) | 150.2 | 7.31 d (2.0) |
| 4 | 106.2 | - | 106.2 | - |
| 5 | 37.5 | 3.70 ddd (8.0, 6.5, 2.0) | 37.4 | 3.67 ddd (8.5, 6.5, 2.0) |
| 6 | 86.3 | 5.59 dt (6.5, 2.0) | 86.3 | 5.56 dt (6.5, 2.0) |
| 7 | 129.0 | 5.75 t (2.0) | 128.9 | 5.69 d (2.0) |
| 8 | 144.4 | - | 144.2 | - |
| 9 | 45.3 | 3.31 m | 45.3 | 3.32 m |
| 10 | 61.7 | 4.69 dd (14.5, 1.0)<br>4.81 dd (14.5, 1.0) | 61.8 | 4.61 dd (14.0, 1.0)<br>4.71 dd (14.0, 1.0) |
| 11 | 172.6 | - | 172.5 | - |
| 12 | 174.1 | - | 172.0 | - |
| 13 | 43.9 | 2.27 2H d (7.0) | 20.6 | 2.01s |
| 14 | 26.8 | 2.09 (m) | | |
| 15 | 22.7 | 0.98 d (6.7) | | |
| 16 | 22.7 | 0.98 d (6.7) | | |
| 1' | 100.0 | 4.70 d (8.0) | 100.1 | 4.73 d (8.0) |
| 2' | 74.6 | 3.21 dd (9.0, 8.0) | 74.6 | 3.26 dd (9.0, 8.0) |
| 3' | 78.4 | 3.40 t (9.0) | 77.7 | 3.44 t (9.0) |
| 4' | 71.6 | 3.30 t (9.0) | 71.6 | 3.40 t (9.0) |
| 5' | 77.9 | 3.37 td (6.5, 2.0) | 75.8 | 3.62 td (6.2, 2.0) |
| 6' | 62.8 | 3.69 dd (12.0, 6.5)<br>3.92 dd (12.0, 2.0) | 64.4 | 4.42 dd (12.0, 6.2)<br>4.54 dd (12.0, 2.0) |
| 1″ | | | 127.6 | - |
| 2″ | | | 115.2 | 6.06 d (1.8) |
| 3″ | | | 146.8 | - |
| 4″ | | | 149.7 | - |
| 5″ | | | 116.5 | 6.79 d (8.2) |
| 6″ | | | 123.1 | 6.97 dd (8.2, 1.8) |
| 7″ | | | 147.3 | 7.60 br d (16.0) |
| 8″ | | | 114.8 | 6.33 br d (16.0) |
| 9″ | | | 169.1 | - |

Recorded at 500 and 175 MHz in $CD_3OD$. Chemical shifts ($\delta$) are expressed in ppm and *J* values are presented in Hz in parenthesis. m: multiplet or overlapped signals.

(1H, dd, $J$ = 8.2, 1.8 Hz) corresponding to 1,3,4-trisubsttuted benzene ring, together with *trans*-double-bond signals at $\delta_H$ 7.60 (1H, br d, $J$ = 16.0 Hz) and 6.33 (1H, br d, $J$ = 16.0 Hz). In the same way, $^{13}$C NMR spectrum of **9** (Table.4) showed additional nine $sp^2$ carbon signals attributed six aromatic carbons ($\delta_c$ 115.2, 116.5, 123.1, 127.6, 146.8 and 149.7), $\alpha,\beta$-unsaturated olefinic carbons ($\delta_c$ 114.8 and 147.3), and carbonyl ester carbon ($\delta_c$ 169.1).

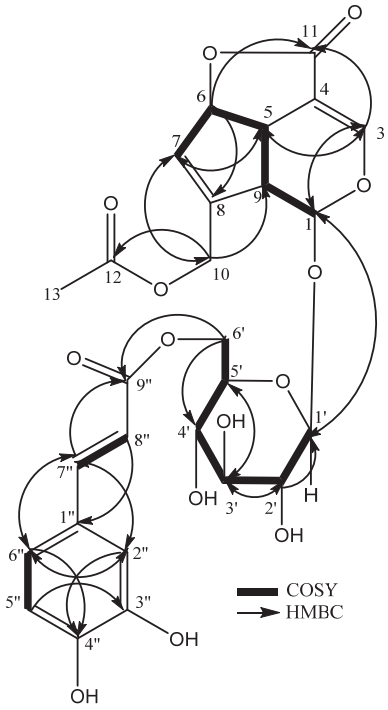


**Figure 21.** HMBC and COSY correlations of **9**

The HMBC cross peaks of H-7″ ($\delta_H$ 7.60)/C2″ ($\delta_c$ 115.2), C-6″ ($\delta_c$ 123.1) and C-9″ ($\delta_c$ 169.1), together with H-8″ ($\delta_H$ 6.33)/C1″ ($\delta_c$ 127.6) (Fig. 21), indicated the presence of *trans*-caffeoyl moiety. The downfield shifts of $H_2$-6′ to $\delta_H$ 4.42 and 4.54 implied that the caffeoyl moiety was linked to C-6′ of glucose moiety, this evidence was supported by HMBC correlation between $H_2$-6′ and C-9″ at ($\delta_c$ 169.1). The highly deshielded chemical shift of an anomeric proton ($\delta_H$ 4.73) and its coupling constant ($J$ = 8.0 Hz) recommended the $\beta$ mode of linkage for glucose moiety. Acid hydrolysis of **9** released D-glucose, while alkaline hydrolysis of **9** yielded caffeic acid which were determined by HPLC using authentic samples and chiral detector (Fig. 23). The relative configuration of **9** was

established by NOESY analysis and coupling constant. The caffeoyl group was assigned an *E* configuration from large coupling constant between H-7″ and H-8″ ($J$ = 16.0 Hz).

In NOESY spectrum (Fig. 22), the correlations of H-5/ H-6 and H-5/H-9 suggested that H-5, H-6 and H-9 are all *β*-orientated. The chemical shift values and the coupling patterns of aglycone moiety were essentially superimposable to aglycone moiety of asperuloside (**16**) [20, 21]. Furthermore, the absolute configuration was established by analysis of the CD spectrum ($\Delta\varepsilon$ = –6.03 at 241 nm) as 1*S*, 5*S*, 6*S*, 9*S*. Correspondingly, **9** was determined to be 6'-*O*-*trans*-caffeoyl asperuloside.

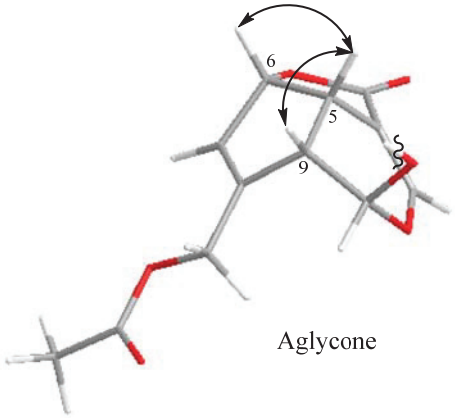


**Figure 22.** Key NOESY correlations of **9**

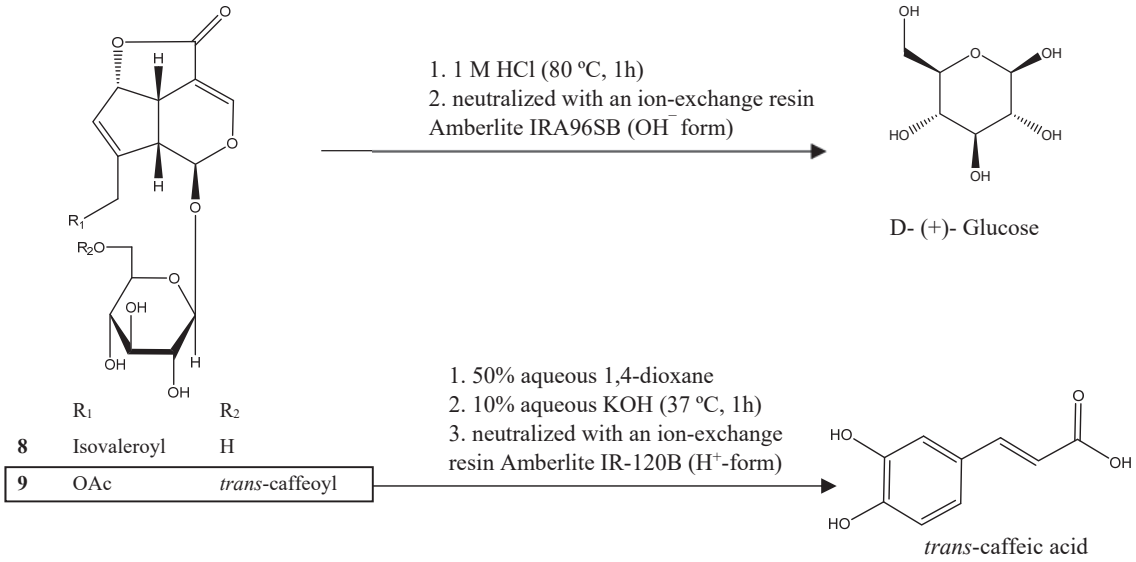


**Figure 23.** Acid hydrolysis of (**8** and **9**) and alkaline hydrolysis of (**9**)

Lasianoside G (**10**) was isolated as a viscous colorless syrup with a specific optical rotation of $[\alpha]_D^{22}$ –55.0 Its molecular formula $C_{36}H_{44}O_{22}$, from its HR-ESI-MS (*m/z* 851.2214 $[M + Na]^+$ (calcd for $C_{36}H_{44}O_{22}Na$ 851.2216), indicating 15 degrees of unsaturation. The UV spectra of **10** exhibited absorption maxima at 236 nm, characteristic for iridoid conjugated enol ether system. Similarly, IR spectra displayed absorption bands corresponding to hydroxy, enone, ester and olefinic groups at 3309, 1735, 1650 and 1630 $cm^{-1}$, respectively.

**Table. 5** The $^{13}C$ and $^1H$ NMR spectroscopic data for **10**

| Position | **10** | | | |
|---|---|---|---|---|
| | Unit A | | Unit B | |
| | $\delta_c$ | $\delta_H$ Multi (*J* in Hz) | $\delta_c$ | $\delta_H$ Multi (*J* in Hz) |
| 1 | 94.1 | 5.86 d (1.0) | 101.8 | 5.05 d (9.0) |
| 3 | 150.1 | 7.15 d (2.0) | 156.3 | 7.70 d (1.0) |
| 4 | 106.3 | - | 107.7 | - |
| 5 | 37.6 | 3.43 ddd (8.5, 6.5, 2.0) | 42.9 | 2.86 ddd (8.0, 6.5, 1.0) |
| 6 | 86.1 | 5.50 dt (6.5, 2.0) | 75.2 | 4.80 m |
| 7 | 129.1 | 5.69 br s | 131.6 | 6.00 d (2.0) |
| 8 | 143.9 | - | 146.5 | - |
| 9 | 45.0 | 3.27 m | 45.8 | 2.74 d (8.0) |
| 10 | 61.9 | 4.62 dd (14.5, 1.0)<br>4.74 dd (14.5, 1.0) | 63.7 | 4.82 m<br>4.95 br d (15.0) |
| 11 | 172.2 | - | 167.6 | - |
| 10-*CO*$CH_3$ | 172.7 | - | 172.2 | - |
| 10-CO*$CH_3$* | 20.6 | 2.06 s | 20.8 | 2.09 s |
| 1' | 98.6 | 4.92 d (8.0) | 100.9 | 4.70 d (7.5) |
| 2' | 74.4 | 4.80 m | 74.9 | 3.27 m |
| 3' | 75.5 | 3.67 dd (9.5, 9.0) | 78.6 | 3.37 dd (9.5, 9.0) |
| 4' | 71.5 | 3.37 dd (9.5, 9.0) | 71.7 | 3.30 m |
| 5' | 78.5 | 3.46 td (6.5, 2.0) | 77.8 | 3.30 m |
| 6' | 62.7 | 3.69 dd (12.0, 6.5)<br>3.94 dd (12.0, 2.0) | 63.0 | 3.61 dd (12.0, 5.5)<br>3.83 dd (12.0, 1.5) |

Recorded at 500 and 125 MHz in $CD_3OD$. Chemical shifts ($\delta$) are expressed in ppm and *J* values are presented in Hz in parenthesis. m: multiplet or overlapped signals.

Duplication of the signals in both $^{1}H$ and $^{13}C$ NMR spectra (Table. 5) of **10** clearly implied its dimeric nature as two set of iridoid glucoside. The proton signals arising in the region of $\delta_H$ 3.27-4.92 in $^{1}H$ NMR spectrum (Table. 5) including two anomeric protons at $\delta_H$ 4.70 (1H, d, $J$ = 7.5 Hz) and 4.92 (1H, d, $J$ = 8.0 Hz) support presence of two glucosyl units in **10**. Furthermore, two $sp^2$ methine proton signals at $\delta_H$ 7.15 (1H, d, $J$ = 2.0 Hz) and 7.70 (1H, d, $J$ = 1.0 Hz), which are characteristic of C-3 protons confirmed the presence of two conjugated enol ether iridoid moieties. Consistent with these observations, the $^{13}C$ NMR spectrum (Table. 5) showed 36 signals comprising four carbonyl carbons ($\delta_c$167.6, 172.2, 172.2 and 172.7), eight olefinic carbons ($\delta_c$ 106.3, 107.7, 129.1, 131.6, 143.9, 146.5, 150.1 and 156.3), six oxygenated carbons (four methines $\delta_c$ 75.2, 86.1, 94.1, 101.8 and two methylenes $\delta_c$ 61.9, 63.7), four $sp^3$ methine carbons ($\delta_c$ 37.6, 42.9, 45.0 and 45.8) together with two anomeric carbons ($\delta_c$ 98.6 and 100.9) and oxygenated carbons arising in the region of $\delta_c$ 62.7- 78.6 were belonged to two glucose moieties. Thus, the two partial structures of **10** were referred as units “A” and “B” and determined to be asperuloside (**16**) and asperulosidic acid [20, 21, 22], respectively.

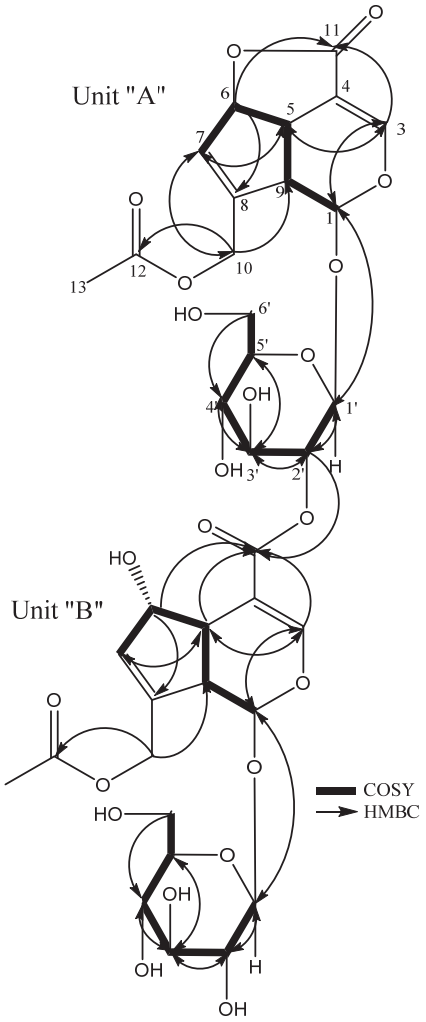


**Figure 24.** HMBC and COSY correlations of **10**

The 1D and 2D NMR data of compound **10** were very similar to those of dimer iridoid glucoside (**15**) that reported in [12]. The only evident difference was observed in glucosyl part of unit “A”, the lower field shift of H-2′ $\delta_H$ 4.80 and upper field shift of $H_2$-6′ $\delta_H$ 3.69 (1H, dd, $J$ = 12.0, 6.5 Hz) and 3.94 (1H, dd, $J$ = 12.0, 2.0 Hz) indicated that **10** was a positional isomer of **15**. The attachment site between “A” and “B” units was deduced to be at C-2′ of unit “A” by ester linkage. This assumption was further verified by correlation from H-2′ ($\delta_H$ 4.80) of unit “A” to C-11 ($\delta_c$ 167.6) of unit “B” in HMBC spectrum (Fig. 24).

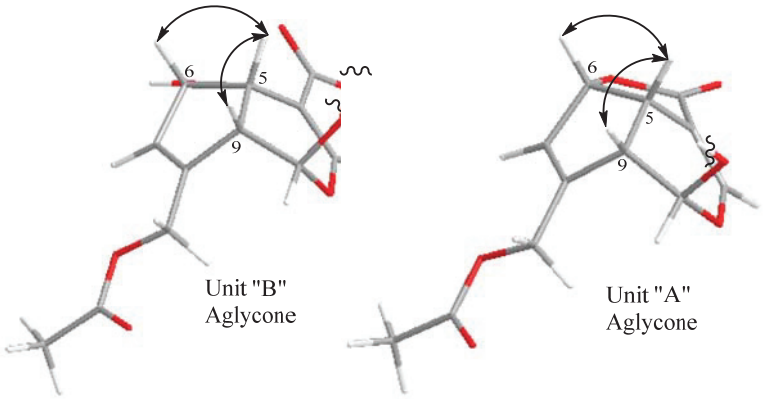


**Figure 25.** Key NOESY correlations of **10**

Moreover, acid hydrolysis of **10** gave D-configurations for both glucosyl unit, which was identified by HPLC analysis with chiral detector, while *β*-anomeric configurations were established from the coupling constant ($J$ = 8.0 Hz) and ($J$ = 7.5 Hz) (Fig. 30). The relative and absolute configuration of both "A" and "B" aglycone parts of **10** were determined to be identical to **16** [20, 21], by comparison of their coupling constant, NOESY experiment (Fig. 25) and CD data. Therefor the structure of **10** was characterized as shown in Figure 2.

Lasianoside H (**11**) was obtained as a viscous colorless syrup, with a specific optical rotation of $[\alpha]^{22}_{D}$ –59.9. It was assigned a molecular formula of $C_{36}H_{44}O_{22}$ by HR-ESI-MS at *m/z* 851.2212 $[M + Na]^+$ (calcd for $C_{36}H_{44}O_{22}Na$ 851.2216) indicated that **11** was also another positional isomer of **15**. Comparison of $^1H$ and $^{13}C$ NMR data (Table. 6) showed that the structure of **11** was similar to that of **15**. The major change was occurred in glucose moiety of unit "A", the chemical shift of H-3′ moved to downfield at $\delta_H$ 5.08 (1H, t, $J$ = 9.0 Hz) and the chemical shift of $H_2$-6′ moved to upfield at $\delta_H$ 3.74 (1H, m) and 3.95 (1H, dd, $J$ = 12.0, 2.0 Hz) suggested that the position of esterification between units "A" and "B" was changed from H-6′ to H-3′. This suggestion was supported by correlation between the H-3′ ($\delta_H$ 5.08) of unit "A" and C-11($\delta_c$ 168.6) of unit "B" in HMBC spectrum (Fig. 26).

**Table. 6** The $^{13}C$ and $^{1}H$ NMR spectroscopic data for **11**

| Position | **11** | | | |
|---|---|---|---|---|
| | Unit A | | Unit B | |
| | $\delta_c$ | $\delta_H$ Multi (*J* in Hz) | $\delta_c$ | $\delta_H$ Multi (*J* in Hz) |
| 1 | 93.4 | 5.99 d (1.4) | 101.3 | 5.07 d (9.0) |
| 3 | 150.3 | 7.33 d (2.0) | 156.1 | 7.77 d (1.3) |
| 4 | 106.2 | - | 108.0 | - |
| 5 | 37.4 | 3.69 ddd (8.0, 6.5, 2.0) | 42.5 | 3.12 ddd (8.0, 6.0, 1.25) |
| 6 | 86.3 | 5.58 dt (6.5, 2.0) | 75.8 | 4.87 m |
| 7 | 129.0 | 5.75 br s | 131.5 | 6.05 d (2.0) |
| 8 | 144.2 | - | 146.1 | - |
| 9 | 45.2 | 3.36 m | 46.4 | 2.69 t (8.0) |
| 10 | 61.9 | 4.69 br d (15.0)<br>4.80 br d (15.0) | 63.8 | 4.82 br d (15.0)<br>4.97 br d (15.0) |
| 11 | 172.6 | - | 168.6 | - |
| 10-*CO*$CH_3$ | 172.3 | - | 172.6 | - |
| 10-CO*CH*$_3$ | 20.7 | 2.11 s | 20.8 | 2.10 s |
| 1' | 100.0 | 4.84 d (8.0) | 100.6 | 4.75 d (8.0) |
| 2' | 72.9 | 3.44 dd (9.5, 8.0) | 74.9 | 3.28 m |
| 3' | 78.7 | 5.08 t (9.0) | 77.9 | 3.32 m |
| 4' | 70.0 | 3.58 t (9.0) | 71.5 | 3.31 m |
| 5' | 78.6 | 3.51 td (6.0, 2.0) | 78.6 | 3.41 m |
| 6' | 62.4 | 3.74 m<br>3.95 dd (12.0, 2.0) | 62.9 | 3.64 dd (12.0, 6.0)<br>3.88 dd (12.0, 2.0) |

Recorded at 500 and 125 MHz in $CD_3OD$. Chemical shifts ($\delta$) are expressed in ppm and *J* values are presented in Hz in parenthesis. m: multiplet or overlapped signals.

The structure of this compound was approved by further analysis of 2D NMR data including COSY, HSQC and HMBC spectra. Acid hydrolysis of **11** revealed that both glucosyl unit were D-configurations (Fig. 30). The relative and absolute configurations of aglycone parts of **11** are identical to those of **10** by comparison of their coupling constant, NOESY experiment (Fig. 27) and CD Cotton effect. From these data, the structure of **11** was characterized as shown in Figure 2.

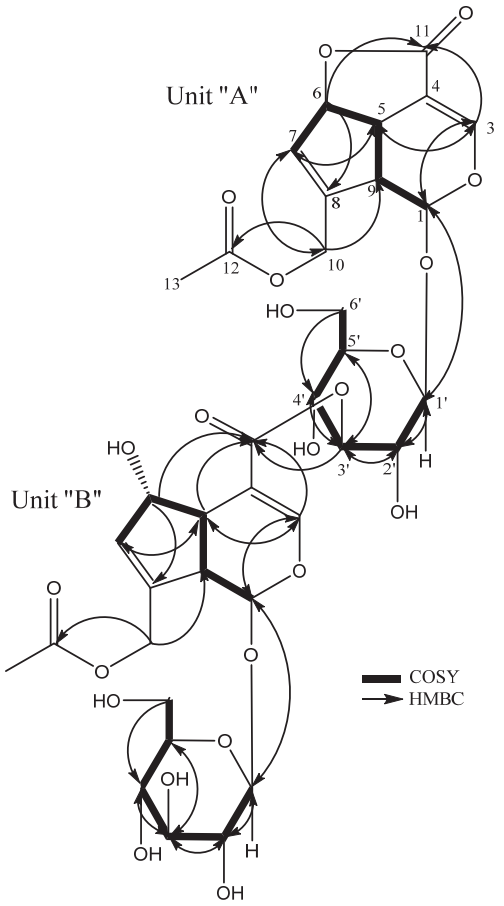


**Figure 26.** HMBC and COSY correlations of **11**

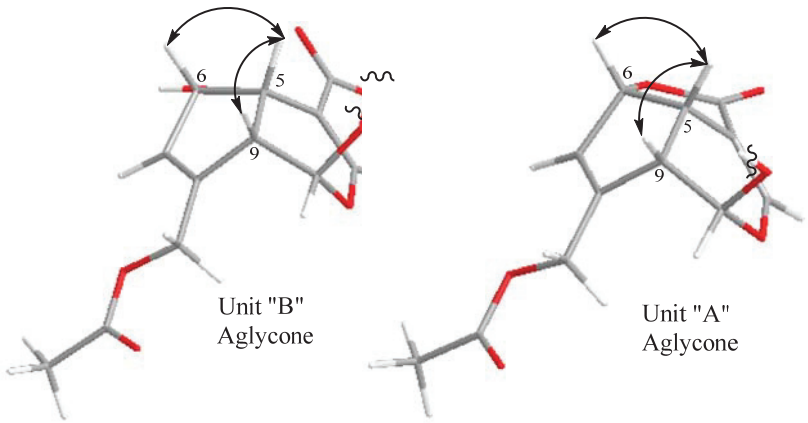


**Figure 27.** Key NOESY correlations of **11**

Lasianoside I (**12**) was isolated as viscous colorless syrup, with a specific optical rotation of $[\alpha]^{22}_{D}$ –60.1. It had molecular formula of $C_{36}H_{44}O_{22}$ established from its $^{13}C$ NMR data and positive mode HR-ESI-MS [*m/z* 851.2215 $[M + Na]^+$ (calcd for $C_{36}H_{44}O_{22}$ Na 851.2216)]. The $^{13}C$ NMR data (Table. 7) showed signals resembling those of **15** except the presence of two $sp^3$ methines C-4 at $\delta_c$ 44.4 and C-3 at 97.3 in unit "B" of **12** instead of resonances of two olefinic carbons at the same position of **15**, in addition to lower field shift for C-11 and C-6 to $\delta_c$ 176.8 and 87.8, respectively. This was supported by absence of an enol ether proton signal in $^1H$ NMR spectrum (Table. 7) and appearance of methine proton at $\delta_H$ 3.36 (1H, m) together with oxymethine proton at $\delta_H$ 5.27 (1H, d, $J$ = 3.5 Hz) corresponding to H-4 and H-3 of unit "B", respectively.

**Table. 7** The $^{13}C$ and $^1H$ NMR spectroscopic data for **12**

| Position | **12** | | | |
|---|---|---|---|---|
| | Unit A | | Unit B | |
| | $\delta_c$ | $\delta_H$ Multi ($J$ in Hz) | $\delta_c$ | $\delta_H$ Multi ($J$ in Hz) |
| 1 | 93.5 | 5.91 d (1.1) | 96.9 | 5.14 d (2.7) |
| 3 | 150.2 | 7.33 d (2.0) | 97.3 | 5.27 d (2.0) |
| 4 | 106.3 | - | 44.4 | 3.36 m |
| 5 | 37.5 | 3.69 ddd (6.5, 6.5, 2.0) | 37.5 | 3.47 m |
| 6 | 86.4 | 5.59 dt (6.5, 2.0) | 87.8 | 5.40 dt (6.5, 2.0) |
| 7 | 128.8 | 5.74 t (2.0) | 125.9 | 6.01 d (2.0) |
| 8 | 144.3 | - | 152.5 | - |
| 9 | 45.4 | 3.37 m | 46.3 | 3.05 m |
| 10 | 61.9 | 4.68 dd (16.0, 1.5)<br>4.79 dd (16.0, 1.5) | 62.8 | 4.68 br d (16.0)<br>5.06 br d (16.0) |
| 11 | 172.6 | - | 176.8 | - |
| 10-*CO*$CH_3$ | 172.2 | - | 172.6 | - |
| 10-CO*$CH_3$* | 20.8 | 2.13 s | 20.8 | 2.09 s |
| 1' | 100.2 | 4.73 d (8.2) | 99.6 | 4.73 d (8.0) |
| 2' | 74.5 | 3.24 dd (9.0, 8.2) | 75.0 | 3.24 dd (9.0, 8.0) |
| 3' | 77.7 | 3.42 m | 78.3 | 3.43 m |
| 4' | 71.1 | 3.42 m | 71.5 | 3.30 m |
| 5' | 76.6 | 3.57 td (5.1, 1.4) | 77.8 | 3.32 m |
| 6' | 68.1 | 4.16 dd (11.7, 5.1)<br>3.95 dd (11.7, 1.4) | 62.8 | 3.67 dd (12.0, 5.0)<br>3.87 br d (12.0) |

Recorded at 500 and 125 MHz in $CD_3OD$. Chemical shifts ($\delta$) are expressed in ppm and $J$ values are presented in Hz in parenthesis. m: multiplet or overlapped signals.

The above data suggested absence of double bond between C-3 and C-4, and indicated presence of γ-lactone ring in the aglycone part of unit “B”. The occurrence of γ-lactone was confirmed by HMBC (Fig. 28) correlation from H-6 ($\delta_H$ 5.40) to C-11 ($\delta_c$ 176.8). A detailed analysis of NMR data supported by COSY, HSQC and HMBC suggested that the two partial structures of **12** were determined to be asperuloside (**16**) [20, 21] and 3,4-dihydro-3-hydroxyasperuloside [23]. The attachment between “A” and “B” units was found to be between C-6′ of unit “A” and C-3 of unit “B” by *O*-linkage due to *J* long correlation between $H_2$-6′ ($\delta_H$ 3.95 and 4.16) and C-3 ($\delta_c$ 97.3) in HMBC spectrum (Fig. 28). HPLC analysis after acid hydrolysis of **12** revealed that both glucosyl unit were D-configurations (Fig. 30).

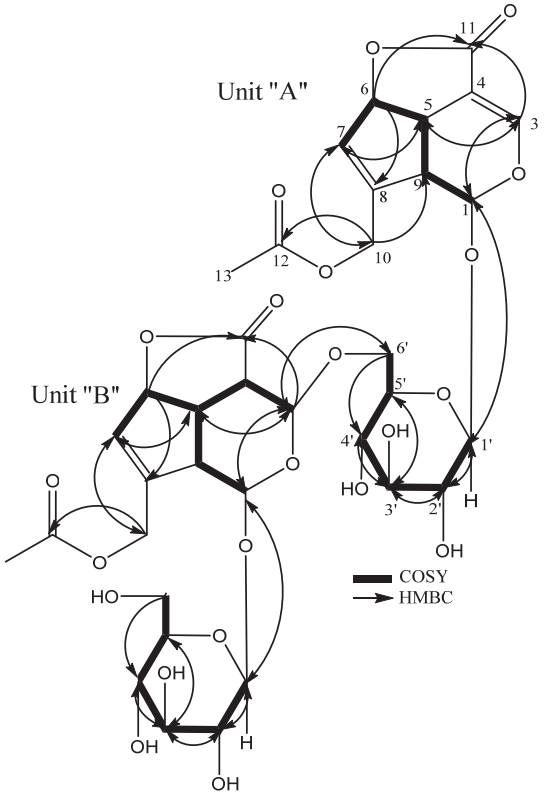


**Figure 28.** HMBC and COSY correlations of **12**

The relative and absolute configuration of unit “A” are similar to **16** by comparison of their NOESY and coupling constant data. On the other hand, indication of the stereochemistry of part “B” was achieved by NOESY (Fig. 29) analysis, particularly for

those of chiral centers H-4, H-5, H-6 and H-9. In NOESY spectrum, the correlations between H-5/H-4, H-6 and H-9 indicated *β*-orientation of H-4, H-5, H-6 and H-9. Base on the above findings, the structure of **12** was assigned as shown in figure 2.

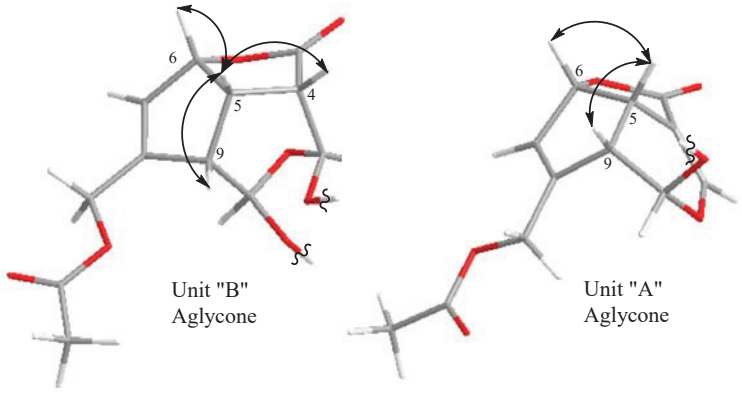


**Figure 29.** Key NOESY correlations of **12**

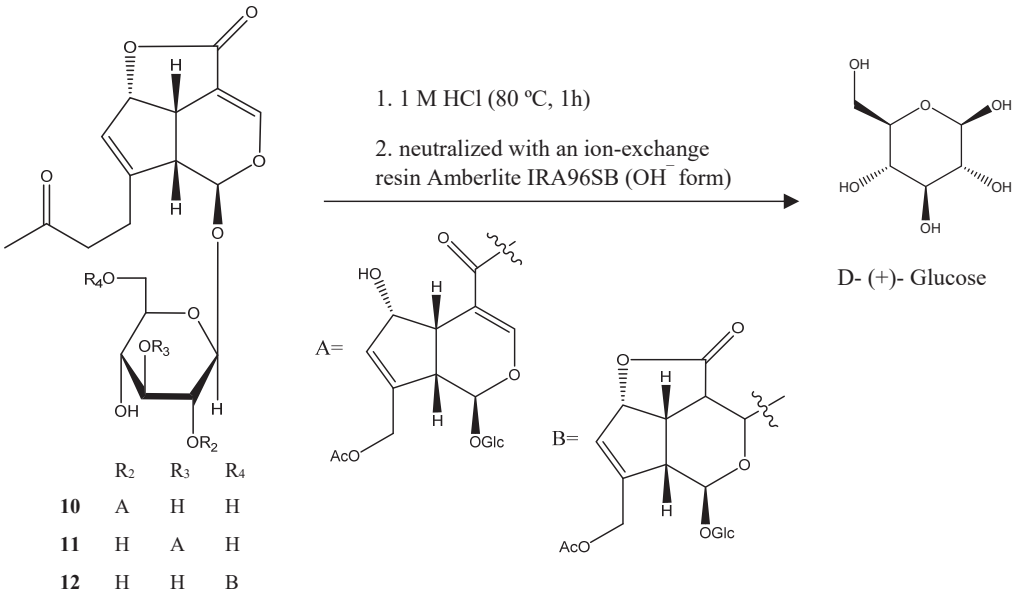


| | $R_2$ | $R_3$ | $R_4$ |
|---|---|---|---|
| **10** | A | H | H |
| **11** | H | A | H |
| **12** | H | H | B |

**Figure 30.** Acid hydrolysis of **10**–**12**

Tripterygiol 7'-*O*-*β*-D-glucopyranoside (**13**) $[\alpha]^{22}_{D}$ –22.5, was isolated as a white amorphous powder. It produced a molecular ion peak at *m/z*: 605.2200, attributed to $[M+Na]^+$ in HR-ESI-MS (calcd for $C_{28}H_{38}O_{13}Na$: 605.2205), indicating nine degrees of

unsaturation. Its UV spectrum revealed the characteristic absorption of typical pattern of non-conjugated phenyl groups at 236 and 272 nm. The IR spectrum showed absorption bands at 3390, 1615, 1518, 1115 and 1033 $cm^{-1}$ corresponding to hydroxyl groups, aromatic rings and ether linkage, respectively.

**Table. 8** The $^{13}C$ and $^{1}H$ NMR spectroscopic data for **13**

| Position | **13** | |
|---|---|---|
| | $\delta_c$ | $\delta_H$ Multi (*J* in Hz) |
| 1 | 133.2 | - |
| 2 | 106.9 | 6.39 s |
| 3 | 149.2 | - |
| 4 | 134.6 | - |
| 5 | 149.2 | - |
| 6 | 106.9 | 6.39 s |
| 7 | 41.3 | 2.44 dd (13.5, 9.8)<br>2.79 dd (13.5, 5.5) |
| 8 | 45.4 | 2.65 m |
| 9 | 74.7 | 3.54 dd (8.3, 5.5)<br>3.82 m |
| 2 x $OCH_3$ | 56.7 | 3.83 s |
| 1' | 131.9 | - |
| 2' | 105.7 | 6.73 s |
| 3' | 149.1 | - |
| 4' | 135.9 | - |
| 5' | 149.1 | - |
| 6' | 105.7 | 6.73 s |
| 7' | 81.0 | 4.86 d (8.5) |
| 8' | 52.2 | 2.40 m |
| 9' | 71.3 | 3.68 m<br>3.75 t (8.5) |
| 2 x $OCH_3$ | 56.7 | 3.85 s |
| 1" | 100.6 | 4.13 d (7.6) |
| 2" | 75.4 | 3.31 m |
| 3" | 78.1 | 3.28 m |
| 4" | 72.1 | 3.27 m |
| 5" | 78.1 | 3.16 ddd (8.5, 6.5, 2.0) |
| 6" | 63.1 | 3.68 dd (12.0, 6.5)<br>3.92 dd (12.0, 2.0) |

Recorded at 500 and 175 MHz in $CD_3OD$. Chemical shifts ($\delta$) are expressed in ppm and *J* values are presented in Hz in parenthesis. m: multiplet or overlapped signals.

The $^{1}H$ and $^{13}C$ NMR spectrum of **13** (Table. 8) displayed signals characteristic to tetrahydrofuran lignans, which were similar to those reported for tripterygiol [24], except for presence of glucose moiety signals. The $^{1}H$ NMR spectrum of **13** (Table. 8) revealed four singlet signals for two pairs of 1,3,4,5-tetrasubstituted aromatic protons at $\delta_H$ 6.39 and 6.73 (each 2H, s), and four methoxy protons at $\delta_H$ 3.83 and 3.85 (each 6H, s). A multiplet at $\delta_H$ 2.40, double doublets at $\delta_H$ 2.44 and 2.79 and a multiplet at $\delta_H$ 2.65 were attributed to H-8′, $H_2$-7 and H-8, respectively. Moreover, $^{1}H$ NMR spectrum showed doublets signals for anomeric proton H-1″ and H-7′ at $\delta_H$ 4.13 (1H, d, $J$ = 7.6 Hz) and 4.86 (1H, d, $J$ = 8.5 Hz), respectively.

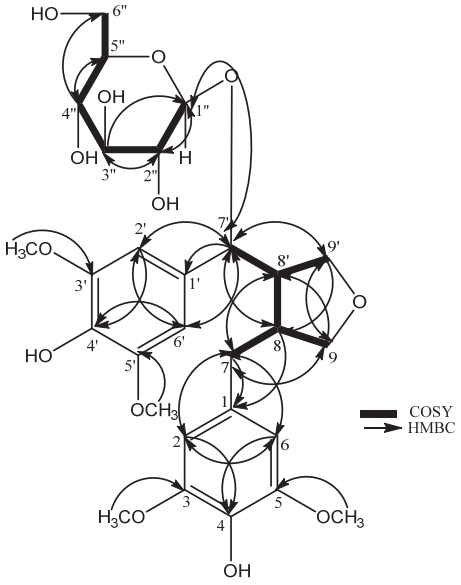


**Figure 31.** HMBC and COSY correlations of **13**

Consistent with these observations, the $^{13}C$ NMR (Table. 8) showed twenty eight carbon signals including six in a glucose part ($\delta_c$ 100.6, 78.1, 78.1, 75.4, 72.1 and 63.1), four methoxy carbons ($\delta_c$ 56.7 x 4), a methylene ($\delta_c$ 41.3), two oxymethylens ($\delta_c$ 74.7 and 71.3), two methines ($\delta_c$ 52.2 and 45.4), an oxymethine ($\delta_c$ 81.0) together with twelve aromatic carbons including eight quaternary carbons ($\delta_c$ 131.9, 133.2, 134.6, 135.9, 149.1 x 2 and 149.2x 2), with four unsubstituted carbons ($\delta_c$ 105.7 x 2 and 106.9x 2).The presence of a tetrahydrofuran ring was indicated by COSY correlations (Fig. 31) from H-8 ($\delta_H$ 2.65), to $H_2$-7 ($\delta_H$ 2.44 and 2.79), $H_2$-9 ($\delta_H$ 3.54 and 3.82) and H-8′ ($\delta_H$ 2.40), and from H-8′ ($\delta_H$

2.40) to H-7′ ($\delta_H$ 4.86), $H_2$-9′ ($\delta_H$ 3.68 and 3.75) and H-8′ ($\delta_H$ 2.65), in addition to HMBC correlations from $H_2$-7 ($\delta_H$ 2.44 and 2.79) to C-9 ($\delta_c$ 74.7), C-8′ ($\delta_c$ 52.2), and C-1 ($\delta_c$ 133.2), and from H-7′ ($\delta_H$ 4.86) to C-9′ ($\delta_c$ 71.3), C-8 ($\delta_c$ 45.4), and C-1′ ($\delta_c$ 131.9). Moreover, HMBC correlations between downfield shifted H-7′ ($\delta_H$ 4.86) and C-1″ ($\delta_c$ 100.6) confirmed the presence of glucose moiety at C-7′. Acid hydrolysis of **13** gave D-glucose (Fig. 33), which was identified by HPLC analysis with chiral detector In NOESY spectrum (Fig. 32), correlations between H-7′/H-8/H-9′*α* indicated that H-7′, H-8 and H-9′*α* are all *α*-oriented, while correlations between H-9*β*/H-8′ indicated that H-9*β* and H-8′ are both *β*-oriented. Based on the above data, compound **13** was elucidate as tripterygiol 7′-*O*-*β*-D-glucopyranoside.

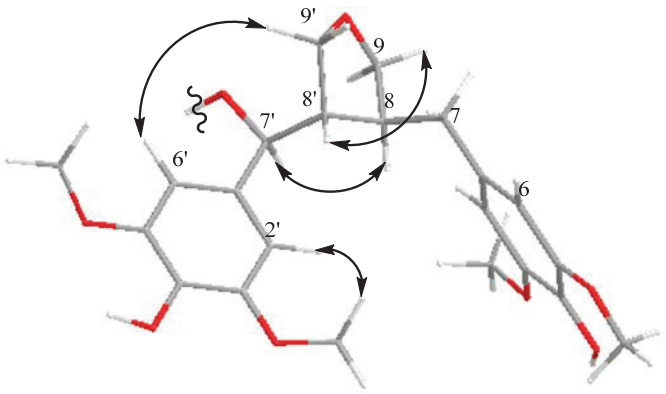


**Figure 32.** Key NOESY correlations of **13**

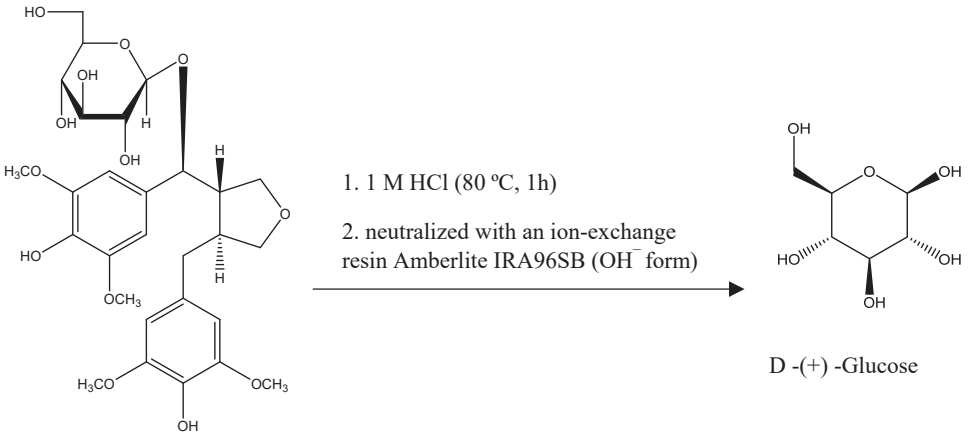


**Figure 33.** Acid hydrolysis of **13**

## 1.4 Bioassay of Chemical constituent:

### 1.4.1. DPPH radical scavenging activity

A series of oxygen centered free radicals and other reactive oxygen species (ROS) are constantly formed in aerobes bodies as a result of different physiological processes. The environmental factors such as radiation, pollution, herbicides, cigarette smoke and certain food can also create free radicals [25]. ROS play a positive role in energy production, cell growth and synthesis of biologically important compounds. Under certain conditions, overproduction of ROS and free radicals lead to induce oxidative stress that responsible for causing a variety of diseases including aging, atherosclerosis, cancer, neuronal disorder, Alzheimer's and cardiovascular diseases [26, 27]. Antioxidant are act as free radical scavengers, reducing agents and quenchers of singlet oxygen molecule, and activators for antioxidant enzymes to suppress the damage induced by free radical in biology system [25].

Humane body has several mechanisms to counteract oxidative stress by producing antioxidant, which are either naturally or externally supplied through foods and/or supplements. These free radicals scavenge and enhance the immune defenses and lower the risk of cancer and degenerative disease by preventing and repairing damages caused by ROS. Therefore, synthetic antioxidants are widely used as potential inhibitor of lipid peroxidation [28]. Later, it was found that the synthetic antioxidants were accumulated in the body causing liver damage and carcinogenesis [29, 30]. This problem encourages the search for safe and effective antioxidants from natural source in past decades. However, it has been demonstrated that the natural antioxidants extracted from herbs and spice have high antioxidant activity.

Free radical scavenging activity of isolated compounds (**1** – **25**) were evaluated using DPPH radical scavenging assay. As shown in Table. 9 and Fig. 34 and 35, a new compound (**9**), together with secoisolariciresinol diglucoside (**23**) and huazhongilexin (**25**) had potent scavenging activities with $IC_{50}$ values 22.5±1.2 $\mu$M, 20.9±1.7 $\mu$M and 24.7±0.42 $\mu$M, respectively, which even exceed that of Trolox ($IC_{50}$: 29.2±0.39 $\mu$M). Moreover, new compounds lasianosides C and D (**5** and **6**) together with 8,8′-bisdihydrosiringenin glucoside (**24**) displayed significant scavenging activity with $IC_{50}$ values 30.2±1.8 $\mu$M, 32.0±1.2 $\mu$M and 33.5±2.3 $\mu$M, respectively. Furthermore,

lasianoside E (**7**) and tripterygiol 7'-*O*-*β*-D-glucopyranoside (**13**) exhibited moderate scavenging activity with $IC_{50}$ values 46.4±2.3 $\mu$M and 42.6±1.4 $\mu$M, respectively, while compound (**21**) ($IC_{50}$: 75.4±0.97 $\mu$M) showed weak scavenging activity. The remaining compounds did not possess significant DPPH radical scavenging properties ($IC_{50}$ > 100 $\mu$M). These results suggested that the radical scavenging activities of **5**, **6**, **7** and **9** were depending on the presence of caffeoyl moieties in structures as previously described [31, 32].

**Table. 9** DPPH free radical scavenging activity of **5** – **7**, **9**, **13**, **21**, **23 – 25**

| Isolated compounds | DPPH ($IC_{50}$ $\mu$M) |
|---|---|
| Lasianoside C (**5**) | 30.2±1.8 |
| Lasianoside D (**6**) | 32.0±1.2 |
| Lasianoside E (**7**) | 46.4±2.3 |
| Compound (**9**) | 22.5±1.2 |
| Compound (**13**) | 42.6±1.4 |
| Grasshopper ketone (**21**) | 75.4±0.97 |
| Secoisolariciresinol diglucoside (**23**) | 20.9±1.7 |
| 8,8′-Bisdihydrosiringenin glucoside (**24**) | 33.5±2.3 |
| Huazhongilexin (**25**) | 24.7±0.42 |
| Trolox | 29.2±0.39 |

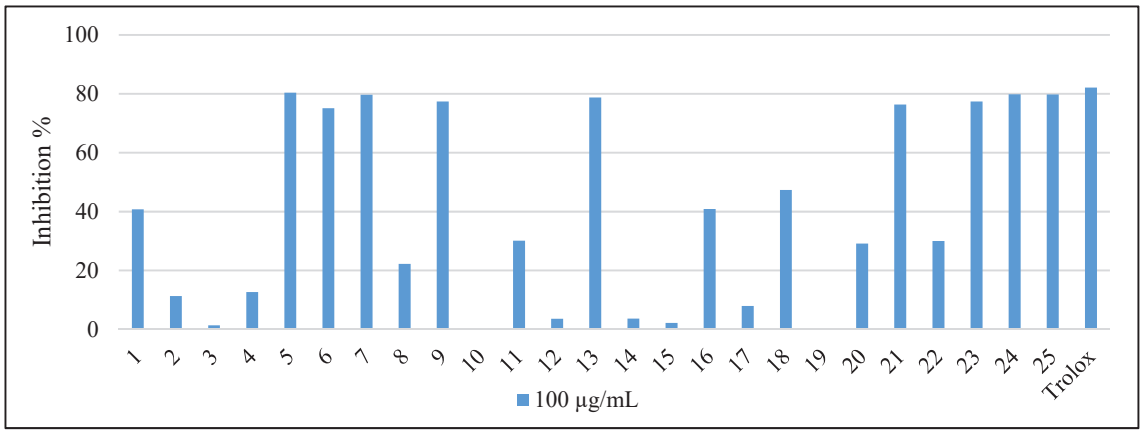


**Figure 34.** DPPH free radical scavenging activity of **1** – **25**

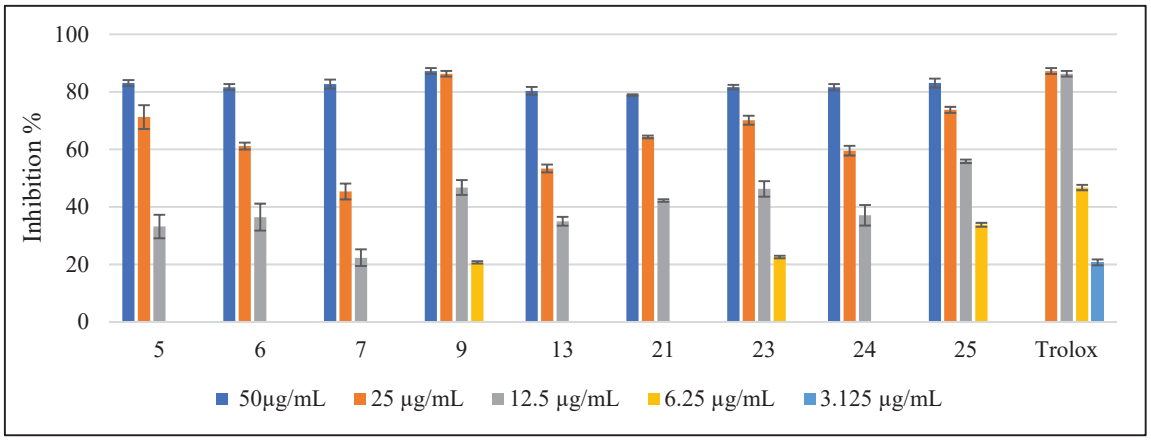


**Figure 35.** DPPH free radical scavenging activity of **5** – **7**, **9**, **13**, **21**, **23** – **25**

## 1.5. Experimental

### 1.5.1. General experimental procedures

NMR measurements were taken on Bruker avance 500 and 700 MHz spectrometers, with tetramethylsilane (TMS) as internal standard (Bruker, Biospin, Rheinstetten). Optical rotations and CD data were performed on JASCO P-1030 and Jasco J-720 polarimeters (Jasco, Eston, MD), respectively. UV and IR spectra were recorded on Jasco V-520 UV/Vis and Horiba FT-710 FT-IR spectrophotometers (Horiba, Kyoto, Japan), respectively. HR-ESI-MS data were obtained using a LTQ Orbitrap XL mass spectrometer (Thermo Fisher Scientific, Waltham, MA). High porous synthetic resin, Diaion HP-20 was purchased from Atlantic research chemical Ltd., (UK). Silica gel column chromatography (CC) and reversed-phase octadecyl silica gel (ODS) were performed on silica gel 60 (230–400 mesh, Merck, Germany), and Cosmosil 75$C_{18}$ - OPN (Nacalai Tesque, Kyoto, Japan; $\Phi = 35$ mm, $L = 350$ mm) columns, respectively. Fractions were checked by thin-layer chromatography (TLC) on precoated silica gel plates 60 $GF_{254}$ (0.25 mm in thickness, Merck), and spots were visualized under UV light (254/365 nm) or by spraying with 10% sulfuric acid reagent. For high pressure liquid chromatography (HPLC) separation, the ODS HPLC column (Cosmosil 5$C_{18}$-AR, Nacalai Tesque, Kyoto, 10 mm x 250 mm, flow rate 2.5 mL/min) was used with a mixture of $H_2O$ and MeOH and the elute was monitored by refractive index and/or a UV detector. The sugars that obtained after acid hydrolysis were analyzed by HPLC using an amino column (Shodex Asahipak NH2P-50 4E (4.6 mm x 250 mm), $CH_3CN$-$H_2O$ (3:1) 1mL/min) together with a chiral detector (Jasco OR-2090*plus*).

### 1.5.2. Plant material

Leaves of *Lasianthus verticillatus* were collected in 2000 from Iriomote Island, Okinawa Prefecture, Japan. A voucher specimen of plant was deposited in Herbarium of the department of pharmacognosy, faculty of pharmaceutical sciences, Hiroshima university (IR0009-LT).

1.5.3. isolated compounds

*1-Acetyl lasianol* (**1**)

Viscous brown syrup $[\alpha]^{22}_{D}$ –32.4 (*c* 1.02, MeOH); HR-ESI-MS (positive ion mode): *m/z*: 279.0841 $[M+Na]^+$ (calcd for $C_{12}H_{16}O_6$ Na 279.0839); UV $\lambda_{max}$ (MeOH) nm (log ε): 276 (3.03); IR (film) $\nu_{max}$: 3418, 2940, 1747, 1731, 1365, 1241, 1190, 1062, 1030 $cm^{-1}$; CD $\lambda_{max}$ (c 1.5 x $10^{-5}$ MeOH) nm (Δε): 288 (–0.003), 218 (+0.040); $^1H$ and $^{13}C$ data see Table 1.

*10-Acetyl lasianol* (**2**)

Viscous colorless syrup $[\alpha]^{22}_{D}$ –63.4 (*c* 0.68, MeOH); HR-ESI-MS (positive ion mode): *m/z*: 279.0841 $[M+Na]^+$ (calcd for $C_{12}H_{16}O_6$ Na 279.0839); UV $\lambda_{max}$ (MeOH) nm (log ε): 278 (2.77); IR (film) $\nu_{max}$: 3405, 2937, 1741, 1731, 1359, 1239, 1186, 1065, 1030 $cm^{-1}$; CD $\lambda_{max}$ (c 3.9 x $10^{-5}$ MeOH) nm (Δε): 280 (–0.129), 210 (+1.242); $^1H$ and $^{13}C$ data see Table 1.

*Lasianoside A* (**3**)

Viscous colorless syrup $[\alpha]^{22}_{D}$ –20.6 (*c* 0.30, MeOH); HR-ESI-MS (positive ion mode): *m/z*: 399.1263 $[M+Na]^+$ (calcd for $C_{16}H_{24}O_{10}Na$, 399.1262); IR (film) $\nu_{max}$: 3390, 2921, 1748, 1194, 1072, 1032 $cm^{-1}$; CD $\lambda_{max}$ (*c* 2.66 x $10^{-5}$ M, MeOH) nm (Δε): 270 (–0.059), 221 (+0.854); $^1H$ and $^{13}C$ data see Tables 2 and 3.

*Lasianoside B* (**4**)

Viscous colorless syrup $[\alpha]^{22}_{D}$ –26.6 (*c* 0.30, MeOH); HR-ESI-MS (positive ion mode): *m/z*: 399.1265 $[M+Na]^+$ (calcd for $C_{16}H_{24}O_{10}Na$, 399.1262); IR (film) $\nu_{max}$: 3372, 2927, 1754, 1171, 1078, 1024 $cm^{-1}$; CD $\lambda_{max}$ (*c* 2.66 x $10^{-5}$ M, MeOH) nm (Δε): 281 (–0.026), 217 (+1.99); $^1H$ and $^{13}C$ data see Tables 2 and 3.

*Lasianoside C* (**5**)

Viscous pale-yellow syrup $[\alpha]^{22}_{D}$ –10.2 (*c* 0.34, MeOH); HR-ESI-MS (positive ion mode): *m/z*: 561.1572 $[M+Na]^+$ (calcd for $C_{25}H_{30}O_{13}Na$, 561.1579); UV (MeOH) $\lambda_{max}$ nm (log ε): 329 (4.74), 300 (4.63), 245 (4.59); IR (film) $\nu_{max}$: 3356, 2913, 1745, 1712, 1623,

1600, 1512, 1359, 1274, 1165, 1032 $cm^{-1}$ ; CD $\lambda_{max}$ (*c* 1.85 x $10^{-5}$ M, MeOH) nm (Δε): 283 (–0.357), 221 (+6.155); $^{1}H$ and $^{13}C$ data see Tables 2 and 3.

*Lasianoside D* (**6**)

Viscous pale-yellow syrup $[\alpha]^{22}_{D}$ –22.9 (*c* 0.27, MeOH); HR-ESI-MS (positive ion mode): *m/z*: 603.1681 $[M+Na]^{+}$ (calcd for $C_{27}H_{32}O_{14}Na$, 603.1684); UV (MeOH) $\lambda_{max}$ nm (log ε): 329 (4.37), 295 (4.27), 233 (4.42); IR (film) $\nu_{max}$: 3396, 2920, 1746, 1732, 1713, 1634, 1608, 1518, 1355, 1264, 1163, 1032 $cm^{-1}$; CD $\lambda_{max}$ (*c* 1.40 x $10^{-5}$ M, MeOH) nm (Δε): 276 (–0.105), 208 (+1.010); $^{1}H$ and $^{13}C$ data see Tables 2 and 3.

*Lasianoside E* (**7**)

Viscous pale-yellow syrup $[\alpha]^{22}_{D}$ –24.5 (*c* 0.40, MeOH); HR-ESI-MS (positive ion mode): *m/z*: 603.1682 $[M+Na]^{+}$ (calcd for $C_{16}H_{24}O_{10}Na$, 603.1684); UV (MeOH) $\lambda_{max}$ nm (log ε): 331 (3.98), 292 (3.90), 240 (3.96); IR (film) $\nu_{max}$: 3361, 2928, 1747, 1738, 1714, 1625, 1602, 1509, 1365, 1271, 1179, 1030 $cm^{-1}$; CD $\lambda_{max}$ (*c* 1.72 x $10^{-5}$ M, MeOH) nm (Δε): 281 (–0.297), 214 (+1.324); $^{1}H$ and $^{13}C$ data see Tables 2 and 3.

*Lasianoside F* (**8**)

Viscous colorless syrup $[\alpha]^{22}_{D}$ –65.5 (*c* 0.88, MeOH); HR-ESI–MS(positive ion mode): *m/z*: 479.1521 $[M+Na]^{+}$ (calcd for $C_{21}H_{28}O_{11}Na$, 479.1524); UV (MeOH) $\lambda_{max}$ nm (log ε) 234 (4.04); IR (film) $\nu_{max}$: 3405, 2960, 1732, 1658, 1634, 1292, 1183, 1163, 1077, 1017, 761 $cm^{-1}$; CD $\lambda_{max}$ (*c* 2.19 x $10^{-5}$ MeOH) nm (Δε): 245 (–4.112); $^{1}H$ and $^{13}C$ data see Table 4.

*6'-O-trans-caffeoyl asperuloside* (**9**)

Viscous colorless syrup $[\alpha]^{22}_{D}$ –62.5 (*c* 0.93, MeOH); HR-ESI-MS (positive ion mode): *m/z*: 599.13710$[M+Na]^{+}$ (calcd for $C_{27}H_{28}O_{14}Na$, 599.1371); UV (MeOH) $\lambda_{max}$ nm (log ε) 331 (4.08), 297 (3.97), 241 (4.04), 234 (4.08); IR (film) $\nu_{max}$: 3389, 2950, 1725, 1658, 1604, 1515, 1444, 1261, 1180, 1074, 1023, 809 $cm^{-1}$; CD $\lambda_{max}$ (*c* 1.73 x $10^{-5}$ MeOH) nm (Δε): 241 (–6.025); $^{1}H$ and $^{13}C$ data see Table 4.

*Lasianoside G* (**10**)

Viscous colorless syrup $[\alpha]^{22}_{D}$ –55.0 (*c* 0.10, MeOH); HR-ESI-MS (positive ion mode): *m/z*: 851.2214 $[M+Na]^+$ (calcd for $C_{36}H_{44}O_{22}Na$, 851.2216); UV (MeOH) $\lambda_{max}$ nm (log ε) 236 (4.10); IR (film) $\nu_{max}$: 3309, 2924, 1735, 1650, 1630, 1260, 1161, 1056, 1032, 669 $cm^{-1}$; CD $\lambda_{max}$ (*c* 2.35 x $10^{-5}$ MeOH) nm (Δε): 235 (–8.036); $^1H$ and $^{13}C$ data see Table 5.

*Lasianoside H* (**11**)

Viscous colorless syrup $[\alpha]^{22}_{D}$ –59.9 (*c* 1.38, MeOH); HR-ESI-MS (positive ion mode): *m/z*: 851.2212 $[M+Na]^+$ (calcd for $C_{36}H_{44}O_{22}Na$, 851.2216): UV (MeOH) $\lambda_{max}$ nm (log ε) 235 (4.31); IR (film) $\nu_{max}$: 3388, 2932, 1729, 1658, 1632, 1261, 1158, 1075, 1044, 787 $cm^{-1}$; CD $\lambda_{max}$ (*c* 1.41 x $10^{-5}$ MeOH) nm (Δε): 245 (–5.734); $^1H$ and $^{13}C$ data see Table 6.

*Lasianoside I* (**12**)

Viscous colorless syrup $[\alpha]^{22}_{D}$ –60.1 (*c* 1.38, MeOH); HR-ESI-MS (positive ion mode): *m/z*: 851.2215 $[M+Na]^+$ (calcd for $C_{36}H_{44}O_{22}Na$, 851.2216); UV (MeOH) $\lambda_{max}$ nm (log ε) 234 (4.23); IR (film) $\nu_{max}$: 3406, 2927, 1738, 1658, 1630, 1254, 1175, 1070, 1051, 1017, 757 $cm^{-1}$; CD $\lambda_{max}$ (*c* 1.14 x $10^{-5}$ MeOH) nm (Δε): 245 (–3.477); $^1H$ and $^{13}C$ data see Table 7.

*Tripterygiol 7'-O-β-D-glucopyranoside* (**13**)

White amorphous powder, $[\alpha]^{22}_{D}$ –22.5 (*c* 1.66, MeOH); HR-ESI-MS (positive ion mode): *m/z*: 605.2200 $[M+Na]^+$ (calcd for $C_{28}H_{38}O_{13}Na$: 605.2205); UV (MeOH) $\lambda_{max}$ nm (log ε) 272 (3.49), 236 (4.11); IR (film) $\nu_{max}$: 3390, 2927, 1615, 1518, 1115, 1033 $cm^{-1}$; $^1H$ NMR (500 MHz, $CD_3OD$) and $^{13}C$ data see Table 8.

*Lasianol* (**14**) [12]

Viscous colorless syrup, HR-ESI-MS: *m/z*: 213.0783 $[M–H]^-$ (calcd for $C_{10}H_{13}O_5$ 213.0763); $^1H$ NMR ($CD_3OD$) *δ*: 2.74 (1H, br d, *J* = 18.3 Hz, H-7*α*), 2.86 (H, m, H-4), 2.94 (1H, dd, *J* = 18.3, 6.2 Hz, H-7*β*), 3.69 (1H, m, H-5), 3.88 (1H, dd, *J* = 10.6, 3.7 Hz, $H_1$-3), 3.96 (1H, dd, *J* = 10.6, 4.1 Hz, $H_1$-3), 4.16 (1H, br d, *J* = 14 Hz, $H_1$-10), 4.19 (1H, br d, *J* = 13.3 Hz, $H_1$-1), 4.21 (1H, br d, *J* = 13.3 Hz, $H_1$-1), 4.32 (1H, br d, *J* = 14 Hz, $H_1$-

10), 5.15 (1H, t, $J$ = 6.3 Hz, H-6) and $^{13}$C NMR ($CD_3OD$) $\delta$: 41.8 ($CH_2$-7), 48.7 (CH-4), 53.0 (CH-5), 56.9 ($CH_2$-10), 58.4 ($CH_2$-1), 63.4 ($CH_2$-3), 83.3 (CH-6), 137.3 (CH-9), 138.4 (CH-8), 181.0 (C-11).

*Bis-iridoid glucoside* (**15**) [12]

Viscous colorless syrup, HR-ESI-MS: *m/z*: 851.2216 $[M+Na]^+$ (calcd for $C_{36}H_{44}O_{22}Na$ 851.2216); $^1$H NMR ($CD_3OD$) $\delta$: 2.07 and 2.11 (each 3H, s, 2 x OAc), 2.68 (1H, t, $J$ = 7.7 Hz, H-9$_B$), 3.08 (1H, ddd, $J$ = 8.0, 6.0, 2.0 Hz, H-5$_B$), 3.26 (1H, m, H-9$_A$), 3.24 (2H, m, H-2′$_A$-2′$_B$), 3.30 (1H, m, H-4′$_B$), 3.32 (1H, m, H-5′$_B$), 3.42 (2H, m, H-3′$_A$-4′$_A$), 3.43 (1H, m, H-3′$_B$), 3.63 (1H, m, H-5′$_A$), 3.64 (1H, m, H$_1$-6′$_B$), 3.69 (1H, ddd, $J$ = 8.0, 6.0, 1.4 Hz, H-5$_A$), 3.88 (1H, dd, $J$ = 12.0, 1.4 Hz, H$_1$-6′$_B$), 4.24 (1H, dd, $J$ = 12.0, 6.3 Hz, H$_1$-6′$_A$), 4.65 (1H, dd, $J$ = 12.0, 2.0 Hz, H$_1$-6′$_A$), 4.66 (1H, br d, $J$ = 14.7 Hz, H$_1$-10$_A$), 4.72 (1H, br d, $J$ = 14.7 Hz, H$_1$-10$_A$), 4.75 (1H, d, $J$ = 7.7 Hz, H-1′$_B$), 4.83 (1H, br d, $J$ = 14.0 Hz, H$_1$-10$_B$), 4.88 (1H, dd, $J$ = 6.0, 2.0 Hz, H-6$_B$), 4.94 (1H, br d, $J$ = 14.0 Hz, H$_1$-10$_B$), 5.09 (1H, d, $J$ = 8.0 Hz, H-1$_B$), 5.59 (1H, d, $J$ = 6.0 Hz, H-6$_A$), 5.76 (1H, m, H-7$_A$), 5.85 (1H, s, H-1$_A$), 6.04 (1H, s, H-7$_B$), 7.33 (1H, d, $J$ = 1.0 Hz, H-3$_A$), 7.74 (1H, s, H-3$_B$), and $^{13}$C NMR ($CD_3OD$) $\delta$: 20.8, 20.8 (each $CH_3$, 2 x OAc), 37.4 (CH-5$_A$), 42.8 (CH-5$_B$), 45.2 (CH-9$_A$), 46.3 (CH-9$_B$), 61.9 ($CH_2$-10$_A$), 62.9 ($CH_2$-6′$_B$), 63.8 ($CH_2$-10$_B$), 64.4 ($CH_2$-6′$_A$), 71.5 (CH-4′$_A$), 71.7 (CH-4′$_B$), 74.6 (CH-2′$_A$), 74.9 (CH-2′$_B$), 75.5 (CH-6$_B$), 75.8 (CH-5′$_A$), 77.6 (CH-5′$_B$), 77.8 (CH-3′$_A$), 78.5 (CH-3′$_B$), 86.4 (CH-6$_A$), 93.2 (CH-1$_A$), 99.9 (CH-1′$_A$), 100.5 (CH-1′$_B$), 101.4 (CH-1$_B$), 106.3 (C-4$_A$), 108.1 (C-4$_B$), 129.2 (CH-7$_A$), 131.8 (CH-7$_B$), 144.1 (C-8$_A$), 146.0 (C-8$_B$), 150.2 (CH-3$_A$), 155.8 (CH-3$_B$), 168.6 (C-11$_B$), 172.2 (C-11$_A$), 172.6 (C-OAc$_A$), 172.6 (C-OAc$_B$).

*Asperuloside* (**16**) [20, 21]

Viscous colorless syrup, HR-ESI-MS: *m/z*: 437.1053 $[M+Na]^+$ (calcd for $C_{18}H_{22}O_{11}Na$ 437.1054); $^1$H NMR ($CD_3OD$) $\delta$: 2.07 (3H, s, OAc), 3.18 (1H, dd, $J$ = 9.5, 8.0 Hz, H-2′), 3.26 (1H, m, H-9), 3.34 (1H, m, H-5′), 3.36 (1H, t, $J$ = 9.5 Hz, H-3′), 3.65 (1H, dd, $J$ = 12.0, 6.5 Hz, H$_1$-6′), 3.67 (1H, m, H-5), 3.91 (1H, dd, $J$ = 12.0, 2.0 Hz, H$_1$-6′), 4.62 (1H, br d, $J$ = 14.0 Hz, H$_1$-10), 4.67 (1H, d, $J$ = 8.0 Hz, H-1′), 4.77 (1H, br d, $J$ = 14.0 Hz, H$_1$-10), 5.56 (1H, d, $J$ = 6.3 Hz, H-6), 5.72 (1H, m, H-7), 5.95 (1H, d, $J$ = 1.0 Hz, H-

1), 7.29 (1H, d, *J* = 1.0 Hz, H-3) and $^{13}$C NMR ($CD_3OD$) *δ*: 20.6 ($CH_3$-OAc), 37.4 (CH-5), 45.3 (CH-9), 61.9 ($CH_2$-10), 62.8 ($CH_2$-6′), 71.6 (CH-4′), 74.6 (CH-2′), 77.9 (CH-5′), 78.4 (CH-3′), 86.3 (CH-6), 93.3 (CH-1), 100.0 (CH-1′), 106.2 (C-4), 128.9 (CH-7), 144.3 (C-8), 150.3 (CH-3), 172.3 (C-11), 172.6 (C-OAc).

*Deacetyl asperuloside* (**17**) [33]

Viscous colorless syrup, HR-ESI-MS: *m/z*: 607.2360 $[M+Na]^+$ (calcd for $C_{28}H_{40}O_{13}Na$ 607.2360); $^1$H NMR ($CD_3OD$) *δ*: 3.21 (1H, dd, *J* = 9.0, 8.0 Hz, H-2′), 3.24 (1H, t, *J* = 9.0 Hz, H-4′), 3.29 (1H, m, H-9), 3.37 (1H, td, *J* = 9.0, 1.4 Hz, H-5′), 3.41 (1H, t, *J* = 9.0 Hz, H-3′), 3.69 (1H, m, $H_1$-6′), 3.69 (1H, m, H-5), 3.94 (1H, dd, *J* = 12.0, 1.4 Hz, $H_1$-6′), 4.19 (1H, br d, *J* = 14.0 Hz, $H_1$-10), 4.23 (1H, br d, *J* = 14.0 Hz, $H_1$-10), 4.70 (1H, d, *J* = 7.7 Hz, H-1′), 5.59 (1H, d, *J* = 6.3 Hz, H-6), 5.66 (1H, m, H-7), 5.97 (1H, s, H-1), 7.31 (1H, d, *J* = 1.0 Hz, H-3) and $^{13}$C NMR ($CD_3OD$) *δ*: 37.5 (CH-5), 45.0 (CH-9), 60.1 ($CH_2$-10), 62.8 ($CH_2$-6′), 71.6 (CH-4′), 74.6 (CH-2′), 77.9 (CH-5′), 78.4 (CH-3′), 86.7 (CH-6), 93.3 (CH-1), 99.3 (CH-1′), 106.5 (C-4), 125.7 (CH-7), 149.8 (C-8), 150.3 (CH-3), 172.9 (C-11).

*Besperuloside* (**18**) [34]

Viscous colorless syrup, $^1$H NMR ($CD_3OD$) *δ*: 3.21 (1H, dd, *J* = 9.0, 8.0 Hz, H-2′), 3.31 (1H, t, *J* = 9.0 Hz, H-4′), 3.37 (1H, td, *J* = 6.2, 2.0 Hz, H-5′), 3.39 (1H, t, *J* = 9.0 Hz, H-3′), 3.40 (1H, t, *J* = 9.0 Hz, H-9), 3.66 (1H, dd, *J* = 12.0, 6.2 Hz, $H_1$-6′), 3.74 (1H, ddd, *J* = 6.5, 6.5, 2.0 Hz, H-5), 3.84 (1H, dd, *J* = 12.0, 2.0 Hz, $H_1$-6′), 4.70 (1H, d, *J* =8.0 Hz, H-1′), 4.94 (1H, dd, *J* = 14.0, 1.0 Hz, $H_1$-10), 5.07 (1H, dd, *J* = 14.0, 1.0 Hz, $H_1$-10), 5.62 (1H, dt, *J* = 6.5, 2.0 Hz, H-6), 5.86 (1H, d, *J* = 2.0 Hz, H-7), 6.09 (1H, d, *J* = 1.0 Hz, H-1), 7.34 (1H, d, *J* = 2.0 Hz, H-3), 7.51 (2H, t, *J* = 8.0Hz, H-3″, 5″), 7.64 (1H, tt, *J* = 8.0, 1.0 Hz, H-4″), 8.07 (2H, dd, *J* = 8.0, 1.0 Hz, H-2″, 6″) and $^{13}$C NMR ($CD_3OD$) *δ*: 37.4 (CH-5), 45.0 (CH-9), 62.6 ($CH_2$-10), 62.7 ($CH_2$-6′), 71.5 (CH-4′), 74.6 (CH-2′), 77.9 (CH-5′), 78.4 (CH-3′), 86.3 (CH-6), 93.4 (CH-1), 100.0 (CH-1′), 106.2 (C-4), 129.4 (CH-7), 129.7 (CH-3″, 5″), 130.7 (CH-2″, 6″), 130.9 (C-1″), 134.6 (CH-4″), 144.3 (C-8), 150.3 (CH-3), 165.9 (C-7″), 172.9 (C-11).

*Deacetyl daphylloside* (**19**) [21]

Viscous colorless syrup, HR-ESI-MS: *m/z*: 427.1209 $[M+Na]^+$ (calcd for $C_{17}H_{24}O_{11}Na$ 427.1211); $^1H$ NMR ($CD_3OD$) $\delta$: 2.56 (1H, t, , $J$ = 8.0 Hz, H-9), 3.02 (1H, ddd, , $J$ = 8.0, 6.5, 1.5 Hz, H-5), 3.23 (1H, m, H-2′), 3.26 (1H, m, H-4′), 3.26 (1H, m, 5′), 3.37 (1H, t, $J$ = 8.5 Hz, H-3′), 3.60 (1H, dd, $J$ = 11.5, 6.0 Hz, $H_1$-6′), 3.74 (3H, s, H-12), 3.85 (1H, dd, $J$ = 11.5, 2.0 Hz, $H_1$-6′), 4.20 (1H, dd, $J$ = 15.0, 1.5 Hz, $H_1$-10), 4.45 (1H, dd, $J$ = 15.0, 1.5 Hz, $H_1$-10), 4.71 (1H, d, $J$ = 8.0 Hz, H-1′), 4.79 (1H, m, H-6), 5.06 (1H, d, $J$ = 8.5 Hz, H-1), 6.01 (1H, d, $J$ = 1.0 Hz, H-7), 7.66 (1H, d, $J$ = 1.0 Hz, H-3) and $^{13}C$ NMR ($CD_3OD$) $\delta$: 42.7 (CH-5), 45.8 (CH-9), 51.9 ($CH_3$-12), 61.7 ($CH_2$-10), 62.8 ($CH_2$-6′), 71.7 (CH-4′), 75.0 (CH-2′), 75.4 (CH-6), 77.8 (CH-5′), 78.6 (CH-3′), 100.5 (CH-1′), 101.5 (CH-1), 108.3 (C-4), 129.8 (CH-7), 151.6 (C-8), 155.4 (CH-3), 169.5 (C-11).

*Daphylloside* (**20**) [21]

Viscous colorless syrup, HR-ESI-MS: *m/z*: 469.1316 $[M+Na]^+$ (calcd for $C_{19}H_{26}O_{12}Na$ 469.1316); $^1H$ NMR ($CD_3OD$) $\delta$: 2.08 (3H, s, OAc), 2.53 (1H, t, , $J$ = 8.0 Hz, H-9), 3.02 (1H, ddd, , $J$ = 8.0, 6.0, 1.5 Hz, H-5), 3.23 (1H, m, H-2′), 3.24 (1H, m, H-4′), 3.24 (1H, m, 5′), 3.37 (1H, t, $J$ = 9.0 Hz, H-3′), 3.60 (1H, dd, $J$ = 11.5, 6.0 Hz, $H_1$-6′), 3.73 (3H, s, H-12), 3.84 (1H, dd, $J$ = 11.5, 1.5 Hz, $H_1$-6′), 4.71 (1H, d, $J$ = 8.0 Hz, H-1′), 4.80 (1H, m, $H_1$-10), 4.80 (1H, m, H-6), 4.93 (1H, br d, $J$ = 15.0 Hz, $H_1$-10), 5.05 (1H, d, $J$ = 8.5 Hz, H-1), 6.01 (1H, d, $J$ = 1.5 Hz, H-7), 7.65 (1H, d, $J$ = 1.5 Hz, H-3) and $^{13}C$ NMR ($CD_3OD$) $\delta$: 20.8 ($CH_3$-OAc), 42.4 (CH-5), 46.3 (CH-9), 51.9 ($CH_3$-12), 62.0 ($CH_2$-6′), 63.8 ($CH_2$-10), 71.6 (CH-4′), 74.9 (CH-2′), 75.4 (CH-6), 77.9 (CH-5′), 78.6 (CH-3′), 100.6 (CH-1′), 101.3 (CH-1), 108.1 (C-4), 131.9 (CH-7), 146.0 (C-8), 155.4 (CH-3), 169.4 (C-11), 172.6 (C-OAc).

*Grasshopper ketone* (**21**) [35]

White amorphous powder, HR-ESI-MS: *m/z*: 247.1305 $[M+Na]^+$ (calcd for $C_{13}H_{20}O_3$ Na 247.1305); $^1H$ NMR ($CD_3OD$) $\delta$: 1.17 (3H, s, H-12), 1.40 (3H, s, H-11), 1.40 (3H, s, H-13), 2.21 (3H, s, H-10), 1.38 and 1.96 (each 1H, m, $H_2$-4), 1.41 and 2.21 (each 1H, m, $H_2$-2), 4.25 (1H, m, H-3), 5.85 (1H, s, H-8), and $^{13}C$ NMR ($CD_3OD$) $\delta$: 26.5 ($CH_3$-10), 29.3 ($CH_3$-11), 30.8 ($CH_3$-13), 32.3 ($CH_3$-12), 37.0 (C-1), 49.7 ($CH_2$-4), 49.9 ($CH_2$-2), 64.6 (CH-3), 72.4 (C-5), 101.1 (CH-8), 119.9 (C-6), 200.9 (C-7), 211.6 (C-9).

*Lauroside A* (**22**) [36, 37]

Viscous colorless syrup, HR-ESI-MS: *m/z*: 411.1993 $[M+Na]^+$ (calcd for $C_{19}H_{32}O_8Na$ 411.1989); $^1H$ NMR ($CD_3OD$) $\delta$: 0.89 (3H, s, H-12), 0.95 (3H, s H-11), 0.96 (3H, s H-13),1.30 (3H, d, $J$ = 6.5 Hz, H-10), 1.81 (1H, br d, $J$ = 14.0 Hz, H-$2_{eq}$), 2.12 (1H, dd, $J$ = 13.5, 3.0 Hz, H-$4_{eq}$), 2.30 (1H, m, H-5), 2.45 (1H, br d, $J$ = 13.5 Hz, H-$4_{ax}$), 2.86 (1H, br d, $J$ = 14.0 Hz, H-$2_{ax}$), 3.18 (1H, m, H-5′), 3.21 (1H, m, H-2′), 3.26 (1H, m, H-3′), 3.30 (1H, m, H-4′), 3.63 (1H, dd, $J$ = 11.5, 5.5 Hz, $H_1$-6′), 3.85 (1H, dd, $J$ = 11.5, 1.5 Hz, $H_1$-6′), 4.34 (1H, d, $J$ = 8.0 Hz, H-1′), 4.53 (1H, quint, H-9), 5.67 (1H, dd, $J$ = 15.5, 8.0 Hz, H-8), 5.80 (1H, br d, $J$ = 15.5 Hz, H-7), and $^{13}C$ NMR ($CD_3OD$) $\delta$: 16.7 ($CH_3$-13), 22.3 ($CH_3$-10), 24.9 ($CH_3$-12), 24.9 ($CH_3$-11), 37.9 (CH-5), 43.6 (C-1), 46.0 ($CH_2$-4), 52.0 ($CH_2$-2), 62.6 ($CH_2$-6′), 71.6 (CH-4′), 74.8 (CH-2′), 74.9 (CH-9), 77.9 (CH-5′), 78.1 (C-6),78.2 (CH-3′), 100.5 (CH-1′), 133.6 (CH-8), 136.8 (CH-7), 214.8 (CH-3).

*Secoisolariciresinol diglucoside* (**23**) [38]

White amorphous powder, HR-ESI-MS: *m/z*: 685.1012 $[M-H]^-$ (calcd for $C_{32}H_{46}O_{15}$ 685.1011); $^1H$ NMR ($CD_3OD$) $\delta$: 2.02 and 2.12 (each 2 H, m, $H_2$-8, 8′), 2.63 (2H, m, $H_1$-7, 7′), 2.72 (2H, dd, $J$ = 14.0, 7.7 Hz, $H_1$-7, 7′), 3.22 (2H, dd, $J$ = 8.4, 8.4 Hz, H-2″, 2‴), 3.24 (2H, m, H-5″, 5‴), 3.30 (2H, m, H-4″, 4‴), 3.37 (2H, t, $J$ = 8.4 Hz, H-3″, 3‴), 3.57 (2H, dd, $J$ = 10.3, 5.5 Hz, $H_1$-9, 9′), 3.68 (2H, m, $H_1$-6″, 6‴), 3.77 (6H, s, 2 x $OCH_3$), 3.89 (2H, d, $J$ = 12.0 Hz, $H_1$-6″, 6‴), 3.91 (2H, dd, $J$ = 10.3, 6.3 Hz, $H_1$-9, 9′), 4.21 (2H, d, $J$ = 7.7 Hz, H-1″, 1‴), 6.65 (2H, d, $J$ = 2.0 Hz, H-2, 2′), 6.65 (2H, d, $J$ = 8.1 Hz, H-5, 5′), 6.68 (2H, dd, $J$ = 8.1, 2.0 Hz, H-6, 6′), and $^{13}C$ NMR ($CD_3OD$) $\delta$: 35.5 ($CH_2$-7, 7′), 41.6 (CH-8), 44.0 (CH-8′), 56.2 (2 x $OCH_3$), 62.7 ($CH_2$-6″), 62.8 ($CH_2$-6‴), 70.4 (CH-4″, 4‴), 71.7 ($CH_2$-9, 9′), 75.2 (CH-2″, 2‴), 78.0 (CH-5″, 5‴), 78.2 (CH-3″, 3‴), 104.6 (CH-1″, 1‴), 113.3 (CH-2), 113.5 (CH-2′), 115.0 (CH-5, 5′), 122.7 (CH-6), 122.8 (CH-6′), 134.0 (C-1, 1′), 145.4 (CH-4, 4′), 148.8 (CH-3, 3′).

*8,8′-Bisdihydrosiringenin glucoside* (**24**) [39]

Viscous colorless syrup, HR-ESI-MS: *m/z*: 607.2360 $[M+Na]^+$ (calcd for $C_{28}H_{40}O_{13}Na$ 607.2360); $^1H$ NMR ($CD_3OD$) $\delta$: 1.93 (1H, m, H-8′), 1.99 (1H, m, H-8), 2.61 (1H, m, H-7), 2.73 (1H, m, H-7), 3.22 (1H, m, H-2″), 3.43 (1H, m, H-4″), 3.44 (1H, m, H-3″), 3.49 (1H, m, H-5″), 3.60 (1H, m, $H_1$-6″), 3.60 (1H, m, $H_1$-9), 3.66 (1H, m, $H_1$-6″), 3.68 (1H, m, $H_1$-9′), 3.70 (1H, m, $H_1$-9), 3.70 (1H, m, $H_1$-9′), 4.80 (1H, d, $J$ = 7.5 Hz, H-1′), 6.40 (2H, m, H-2′, 6′), 6.43 (2H, m, H-2, 6), and $^{13}C$ NMR ($CD_3OD$) $\delta$: 36.4 ($CH_2$-7′), 36.7 ($CH_2$-7), 43.6 (CH-8′), 44.3 (CH-8), 56.6 and 56.8 (2 x $OCH_3$), 61.9 ($CH_2$-9′), 62.1 ($CH_2$-9), 62.5 ($CH_2$-6″), 71.2 (CH-4″), 75.7 (CH-2″), 77.7 (CH-3″), 78.3 (H-5″), 105.7 (CH-1″), 107.2 (CH-2′, 6′), 133.0 (C-4′), 134.3 (C-4), 139.4 (C-1, 1′), 149.0 (CH-3′, 5′), 152.4 (CH-3, 5).

*Huazhongilexin* (**25**) [40]

Viscous colorless syrup, HR-ESI-MS: *m/z*: 459.1624 $[M+Na]^+$ (calcd for $C_{22}H_{28}O_9$ Na 459.1626); $^1H$ NMR ($CD_3OD$) $\delta$: 2.31 (2H, m, H-8, 8′), 3.62 (2H, dd, $J$ = 11.5, 5.0 Hz, $H_1$-9, 9′), 3.70 (2H, dd, $J$ = 11.5, 3.5 Hz, $H_1$-9, 9′), 3.71 (12H, 4 x $OCH_3$), 5.00 (2H, d, $J$ = 8.5 Hz, H-7, 7′), 6.73 (4H, s, H-2, 2′, 6, 6′), and $^{13}C$ NMR ($CD_3OD$) $\delta$: 55.1 (CH-8, 8′), 56.8 (4 x $OCH_3$), 61.6 (CH-9, 9′), 84.6 (CH-7, 7′), 104.8 (CH-2, 2′, 6, 6′), 132.8 (C-4, 4′), 147.9 (C-3, 3′, 5, 5′).

### 1.5.4. Acid hydrolysis

Each glucoside (**3** – **13**) was hydrolyzed by heating in 1 M HCl (1.0 mL) at 80 ºC for 3hr. The solution was neutralized with Amberlite IRA96SB ($OH^-$ form) and filtered. The filtrates were partitioned with equal volume of EtOAc. The aqueous layer for a solution was directly analyzed by HPLC with an amino column [Asahipak $NH_2$P-50 4E, $CH_3CN$-$H_2O$ (3:1), 1mL/min] and a chiral detector (JASCO OR-2090plus) in comparison with (D-glucose) as authentic. The peaks were appeared at $t_R$ 8.1 min coincided with that of D-glucose [41].

### 1.5.5. Alkaline hydrolysis

A solution of 3.0 mg of each compound (**5 – 7**, **9**) in 50% aqueous 1,4-dioxane (0.5 mL) was treated with 10% aqueous KOH (0.5 mL) and stirred at 37 ºC for 3 h. The reaction mixture was neutralized with an ion-exchange resin (Amberlite IR-120B) ($H^+$-form), then filtrated. After that, it was evaporated *in vacuo* and dissolved in EtOAc, then it was subjected to HPLC analysis [Cosmosil C18-PAQ, MeOH-$H_2O$ (45:50) with 0.1%TFA, 1mL/min)] with UV (245 nm) detector to identify the caffeic acid ($t_R$ 11.4 min) [42].

1.5.6. DPPH radical scavenging activity

The reagents, 2,2-diphenyl-1-picrylhydrazyl (DPPH) and (*S*)-(–)-6-hydroxy-2,5,7,8-tetramethylchroman-2-carboxylic acid (Trolox) from Aldrich Chemical Co. were used to test anti-radical activities (DPPH) of isolated compounds. The tested compounds were added in 96-well microtiter plate with 100 $\mu$L of MeOH, their absorbances were measured at 515nm as $A_{blank}$. Then, a 100 $\mu$L of DPPH solution (200 $\mu$M) was added to each well, followed by incubation in dark chamber at room temperature for 30 min before measurement of the absorbance ($A_{sample}$) again.

The % inhibition was calculated using the following equation of free radicals:

$$\% \text{ Inhibition} = [1 - (A_{sample} - A_{blank})/ (A_{control} - A_{blank})] \times 100$$

where $A_{control}$ is the absorbance of DMSO with all reagents. Trolox was used as positive control. All the tests were performed in triplicate and $IC_{50}$ values were determined by linear regression [43].

# CHAPTER 2

## *Cadaba rotundifolia*

## (Saudi plant)

## 2.1. Introduction

*Cadaba rotundifolia* Forssk. (Fig. 36) is an erect shrub, drooping much branches with young twinges covered with short glandular hair. It's distribution was recorded from Kenya, Ethiopia, Djibouti, Somalia Northwards to Sudan; Eastwards to Saudi Arabia, Yemen and Oman [44]. In Saudi Arabia, *C. rotundifolia* is distributed in southern west region [45]. It can reach 100-400 cm in height and their old stem are suberulous with glandular hairs. The leaves are simple, elliptic, ovate, orbicular, leathery, 25-45 x 22-38 mm with cuneate base and bluish green color. Their flower 20-22 mm, zygomorphic, bracteate and have inflorescence terminal raceme, pedicel 10-16 mm. The fruits are fleshy berry, cylindrical, 25-50 x 2-8 mm. The seeds are reniform, embedded in scarlet pulp [44]. It is belonging to Capparaceae and it has local name as (Qadab). Traditionally it used for abscesses and tumors in Sudan [46].

**Figure 36.** *Cadaba rotundifolia*

Previous phytochemical investigations of different *Cadaba* species led to isolation of a variety of secondary metabolites. The spermidine alkaloid cadabicine, terpenes, 12-aminododecanoic acid, stachydrine and its 3-hydroxylated derivative together with two

flavonol glycosides were isolated from *C. farinose* [47, 48]. The aerial parts of *C. glandulosa* gave flavonoids with anti-inflammatory activity [49], while the roots of *C. trifoliata* proved to be a rich source of tannins, steroids, alkaloids, and phenolic compounds [50].

Previous chemical study of the ethanolic extract of *C. rotundifolia* root yielded a quaternary alkaloid (3-hydroxystachydrine) [46]. According to [51], *C. rotundifolia* organic solvent extracts showed selective antibacterial activity at the level of organic solvent extract and bacterial strains. The study tested different organic solvent extract of *C. rotundifolia* against three Gram-positive and four Gram-negative bacteria, using Ciprofloxacin as reference control. The highest inhibitory effects obtained against *B. cereus*, *E. coli* and *P. aeruginosa* regardless the kind of organic solvent. Petroleum ether extract exhibited the highest inhibitory effect on the growth of all tested bacteria in comparison with the rest of organic solvent, while the lowest inhibitory effect exhibited by aqueous extract.

No reports on the constituents of *C. rotundifolia* grown in Saudi Arabia has been issued so far, so a comprehensive study of the plant constituents was undertaken. This study reports isolation of four new acylated kaempferol glycosides derivatives (**26, 28, 32** and **33**), together with **16** known compounds (**34** – **45**) by various chromatographic techniques. The structures of isolated compounds were characterized by physical and spectroscopic data analyses including 1D and 2D NMR, IR, UV, HR-ESI-MS. In addition, all the obtained compounds were evaluated for their free radical scavenging properties by DPPH radical scavenging assay as well as AGEs formation and collagenase assay.

## 2.2. Extraction and Isolation of Chemical Constituents

The air-dried powdered aerial parts (6.0 Kg) of *C. rotundifolia* Forssk. were extracted with methanol (10 L x 7) till exhaustion and then concentrated under reduced pressure to give a viscous gummy material (800 g). This residue was suspended in 900 mL of distilled water and fractionated by shaking with petroleum ether (bp. 60-80 ºC)(3 L x 5, 132.9 g), $CH_2Cl_2$ (3 L x 5, 6 g), EtOAc (3 L x 5, 10.9 g) and 1-BuOH (3 L x 5, 118 g), respectively.

Part of 1-BuOH fraction (112 g) was fractionated on Diaion HP-20 column chromatography (Φ = 6 cm, *L* = 35 cm, 900 g), The column was eluted initially with $H_2O$, then with MeOH / $H_2O$ stepwise gradient with increasing MeOH content using (20, 40, 60, 80, 100% MeOH, respectively, 3 L each), yielding five fractions (Frs. Cr1 – Cr5).

The fraction Cr2 (10.7 g) was proceeded on silica gel column chromatography (Φ = 3 cm, *L* = 15 cm, 100 g) with increasing amount of methanol in chloroform (20:1, 10:1, 7:1, 5:1, 3:1, 1:1, finally with 100% MeOH, 500 ml each) yielding seven fractions (Frs. Cr2.1 – Cr2.7).

The fraction Cr2.4 (3.5 g) was subjected to open reversed phase (ODS) column chromatography in 10% aq. methanol (400 mL) – 100% methanol (400 mL), linear gradient, lead 8 fractions (Frs. Cr2.4.1 –Cr2.4.8). The residue of fraction Cr2.4.4 (187 mg) was purified by preparative HPLC, 46% aq. acetone to give **43** (myricetin, 5.0 mg) and **45** (phloretin, 25.1 mg).

The fraction Cr2.5 (2.4 g) was subjected to open reversed phase (ODS) column chromatography in 10% aq. methanol (400 mL) – 100% methanol (400 mL), linear gradient, lead seven fractions (Frs. Cr2.5.1 –Cr2.5.7). The residue of fraction Cr2.5.4 (554 mg) was purified by preparative HPLC, 25% aq. acetone to give **34** (kaempferol 3,4′-di-*O*-*β*-D-glucoside, 4.2 mg).

The fraction Cr2.7 (2.6 g) was subjected to open reversed phase (ODS) column chromatography in 10% aq. methanol (400 mL) – 100% methanol (400 mL), linear gradient, lead six fractions (Frs. Cr2.7.1 –Cr2.7.6). The residue of fraction Cr2.7.2 (632 mg) was purified by preparative HPLC, 25% aq. acetone to give **40** (myricetin 3-*O*-[2,6-di-*O*-L-rhamnopyranosyl]-*β*-glucoside, 5.6 mg) and **41** (myricetin 3-*O*-*β*-neohesperidoside, 11.0 mg).

Then residue of fraction Cr2.7.3 (1.2 g) also was purified by preparative HPLC, 28% aq. acetone to give **35** (kaempferol 3-*O*-[2,6-di-*O*-L-rhamnopyranosyl]-*β*-D-glucoside, 17.3 mg) and **44** (beitingxinhuagtong, 9.2 mg).

Other fraction Cr3 (15.5 g) was proceeded on silica gel column chromatography (Φ = 3 cm, *L* = 20 cm, 150 g) with increasing amount of methanol in chloroform (20:1, 10:1, 7:1, 5:1, 3:1, 1:1, then 100% MeOH, 400 mL each), yielding seven fractions (Frs. Cr3.1 – Cr3.7). The fraction Cr3.3 (2.9 g) was subjected to open reversed phase (ODS) column chromatography in 10% aq. methanol (400 mL) – 100% methanol (400 mL), linear gradient, lead nine fractions (Frs. Cr3.3.1 –Cr3.3.9). The residue of fraction Cr3.3.4 (645 mg) was purified by preparative HPLC, 28% aq. acetone to give **38** (kaempferol 3-*O*-*β*-D-glucoside, 30.1 mg).

The fraction Cr3.4 (2.8 g) was subjected to open reversed phase (ODS) column chromatography in 10% aq. methanol (400 mL) – 100% methanol (400 mL), linear gradient, lead seven fractions (Frs. Cr3.4.1 –Cr3.4.7). The residue of fraction Cr3.4.2 (1.2 g) was purified by preparative HPLC, 28% aq. acetone to give **42** (myricetin 3-*O*-*β*-D-glucoside, 15.2 mg). The residue of fraction Cr3.4.4 (187 mg) also was purified by preparative HPLC, 40% aq. acetone to give **26** (kaempferol 3-*O*-[2-*O*-(*trans*-feruloyl)-3-*O*-*β*-D-glucopyranosyl]-*β*-D-glucopyranoside, 7.4 mg) and **30** (kaempferol 3-*O*-[2-*O*-(*trans*-*p*-coumaroyl)-3-*O*-*β*-D-glucopyranosyl]-*β*-D-glucopyranoside, 2.0 mg).

The fraction Cr3.5 (4.4 g) was subjected to open reversed phase (ODS) column chromatography in 10% aq. methanol (400 mL) – 100% methanol (400 mL), linear gradient, lead seven fractions (Frs. Cr3.5.1 –Cr3.5.7). The residue of fraction Cr3.5.4 (692 mg) was purified by preparative HPLC, 28% aq. acetone to give **36** (kaempferol 3-*O*-*β*-neohesperidoside, 39.0 mg) and **37** (kaempferol 3-*O*-*β*-rutinoside, 20.0 mg). The other residue of fraction Cr3.5.5 (65.7 mg) was purified by preparative HPLC, 32% aq. acetone to give **39** (rhamnocitrin 3-*O*-*β*-neohesperidoside, 3.0 mg).

The fraction Cr3.6 (760 mg) was subjected to open reversed phase (ODS) column chromatography in 10% aq. methanol (200 mL) – 100% methanol (200 mL), linear gradient, lead seven fractions (Frs. Cr3.6.1 –Cr3.6.7). The residue of fraction Cr3.6.4 (923 mg) was purified by preparative HPLC, 25% aq. acetone. The following compounds were separated, **27** (kaempferol 3-*O*-*β*-neohesperidoside-7-*O*-[2-*O*-(*cis*-*p*-coumaroyl)-3-*O*-*β*-D-glucopyranosyl]-

β-D-glucopyranoside, 5.0 mg), **31** (kaempferol 3-*O*-*β*-neohesperidoside-7-*O*-[2-*O*-(trans-*p*-coumaroyl)-3-*O*-*β*-D-glucopyranosyl]-*β*-D-glucopyran-oside, 12.0 mg), **32** (kaempferol 3-*O*-*β*-neohesperidoside-7-*O*-[2-*O*-(*trans*-feruloyl)]-*β*-D-glucopyranoside, 2.0 mg) and **33** (kaempferol 3-*O*-*β*-neohesperidoside-7-*O*-[2-*O*-(*trans*-*p*-coumaroyl)]-*β*-D-glucopyranoside, 10.0 mg). The other residue of fraction Cr3.6.5 (963 mg) was purified by preparative HPLC, 35% aq. acetone, to give **28** (kaempferol 3-*O*-[2,6-di-*O*-L-rhamnopyranosyl]-*β*-D-glucopyranoside-7-*O*-[6-*O*-(*trans*-feruloyl)]-*β*-D-glucopyranoside, 7.8 mg) and **29** (kaempferol 3-*O*-[2,6-di-*O*-L-rhamnopyranosyl]-*β*-D-glucopyranoside-7-*O*-[6-*O*-(*trans*-*p*-coumaroyl)]-*β*-D-glucopyranoside, 2.0 mg). The isolation procedures are presented in (Chart. 3).

**CHART 3.** Extraction and isolation

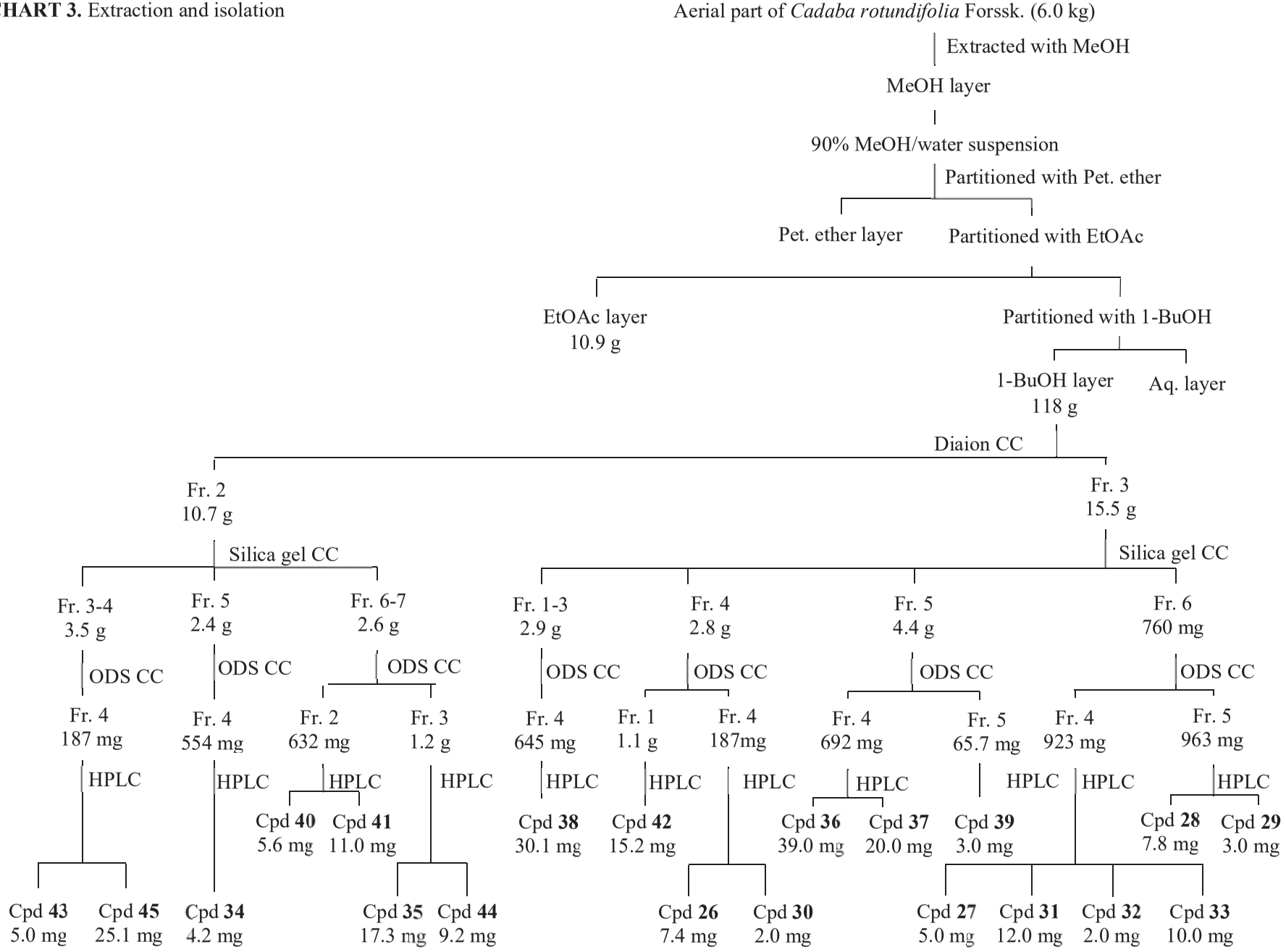

## 2.3. Structural Elucidations of Chemical Constituents

The 1-BuOH fraction of aerial part of *Cadaba rotundifolia* was subjected to fractionation by Diaion HP-20 and silica gel columns, respectively. The resulting fractions were separated on octadecylsilane (ODS) column chromatography, then purified by preparative high-performance liquid chromatography (HPLC) to obtain **20** compounds (Fig. 36).

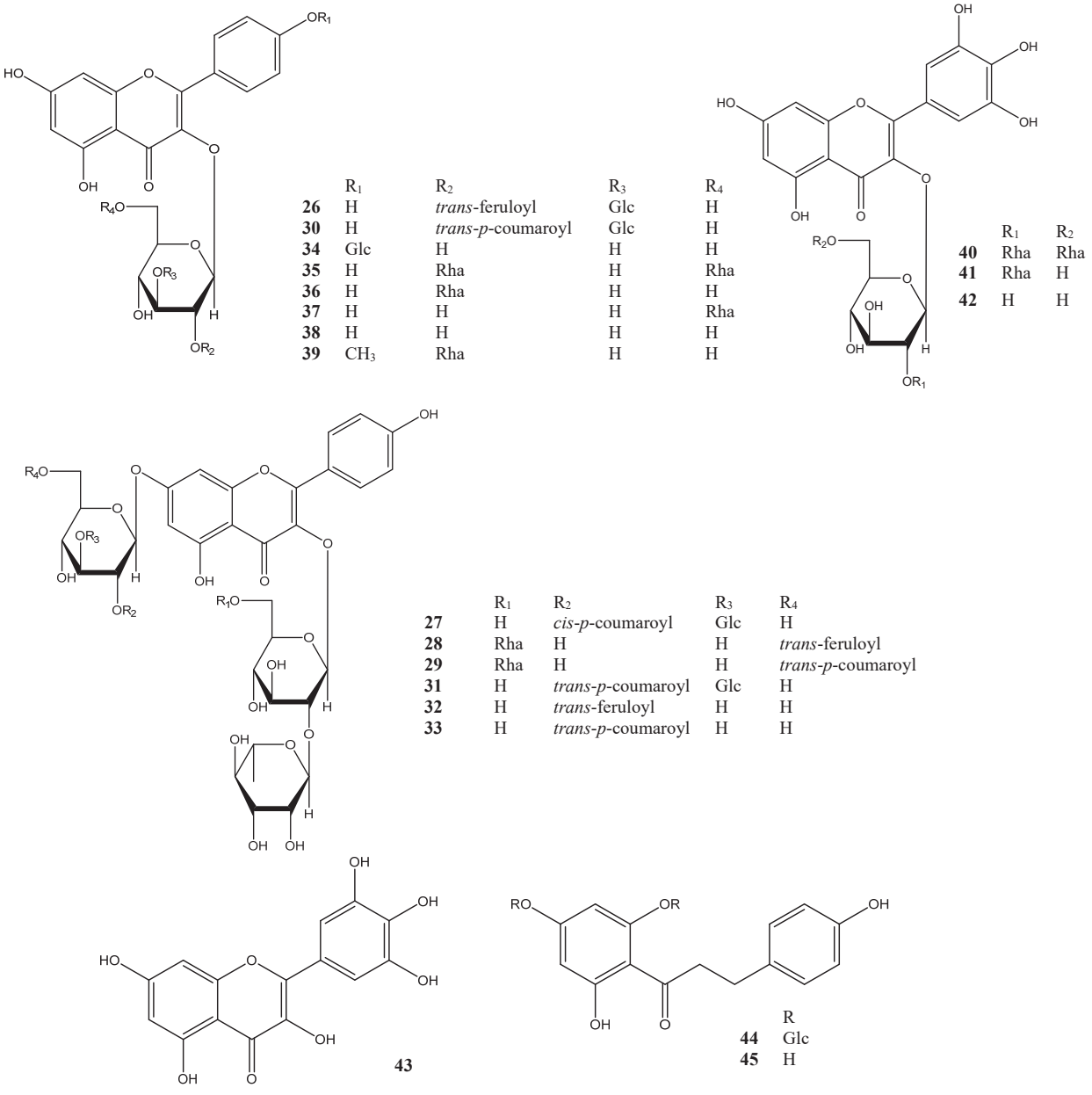


**Figure 36.** Isolated compounds from *Cadaba rotundifolia* (**26-45**)

The NMR spectroscopic analysis of isolated compounds revealed structural similarities and indicated the presence of flavonoids, especially flavonol skeleton and their glycosides and acylated glycosides derivatives [kaempferol skeleton (**26** – **38**), rhamnetin skeleton (**39**), myricetin skeleton (**40** – **43**)] together with dihydrochalcone skeleton compound and its glycoside derivative (**44** and **45**). The known compounds were identified as kaempferol 3-*O*-[2-*O*-(*trans-p*-coumaroyl)-3-*O*-*β*-D-glucopyranosyl]-*β*-D-glucopyranoside (**30**), kaempferol 3-*O*-*β*-neohesperidoside-7-*O*-[2-*O*-(*trans-p*-coumaroyl)-3-*O*-*β*-D-glucopyranosyl]-*β*-D-glucopyranoside (**31**), kaempferol 3-*O*-*β*-neohesperidoside-7-*O*-[2-*O*-(*trans*-feruloyl)]-*β*-D-glucopyranoside (**32**), kaempferol 3-*O*-*β*-neohesperidoside-7-*O*-[2-*O*-(*trans-p*-coumaroyl)]-*β*-D-glucopyranoside (**33**), kaempferol 3,4′-di-*O*-*β*-D-glucoside (**34**), kaempferol 3-*O*-[2,6-di-*O*-L-rhamnopyranosyl]-*β*-D-glucoside (**35**), kaempferol 3-*O*-*β*-neohesperidoside (**36**), kaempferol 3-*O*-*β*-rutinoside (**37**), kaempferol 3-*O*-*β*-D-glucoside (**38**), rhamnocitrin 3-*O*-*β*-neohesperidoside (**39**), myricetin 3-*O*-[2,6-di-*O*-L-rhamnopyranosyl]-*β*-D-glucoside (**40**), myricetin 3-*O*-*β*-neohesperidoside (**41**), myricetin 3-*O*-*β*-D-glucoside (**42**), myricetin (**43**), beitingxinhuagtong C (**44**), phloretin (**45**).

Compound (**26**) was isolated as a yellow amorphous powder, soluble in methanol with a negative optical rotation ($[\alpha]^{22}{}_{D}$ –79.0). Its molecular formula, $C_{37}H_{38}O_{19}$, was determined from the positive HR-ESI-MS analysis (*m/z* 809.1888 $[M + Na]^+$,calcd for $C_{37}H_{38}O_{19}Na$ 809.1899). It had UV spectrum typical of acylated kaempferol glycoside ($\lambda_{max}$ 327, 267 nm) [52, 53]. The IR spectrum suggested the presence of hydroxy (3388 $cm^{-1}$), *α*,*β*-unsaturated carbonyl ester (1710 $cm^{-1}$), *α*,*β*-unsaturated ketone (1658 $cm^{-1}$), aromatic ring (1513, 1446 $cm^{-1}$) and ether (1176, 1070 $cm^{-1}$) functions. The protons and carbons resonances in $^1H$ and $^{13}C$ NMR spectra were clarified the aromatic and glycosidic nature of **26**. It was found that the $^1H$ NMR spectrum of **26** displayed features resembling to those of **30** [54], they were almost identical in both aglycon and glycosides units. The major differences were in the signals relative to the acyl moiety. The $^1H$ NMR spectrum of **26** (Table. 10) exhibited *meta*-coupled resonances at $\delta_H$ 6.17 and 6.37 (each 1H, d, $J$ = 2.0 Hz), were characteristic to H-6 and H-8 of the A-ring, respectively. The $^1H$–$^1H$ correlation spectroscopy (COSY) (Fig. 37) and $^1H$ NMR spectra of **26** displayed two *ortho*-coupled doublet resonances at

$\delta_H$ 8.01 and 6.91 (each 2H, d, $J$ = 8.8 Hz) assignable to H-2′/6′ and H-3′/5′ of the B-ring, respectively, which indicated the presence of kaempferol aglycone (Fig. 37).

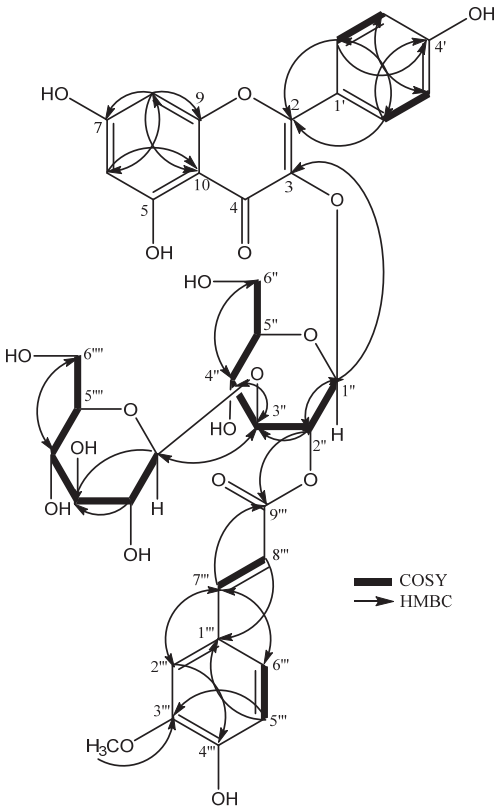


**Figure 37.** HMBC and COSY correlations of **26**

The $^1$H NMR spectrum of **26** (Table. 10) also gave signals attributed to an ABX coupling system for 1, 3, 4-trisubstituted aromatic moiety at $\delta_H$ 6.83 (1H, d, $J$ = 8.2 Hz), 7.09 (1H, d, $J$ = 8.2, 1.8 Hz) and 7.20 (1H, d, $J$ = 1.8 Hz), and two coupled *trans* olefinic protons at $\delta_H$ 6.40 (1H, br d, $J$ = 15.9 Hz) and 7.68 (1H, br d, $J$ = 15.9 Hz), together with singlet signal for a methoxy group at $\delta_H$ 3.92 suggested the presence of cinnamic acid derivative. The two anomeric proton resonances, which occur at $\delta_H$ 5.73 (1H, d, $J$ = 8.0 Hz) and 4.43 (1H, d, $J$ = 7.8 Hz) correspond to two glucose moieties. The $\beta$-anomeric configuration for the sugars were determine from their magnitudes of $J_{1,2}$ coupling constants. In addition, Acid hydrolysis of **26** released D-glucose (Fig. 38). The $^{13}$C NMR spectrum (Table. 10) of **26** showed 37 carbon resonances, 12 signals were assigned to two $\beta$-glucose units, 15 signals were consisted with kaempferol aglycone and the remaining 10 signals were ascribed to ferulic acid or isoferulic acid.

**Table 10** The $^{13}C$ and $^{1}H$ NMR spectroscopic data of **26**

| Position | **26** | |
|---|---|---|
| | $\delta_C$ | $\delta_H$ Multi (*J* in Hz) |
| 2 | 158.4 | - |
| 3 | 134.8 | - |
| 4 | 179.2 | - |
| 5 | 163.2 | - |
| 6 | 99.8 | 6.17 d (2.0) |
| 7 | 165.8 | - |
| 8 | 94.6 | 6.37 d (2.0) |
| 9 | 158.5 | - |
| 10 | 105.8 | - |
| 1′ | 122.7 | - |
| 2′ | 132.2 | 8.01 d (8.8) |
| 3′ | 116.3 | 6.91 d (8.8) |
| 4′ | 161.6 | - |
| 5′ | 116.3 | 6.91 d (8.8) |
| 6′ | 132.2 | 8.01 d (8.8) |
| 3-*O*-glucose | | |
| 1″ | 100.5 | 5.73 d (8.0) |
| 2″ | 74.6 | 5.23 dd (9.5, 8.0) |
| 3″ | 84.9 | 3.91 t (9.5) |
| 4″ | 70.0 | 3.55 t (9.5) |
| 5″ | 78.4 | 3.39 ddd (9.5, 5.5, 2) |
| 6″ | 62.4 | 3.62 dd (12.0, 5.5) |
| | | 3.81 dd (12.0, 2.0) |
| 2″-*O*-feruloyl | | |
| 1‴ | 127.8 | - |
| 2‴ | 111.7 | 7.20 d (1.8) |
| 3‴ | 149.3 | - |
| 4‴ | 150.6 | - |
| 5‴ | 116.4 | 6.83 d (8.2) |
| 6‴ | 124.3 | 7.09 dd (8.2, 1.8) |
| 7‴ | 147.5 | 7.68 br d (15.9) |
| 8‴ | 115.5 | 6.40 br d (15.9) |
| 9‴ | 168.5 | - |
| O*CH₃* | 56.4 | 3.92 s |
| 3″-*O*-glucose | | |
| 1⁗ | 104.9 | 4.43 d (7.8) |
| 2⁗ | 74.8 | 3.21 dd (8.8, 7.8) |
| 3⁗ | 77.7 | 3.31 t (8.8) |
| 4⁗ | 71.4 | 3.28 t (8.8) |
| 5⁗ | 78.1 | 3.34 m |
| 6⁗ | 62.5 | 3.62 dd (11.9, 2.2) |
| | | 3.88 dd (11.9, 6.0) |

Recorded at 700 and 175 MHz in $CD_3OD$. Chemical shifts ($\delta$) are expressed in ppm and *J* values are presented in Hz in parenthesis. m: multiplet or overlapped signals.

The correlations observed between the protons and carbons resonances from H-7‴ ($\delta_H$ 7.68) to C-2‴ ($\delta_c$ 111.7), C-6‴ ($\delta_c$ 124.3) and an ester carbonyl C-9‴ ($\delta_c$ 168.5), and from the protons of methoxy group ($\delta_H$ 3.92) to C-3‴ ($\delta_c$ 149.3) in HMBC spectrum (Fig. 37) indicated the

presence of feruloyl unit. According to coupling constant of olefinic protons H-7‴ and H-8‴ ($J$ = 15.9 Hz), the configuration of feruloyl moiety was determined as *trans*. Alkaline hydrolysis afforded ferulic acid (Fig. 38) identified by HPLC comparing with authentic sample. Full assignments of $^{1}H$ and $^{13}C$ resonances of the structural fragments of **26** were achieved by analysis of COSY, HSQC and HMBC. A correlation between anomeric proton H-1″ ($\delta_H$ 5.73) and $\delta_c$ 134.8 in HMBC spectrum (Fig. 37) define C-3 of kaempferol as a site of *O*-glucosylation. Moreover, the interglucosidic linkage of the disaccharide moiety was determined by HMBC cross-peak between H-3″ ($\delta_H$ 3.91) and C-1‴ ($\delta_c$ 104.9). The *E*-feruloyl unit was linked to C-2″ based on the correlations of the H-2″ ($\delta_H$ 5.23) with C-1″ ($\delta_c$ 100.5), C-3″ ($\delta_c$ 84.9) and ester carbonyl carbon C-9‴ ($\delta_c$ 168.5). Therefore, the structure of compound **26** was determined as kaempferol 3-*O*-[2-*O*-(*trans*-feruloyl)-3-*O*-*β*-D-glucopyranosyl]-*β*-D-glucopyranoside.

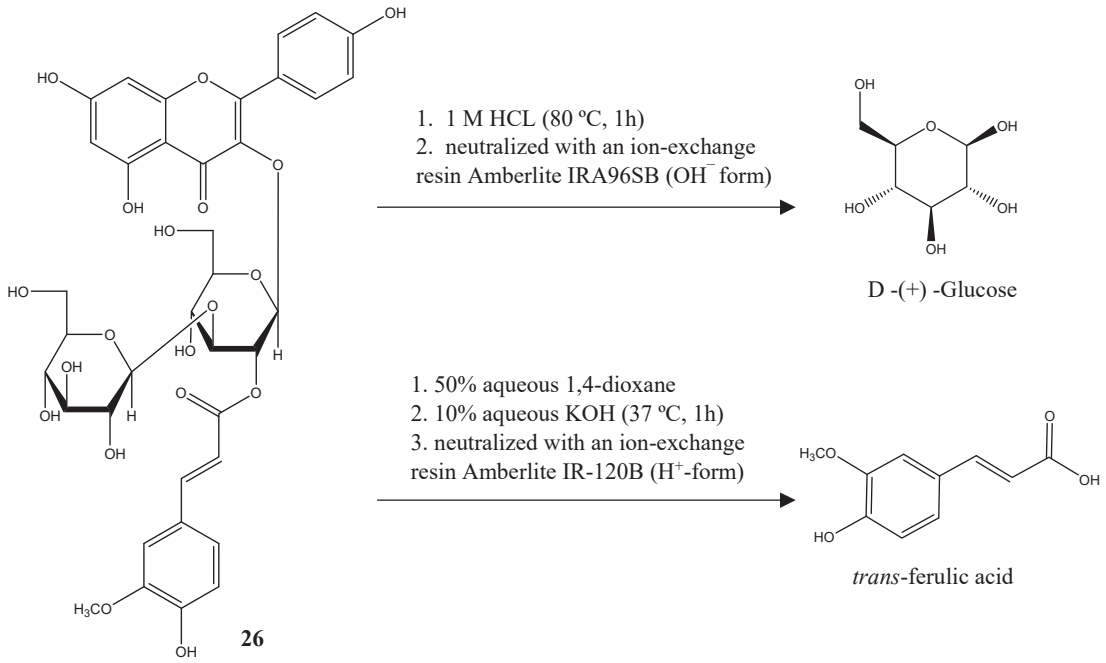


**Figure 38.** Acid and alkaline hydrolysis of **26**

Compound (**27**) was isolated as a yellow amorphous powder, with a positive optical rotation ([α] $^{22}{}_{D}$+14.5). Its molecular formula was determined to be $C_{48}H_{56}O_{27}$ by HR-ESI-MS positive spectrum (*m/z* 1087.2878 $[M + Na]^+$, calcd for $C_{48}H_{56}O_{27}Na$ 1087.2901). The UV profile of **27** was $\lambda_{max}$ 316, 267 nm, which was similar to those of the kaempferol glycoside acylated by a hydroxy cinnamic acid [57, 58, 60]. The IR spectrum indicated absorptions of hydroxy (3397 cm⁻

[1]), *α*,*β*-unsaturated carbonyl ester (1721 $cm^{-1}$), *α*,*β*-unsaturated ketone (1657 $cm^{-1}$), aromatic ring (1512, 1442 $cm^{-1}$) and ether (1157, 1072 $cm^{-1}$) functions. The above features were confirmed by $^1$H NMR spectrum which revealed a set of kaempferol signals, *p*-coumaroyl group and glycoside moieties. The kaempferol aglycone of **27** was represented in $^1$H NMR spectrum (Tables. 11 and 12) as two *ortho*-coupled resonances of the B-ring at $\delta_H$ 8.06 and 6.89 (each 1H, d, $J$ = 8.9 Hz), were typical of H-2′/6′ and H-3′/5′, respectively, in addition to two *meta*-coupled proton resonances at $\delta_H$ 6.37 and 6.65 (each 1H,br s), attributed to H-6 and H-8 of the A-ring, respectively.

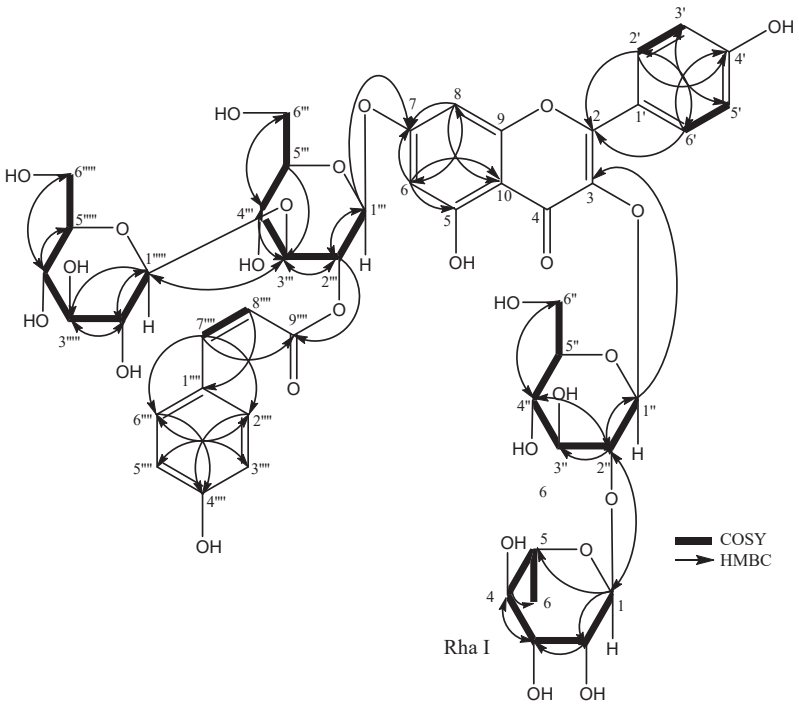


**Figure 39.** HMBC and COSY correlations of **27**

In comparison with literature, the downfield shifts of H-6 and H-8 in $^1$H NMR spectrum suggested the presence of substitution at kaempferol C-7, while the substitution at C-3 was evident from the downfield shift of C-2 to ($\delta_c$ 159.2) in $^{13}$C NMR spectrum. Moreover, the $^1$H NMR spectrum (Tables. 11 and 12) exhibited two olefinic protons at $\delta_H$ 5.83 and 6.86 with a coupling constant of 12.9 Hz. Similarly, the AA′BB′ aromatic coupling system at $\delta_H$ 6.67 and 7.55 (each 1H, d, $J$ = 8.6 Hz) were attributed to a *trans*-*p*-coumaroyl unit, which was confirmed by correlation

of olefinic proton ($\delta_H$ 5.83 and 6.86) with the ester carbonyl carbon at $\delta$c 167.2 and aromatic carbons ($\delta$C 127.6; C-1‴′ and 133.4; C-2/6‴′) in HMBC spectrum (Fig. 37).

**Table 11** The $^{13}$C and $^{1}$H NMR spectroscopic data of **27**

| Position | **27** | | | | |
|---|---|---|---|---|---|
| | $\delta_C$ | $\delta_H$ Multi (*J* in Hz) | Position | $\delta_C$ | $\delta_H$ Multi (*J* in Hz) |
| 2 | 159.2 | - | 2‴-*O*-*p*-coumaroyl | | |
| 3 | 134.7 | - | 1‴′ | 127.6 | - |
| 4 | 179.5 | - | 2‴′ | 133.4 | 7.55 d (8.6) |
| 5 | 163.0 | - | 3‴′ | 115.9 | 6.67 d (8.6) |
| 6 | 100.4 | 6.37 br s | 4‴′ | 160.0 | - |
| 7 | 163.8 | - | 5‴′ | 115.9 | 6.67 d (8.6) |
| 8 | 95.7 | 6.65 br s | 6‴′ | 133.4 | 7.55 d (8.6) |
| 9 | 157.9 | - | 7‴′ | 145.0 | 6.86 br d (12.9) |
| 10 | 108.0 | - | 8‴′ | 116.6 | 5.83 br d (12.9) |
| 1′ | 122.8 | - | 9‴′ | 167.2 | - |
| 2′ | 132.3 | 8.06 d (8.9) | 3‴-*O*-glucose | | |
| 3′ | 116.2 | 6.89 d (8.9) | 1‴′′ | 105.0 | 4.40 d (7.8) |
| 4′ | 161.6 | - | 2‴′′ | 74.7 | 3.20 dd (8.5, 7.8) |
| 5′ | 116.2 | 6.89 d (8.9) | 3‴′′ | 77.8 | 3.31 m |
| 6′ | 132.3 | 8.06 d (8.9) | 4‴′′ | 71.4 | 3.29 m |
| 3-*O*-glucose | | | | | 5‴′′ |
| 1″ | 100.2 | 5.72 d (7.6) | 6‴′′ | 62.5 | 3.87 dd (11.5, 5.4)<br>3.64 dd (11.5, 1.3) |
| 2″ | 80.0 | 3.60 m | | | |
| 3″ | 78.9 | 3.55 t (9.0) | | | |
| 4″ | 71.8 | 3.26 t (9.0) | | | |
| 5″ | 78.1 | 3.31 m | | | |
| 6″ | 62.6 | 3.47 dd (12.0, 5.9)<br>3.71 dd (12.0, 2.1) | | | |
| Rha<br>(2″-*O*-rhamnose) | | | | | |
| 1 | 102.6 | 5.22 d (1.3) | | | |
| 2 | 72.4 | 3.99 m | | | |
| 3 | 72.3 | 3.76 m | | | |
| 4 | 74.0 | 3.33 t (9.6) | | | |
| 5 | 69.9 | 4.02 dq (9.6, 6.18) | | | |
| 6 | 17.6 | 0.96 d (6.18) | | | |
| 7-*O*-glucose | | | | | |
| 1‴ | 99.6 | 5.29 d (7.8) | | | |
| 2‴ | 73.4 | 5.25 dd (9.0, 7.8) | | | |
| 3‴ | 84.3 | 3.92 t (9.0) | | | |
| 4‴ | 69.8 | 3.76 m | | | |
| 5‴ | 78.2 | 3.78 | | | |
| 6‴ | 62.2 | 3.75 dd (12.0, 5.1)<br>3.94 dd (12.0, 1.6) | | | |

Recorded at 600 and 150 MHz in $CD_3OD$. Chemical shifts ($\delta$) are expressed in ppm and *J* values are presented in Hz in parenthesis. m: multiplet or overlapped signals.

The sugar units in **27** were represented in $^{1}$H NMR spectra as four anomeric proton signals at $\delta_H$ 4.40 (1H, d, $J$ = 7.8 Hz), 5.22 (1H, d, $J$ = 1.3 Hz), 5.29 (1H, d, $J$ = 7.8 Hz), 5.72 (1H, d, $J$ = 7.6 Hz) indicated tetraglycosidic nature of **27**. Identification of the sugars residues was carried out by careful analysis of 1D and 2D data as well as comparison with reported literature. Based on these data analysis and acid hydrolysis results together with the magnitudes of $J_{1,2}$ coupling constants and one methyl group at 0.96 (3H, d, $J$ = 6.18 Hz), the sugars were identified as three *β*-D-glucopyranose and an *α*-L-rhamnopyranose. On other hand, Alkaline hydrolysis of **27** afforded *cis*-*p*-coumaric acid (Fig. 42).

The spectroscopic data of **27** (Tables. 11 and 12) clarified that it is an isomer of **31** [55]. The relatively smaller coupling constant ($J$ = 12.9 Hz) and the chemical shift values of H-7‴′ and H-8‴′ ($\delta_H$ 6.86 and 5.83, respectively) indicated **27** as a *cis* isomer. The positions of glycosides and *p*-coumaroyl moiety in relation to each other and kaempferol aglycone were determined using HMBC spectrum (Fig. 39). The anomeric protons of two glucose moieties at $\delta_H$ 5.72 and 5.29 have long-rang correlations with C-3 ($\delta_c$ 134.7) and C-7 ($\delta_c$ 163.8) of the kaempferol aglycone, respectively.

The COSY correlation (Fig. 39) of H-2″ at ($\delta_H$ 3.60) with H-1″ at ($\delta_H$ 5.72), together with correlation observed in HMBC spectrum between H-2″and C-1 of Rha at $\delta_c$ 102.6 confirmed the presence of *β*-neohesperidoside structure at C-3 of kaempferol. Moreover, the correlations of H-2‴ ($\delta_H$ 5.25) with H-1‴ ($\delta_H$ 5.29) and H-3‴ ($\delta_H$ 3.92) in COSY spectrum, and the correlations from H-2‴ to C-9‴′ ($\delta_c$ 167.2), and from H-3‴ to C-1‴′ ($\delta_c$ 105.0) in HMBC spectrum confirmed the presence of 7-*O*-[2-*O*-(*cis*-*p*-coumaroyl)-3-*O*-*β*-D-glucpyranosyl]-*β*-D-glucopyranose at kaempferol aglycone. The structure of **27** was therefore identified as kaempferol 3-*O*-*β*-neohesperidoside-7-*O*-[2-*O*-(*cis*-*p*-coumaroyl)-3-*O*-*β*-D-glucopyranosyl]-*β*-D-glucopyranoside.

Compound (**28**) was obtained as a yellow amorphous powder with a negative optical rotation ($[\alpha]^{22}_{D}$ –82.5). A $C_{49}H_{58}O_{27}$ molecular formula was deduced from the sodiated molecular ion peak at *m*/*z* 1101.3021 (calcd for $C_{49}H_{58}O_{27}$ Na 1101.3058) by HR-ESI-MS measurement. It displayed characteristic UV maxima of acylated kaempferol glycoside at $\lambda_{max}$ 329, 268 nm, similar to those of **26**. The IR spectrum exhibited absorptions of hydroxy (3389 cm$^{-1}$), *α*,*β*-unsaturated carbonyl ester (1712 cm$^{-1}$), *α*,*β*-unsaturated ketone (1651 cm$^{-1}$), aromatic ring (1513, 1455 cm$^{-1}$) and ether (1180, 1071 cm$^{-1}$) functions. Analysis of $^{1}$H and $^{13}$C NMR spectra of **28** (Tables. 12

and13) indicated the presence of kaempferol residue, four hexose sugar moieties, and *E*-feruloyl unit. The $^1$H spectrum (Tables. 12 and13) displayed four downfield doublets signals at $\delta_H$ 6.46 (1H, d, $J$ = 2.1 Hz), 6.61 (1H, d, $J$ = 2.1 Hz), 6.76 (2 H, d, $J$ = 8.9 Hz) and 7.93 (2 H, d, $J$ = 8.9 Hz) assignable to H-6, 8, 3′/5′ and 2′/6′, respectively, belonging to kaempferol aglycone.

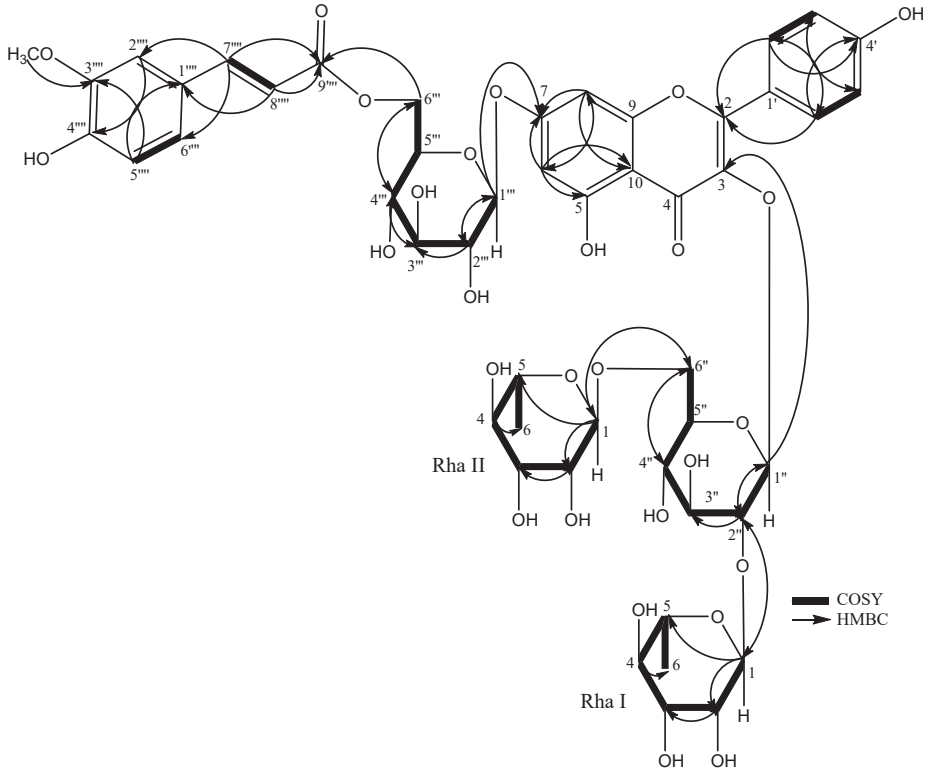


**Figure 40.** HMBC and COSY correlations of **28**

Moreover, the characteristic signals of *E*-feruloyl moiety were observed in $^1$H NMR spectrum as five downfield doublets at $\delta_H$ 6.28 (1H, br d, $J$ = 15.8 Hz), 6.67 (1H, d, $J$ = 8.2 Hz), 6.85 (1H, d, $J$ = 8.2, 1.7 Hz), 6.98 (1H, d, $J$ = 1.7 Hz) and 7.50 (1H, br d, $J$ = 15.8 Hz), corresponding to H-8′′′′, 5′′′′, 6′′′′, 2′′′′ and 7′′′′, respectively, in addition to singlet signal of a methoxy group at $\delta_H$ 3.75. Full assignment of 1D NMR spectra of **28** was achieved by analysis of COSY, HSQC and HMBC data, which confirmed presence of 3,7-*O*-glycosidic kaempferol residue together with *E*-feruloyl unit. Acid hydrolysis of **28** with 1N HCl released D-glucose and L-rhamnose, while alkaline hydrolysis afforded ferulic acid. These results were identified by HPLC comparing with authentic samples (Fig. 42). The $^1$H NMR spectrum of **28** exhibited resonances for anomeric protons of *O*-linked sugars at $\delta_H$ 4.98 (1H, d, $J$ = 7.4 Hz) and 5.51 (1H,

d, $J$ = 7.6 Hz), corresponding to two D-glucose, and 4.38 (1H, d, $J$ = 1.3 Hz) and 5.14 (1H, d, $J$ = 1.1 Hz), together with typical doublets of two methyl group at $\delta_H$ 0.88 (3H, d, $J$ = 6.2 Hz) and 0.96 (3H, d, $J$ = 6.2 Hz), corresponding to two L-rhamnose moieties.

Full assignment of $^{1}H$ and $^{13}C$ NMR data of each sugar was achieved using standard 2D NMR data (Tables. 13 and 14). The configurations of these sugars were identified from their magnitudes of $J_{1,2}$ coupling constants and chemical shifts as $\beta$-D-glucopyranose and $\alpha$-L-rhamnopyranose. The glycosidation sites on kaempferol aglycone of **28** were determined from long-rang correlations exhibited in HMBC spectrum from H-1″ $\delta_H$ 5.51 to C-3 ($\delta_c$ 134.6), and from H-1‴ 4.98 to C-7 (164.4). Both C-2″ and C-6″ of the $\beta$-glucose attached at C-3 were low field shifted in $^{13}C$ NMR spectrum (Table. 12) to ($\delta_c$ 79.7) and ($\delta_c$ 68.3), respectively, and glycosylated by two $\alpha$-L-rhamnopyranosyl moieties (Rha I and Rha II, respectively), according to HMBC correlations (Fig. 40), their connectivities detected by the cross peaks between H-2″ ($\delta_H$ 3.52) and C-1 of Rha I ($\delta_c$ 102.5), and between $H_2$-6″ ($\delta_H$ 3.27 and 3.71) and C-1 of Rha II ($\delta_c$ 102.2). Furthermore, the HMBC correlations from significant downfield shifted protons of $H_2$-6‴ of the $\beta$-glucose attached at C-7 at $\delta_H$ 4.17 and 4.75 to C-9‴″ at ($\delta_c$ 169.1) indicated the position of acetylation, thus defining the *E*-feruloyl linkage site. Therefore, the structure of compound **28** was elucidated as kaempferol 3-*O*-[2,6-di-*O*-L-rhamnopyranosyl]-$\beta$-D-glucopyranoside-7-*O*-[6-*O*-(*trans*-feruloyl)]-$\beta$-D-glucopyranoside.

Compound (**29**) was isolated as a yellow amorphous powder, with a negative optical rotation ($[\alpha]_D^{22}$ –81.6). Its molecular formula was established as $C_{48}H_{56}O_{26}$ by its HR-ESI-MS positive spectrum (*m/z* 1071.2925 $[M + Na]^+$, calcd for $C_{48}H_{56}O_{26}Na$ 1071.2952), suggesting the lake of one methoxy group compared to **28**. Analysis of 2D experiments of **29** including COSY, HSQC and HMBC and comparison of its $^{1}H$ and $^{13}C$ NMR values with those of **28** (Tables. 12 and 13) showed that **29** was kaempferol tetraglycoside acylated with a cinnamic acid derivative.

The $^{1}H$ and $^{13}C$ NMR spectra of **29** revealed identical glycosylation profile to that of **28**. Comparison of the HMBC correlations (Fig. 41) of **29** with those of **28** (Fig. 40) detected the same pattern of connectivity defining linkages between the glycosyl moieties and the kaempferol residue, and between the glycosyl moieties themselves. Thus, the difference between **28** and **29** should be located at the cinnamoyl derivative substituent.

**Table 12.** The $^{13}C$ and $^{1}H$ NMR spectroscopic data of **28** and **29**

| Position | **28** | | Position | **29** | |
|---|---|---|---|---|---|
| | $\delta_C$ | $\delta_H$ Multi (*J* in Hz) | | $\delta_C$ | $\delta_H$ Multi (*J* in Hz) |
| 2 | 159.4 | - | 2 | 159.4 | - |
| 3 | 134.6 | - | 3 | 134.6 | - |
| 4 | 179.5 | - | 4 | 179.5 | - |
| 5 | 162.9 | - | 5 | 162.9 | - |
| 6 | 100.7 | 6.46 d (2.1) | 6 | 100.7 | 6.45 d (2.1) |
| 7 | 164.4 | - | 7 | 164.4 | - |
| 8 | 96.3 | 6.61 d (2.1) | 8 | 96.2 | 6.62 d (2.1) |
| 9 | 157.8 | - | 9 | 157.8 | - |
| 10 | 107.7 | - | 10 | 107.7 | - |
| 1′ | 122.8 | - | 1′ | 122.8 | - |
| 2′ | 132.2 | 7.93 d (8.9) | 2′ | 132.2 | 7.95 d (8.8) |
| 3′ | 116.2 | 6.76 d (8.9) | 3′ | 116.9 | 6.77 d (8.8) |
| 4′ | 161.4 | - | 4′ | 161.5 | - |
| 5′ | 116.2 | 6.76 d (8.9) | 5′ | 116.9 | 6.77 d (8.8) |
| 6′ | 132.2 | 7.93 d (8.9) | 6′ | 132.2 | 7.95 d (8.8) |
| 3-*O*-glucose | | | 3-*O*-glucose | | |
| 1″ | 100.3 | 5.51 d (7.6) | 1″ | 100.3 | 5.51 d (7.6) |
| 2″ | 79.7 | 3.52 dd (9.6, 7.6) | 2″ | 79.8 | 3.52 dd (9.6, 7.6) |
| 3″ | 79.0 | 3.45 m | 3″ | 79.0 | 3.44 m |
| 4″ | 72.0 | 3.13 t (9.12) | 4″ | 71.7 | 3.19 m |
| 5″ | 77.2 | 3.24 m | 5″ | 77.2 | 3.24 m |
| 6″ | 68.3 | 3.27 m | 6″ | 68.3 | 3.27 m |
| | | 3.71 m | | | 3.71 m |
| Rha I | | | Rha I | | |
| (2"-*O*-rhamnose) | | | (2"-*O*-rhamnose) | | |
| 1 | 102.5 | 5.14 d (1.1) | 1 | 102.5 | 5.14 d s |
| 2 | 72.3 | 3.90 m | 2 | 72.3 | 3.90 m |
| 3 | 72.3 | 3.69 m | 3 | 72.3 | 3.69 m |
| 4 | 74.0 | 3.25 m | 4 | 74.7 | 3.42 m |
| 5 | 69.9 | 3.93 dq (9.5, 6.2) | 5 | 69.9 | 3.68 dq (9.6, 6.2) |
| 6 | 17.6 | 0.88 d (6.2) | 6 | 17.6 | 0.96 d (6.2) |
| Rha II | | | Rha II | | |
| (6"-*O*-rhamnose) | | | (6"-*O*-rhamnose) | | |
| 1 | 102.2 | 4.38 d (1.3) | 1 | 102.2 | 4.36 d s |
| 2 | 72.0 | 3.38 m | 2 | 72.0 | 3.37 m |
| 3 | 72.0 | 3.34 dd (9.4, 3.4) | 3 | 72.0 | 3.33 dd (9.4, 3.4) |
| 4 | 73.8 | 3.12 t (9.4) | 4 | 74.0 | 3.25 m |
| 5 | 69.7 | 3.30 m | 5 | 69.7 | 3.25 m |
| 6 | 17.8 | 0.96 d (6.2) | 6 | 17.8 | 0.88 d (6.2) |
| 7-*O*-glucose | | | 7-*O*-glucose | | |
| 1‴ | 101.6 | 4.98 d (7.4) | 1‴ | 101.6 | 4.98 d (7.3) |
| 2‴ | 74.7 | 3.42 m | 2‴ | 73.8 | 3.41 t (9.4) |
| 3‴ | 77.8 | 3.43 m | 3‴ | 77.8 | 3.42 m |
| 4‴ | 71.7 | 3.34 m | 4‴ | 71.8 | 3.34 t (9.4) |
| 5‴ | 75.8 | 3.72 m | 5‴ | 75.7 | 3.72 m |
| 6‴ | 64.6 | 4.17 dd (12.0, 2.0) | 6‴ | 64.6 | 4.18 dd (12.0, 2.1) |
| | | 4.57 dd (12.0,6.9) | | | 4.54 dd (12.0, 7.0) |

Recorded at 600 and 150 MHz in $CD_3OD$. Chemical shifts ($\delta$) are expressed in ppm and *J* values are presented in Hz in parenthesis. m: multiplet or overlapped signals.

**Table 13** The $^{13}C$ and $^{1}H$ NMR spectroscopic data of **28** and **29** (continued)

| Position | **28** | | Position | **29** | |
|---|---|---|---|---|---|
| | $\delta_C$ | $\delta_H$ Multi (*J* in Hz) | | $\delta_C$ | $\delta_H$ Multi (*J* in Hz) |
| 6‴ -*O*-feuryl | | | 6‴ -*O*-coumaroyl | | |
| 1⁗ | 127.6 | - | 1⁗ | 127.1 | - |
| 2⁗ | 111.6 | 6.98 d (1.7) | 2⁗ | 131.2 | 7.25 d (8.6) |
| 3⁗ | 149.2 | - | 3⁗ | 116.2 | 6.66 d (8.6) |
| 4⁗ | 150.5 | - | 4⁗ | 161.2 | - |
| 5⁗ | 116.5 | 6.67 d (8.2) | 5⁗ | 116.2 | 6.66 d (8.6) |
| 6⁗ | 124.2 | 6.85 d (8.2, 1.7) | 6⁗ | 131.2 | 7.25 d (8.6) |
| 7⁗ | 147.3 | 7.50 br d (15.8) | 7⁗ | 147.1 | 7.50 br d (15.9) |
| 8⁗ | 115.1 | 6.28 br d (15.8) | 8⁗ | 114.7 | 6.24 br d (15.9) |
| 9⁗ | 169.1 | - | 9⁗ | 169.1 | - |
| O*CH*$_3$ | 56.5 | 3.75 s | O*CH*$_3$ | | |

Recorded at 600 and 150 MHz in $CD_3OD$. Chemical shifts ($\delta$) are expressed in ppm and *J* values are presented in Hz in parenthesis.

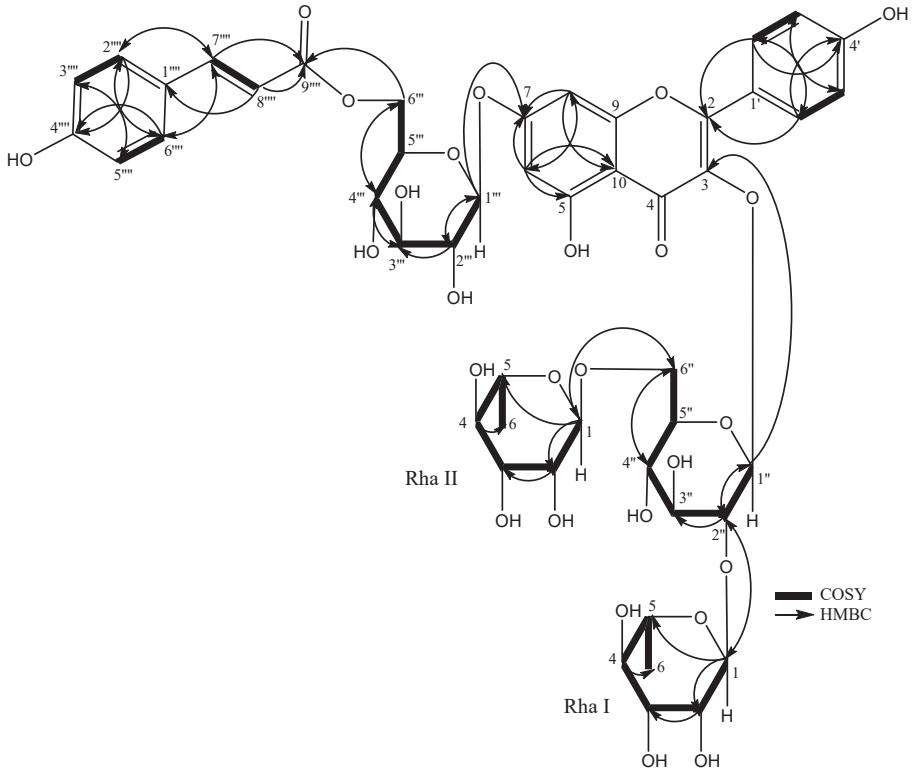


**Figure 41.** HMBC and COSY correlations of **29**

In particular, the $^{1}H$ NMR spectrum (Table. 13) showed the typical coupling pattern (AA′BB′ system) of 1,4-disubstituted aromatic moiety at $\delta_H$ 6.66 and 7.25 (each 2H, d, $J$ = 8.6 Hz) and two *trans*-coupled double bond protons at $\delta_H$ 6.24 and 7.50 (each 1H, br d, $J$ = 15.9 Hz), as well as to an ester carbonyl ($\delta_c$ 169.1) in $^{13}C$ NMR spectrum assignable to *p*-coumaroyl unit. In HMBC spectrum (Fig. 41), the cross peaks between $H_2$-6‴ ($\delta_H$ 4.18 and 4.54) and C-9⁗ ($\delta_c$ 169.1)

placed *p*-coumaroyl unit at C-6‴. The sugar units were identified as D-glucose and L-rhamnose by acid hydrolysis of **29**, followed by HPLC analysis with chiral detector in comparison with authentic samples (Fig. 42). Anomeric configurations were determined from the magnitudes of $J_{1,2}$ coupling constants in $^{1}$H NMR spectrum. Therefore, the structure of **29** was that of acylated kaempferol tetraglycoside, kaempferol 3-*O*-[2,6-di-*O*-L-rhamnopyranosyl]-*β*-D-glucopyranoside-7-*O*-[6-*O*-(*trans*-*p*-coumaroyl)]-*β*-D-glucopyranoside.

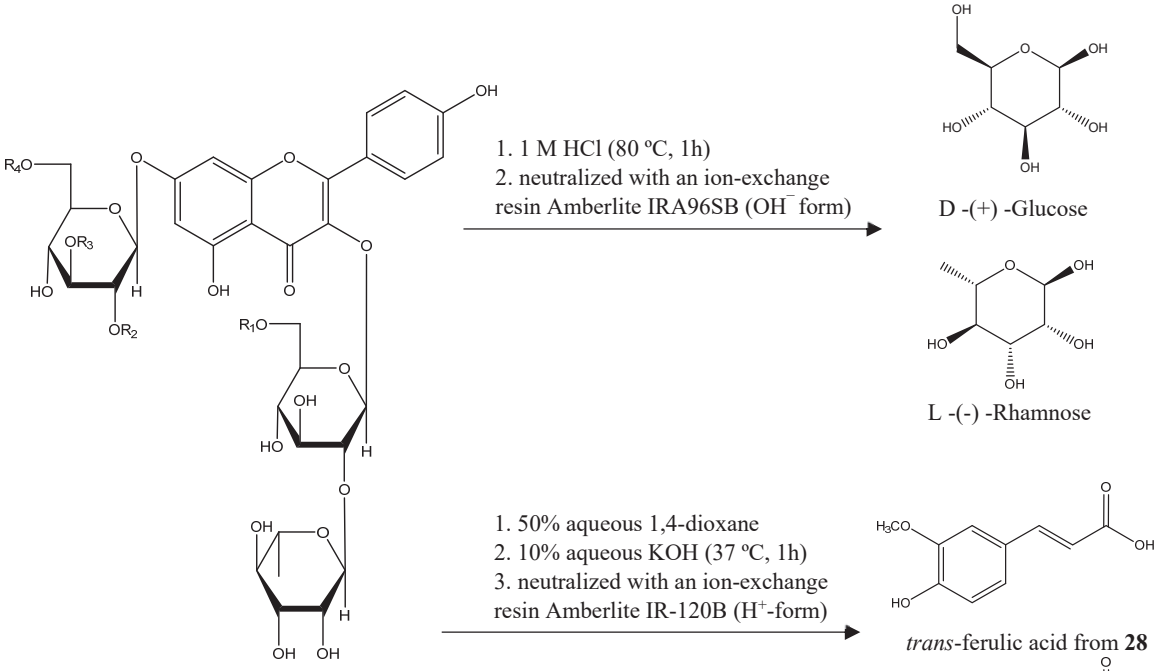


| | $R_1$ | $R_2$ | $R_3$ | $R_4$ |
|---|---|---|---|---|
| **27** | H | *cis*-*p*-coumaroyl | Glc | H |
| **28** | Rha | H | H | *trans*-feruloyl |

**Figure 42.** Acid hydrolysis of **27 – 29** and alkaline hydrolysis of **27 – 28**

## 2.4 Bioassay of Chemical constituent:

### 2.4.1. DPPH radical scavenging activity

Oxidative stress is a general term used to describe a series of imbalance in organisms between the production of reactive oxygen species (ROS) and the antioxidant defense mechanism. Reactive oxygen species (ROS), such as hydroxy radical, hydrogen peroxide, and superoxide anions, are produced as a by-product in aerobic organisms [56]. Under oxidative stress condition, over production of ROS may damage membrane lipids and DNA, and affect the function of cellular proteins. For these reasons, oxidative stress contributes to general decline in optimum bodily functions (the aging processes), and may involve in the pathogenesis of several disorders, whether as a cause or as an effect.

Antioxidants are compounds that can delay, inhibit or prevent the oxidation of oxidizable matters by scavenging free radicals and diminish oxidative stress. As we mention in chapter (1) that the synthetic antioxidants accumulated in the body cause liver dysfunction and carcinogenesis [29, 30]. During past decades, interest in polyphenols, including flavonoids, has considerably increased due to the discovery of their various biological properties, principally their antioxidant effects and therefore their possible role in prevention of several chronic diseases involving oxidative stress [57].

Flavonoids are a diverse group of compounds, which are widely distributed in the plant kingdom. Natural flavonoids are known for their significant scavenging properties on oxygen radicals by both *in vivo* and *in vitro* [58-61]. *C. rotundifolia* 1-BuOH fraction is rich with flavonoids especially kaempferol and myricetin together with their derivatives. Isolated compounds (**26** – **45**) from 1-BuOH fraction of *C. rotundifolia* were evaluated for DPPH radical scavenging assay activity (Table. 14) (Fig. 43 and 44) using Trolox as positive control ($IC_{50}$: 29.2±0.39 $\mu$M). The results showed that compounds **42** and **43** exhibited potent radical scavenging activity with $IC_{50}$ values of 14.5 and 11.7 $\mu$M, respectively. On the other hand, compounds **40** and **41** showed moderate activity with $IC_{50}$ values of 43.0 and 31.8 $\mu$M, respectively. These results are consistent with previous studies on the effectiveness of myricetin as a potent antioxidant agent which could prevent and slow the progress of ageing or various diseases associated with oxidative stress.

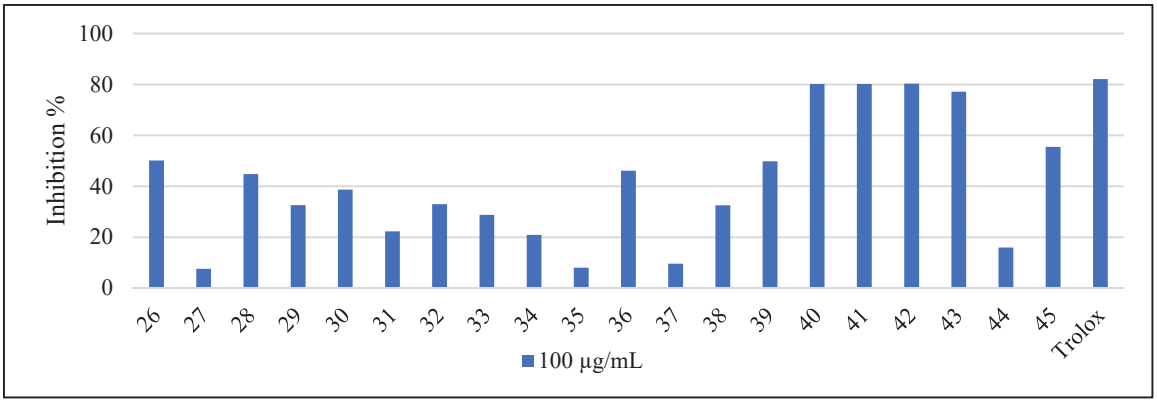


**Figure 43.** DPPH free radical scavenging activity of **26** – **45**

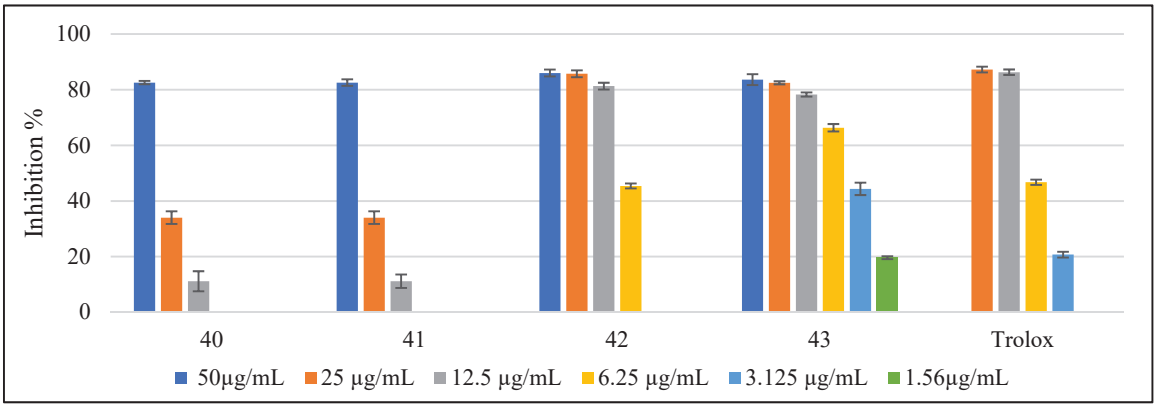


**Figure 44.** DPPH free radical scavenging activity of **40** – **43**

### 2.4.2. AGE's formation

Reactive oxygen species (ROS) are generated in body as by-product of many physiological processes [62]. ROS are highly reactive radical molecules, such as free radical, oxygen ion and peroxides [63]. It was found that ROS playing a dual role as both beneficial and harmful species according to their concentration. In low to moderate concentration, ROS play important role in energy production and intercellular signaling, but at high concentration it can be toxic and cause damage to biomolecules [64]. Over production of ROS is known as oxidative stress, which is the major cause of many disorders including aging and diseases [25, 26].

Moreover, the oxidative stress is the main contributor to the skin aging process and accelerate the formation of Advanced Glycation End-products (AGEs). AGEs are oxidative products originate from non-enzymatic glycation reaction between sugars and proteins similar to the Maillard reaction, nucleic acids or lipids in hyperglycemic environments or during aging [65].

**Table 14.** Bioactivities of **26**, **31**, **33**, **35** and **40** – **43** from *C. rotundifolia*

| Isolated compounds | DPPH ($IC_{50}$ $\mu$M) | AGEs ($IC_{50}$ $\mu$M) | Collagenase ($IC_{50}$ $\mu$M) |
|---|---|---|---|
| Kaempferol-3-*O*-[2-*O*-(*trans*-feruloyl)-3-*O*-*β*-D-glucopyranosyl]-*β*-D-glucopyranoside (**26**) | >100 | >100 | 94.5±3.1 |
| Kaempferol 3-*O*-*β*-neohesperidoside-7-*O*-[2-*O*-(*trans*-*p*-coumaroyl)-3-*O*-*β*-D-glucopyranosyl]-*β*-D-glucopyranoside (**31**) | >100 | >100 | 79.8±3.3 |
| Kaempferol 3-*O*-*β*-neohesperidoside-7-*O*-[2-*O*-(*trans*-*p*-coumaroyl)]-*β*-D-glucopyranoside (**33**) | >100 | >100 | 88.3±2.3 |
| Kaempferol 3-*O*-[2,6-di-*O*-L-rhamnopyranosyl]-*β*-D-glucoside (**35**) | >100 | 85.5±3.5 | 64.0±1.9 |
| Myricetin 3-*O*-[2,6-di-*O*-L-rhamnopyranosyl]-*β*-glucoside (**40**) | 43.0±1.15 | >100 | >100 |
| Myricetin 3-*O*-*β*-neohesperidoside (**41**) | 31.8±0.63 | >100 | >100 |
| Myricetin 3-*O*-*β*-D-glucoside (**42**) | 14.5±1.15 | 96.5±1.8 | >100 |
| Myricetin (**43**) | 11.7±1.8 | 34.9±1.2 | >100 |
| Trolox | 29.2±0.39 | n.d | n.d |
| Aminoguanidine hydrochloride | n.d | 7818±34.4 | n.d |
| Caffeic acid | n.d | n.d | 129±3.3 |

n.d= not determined

Briefly, the Maillard reaction can be divided into two stages. The early glycation is reversible and involve the production of unstable Schiff base from carbonyl group of a reducing sugar and the primary amino groups of a protein (lysine, arginine) [66]. Reorganization then leads to the formation of more stable ketoamine (Amadori product). During the last stage, complex irreversible oxidation, condensation and cyclisation reaction lead to AGEs by intra- and intermolecular protein cross-linkage [67, 68]. These reaction in addition to the oxidation by ROS lead to diverse AGEs products (fluorescence, non-fluorescence and non-cross-linking) [69, 70]. AGEs are involving in the pathogenesis of numerous diseases probably because of their ability to react with a great variety of biomolecules that lead to decrease flexibility and modification of intracellular protein [71].

Furthermore, interaction of AGEs with their cellular receptors (RAGE) in skin leading to inflammation and subsequent disease [72]. Accumulation of AGEs in tissue with sustained hyperglycemia contribute to development of diabetic complications. Therefore, the following study have been performed to develop AGE inhibitor, which could be useful in the prevention or reduction of diabetic complications [73].

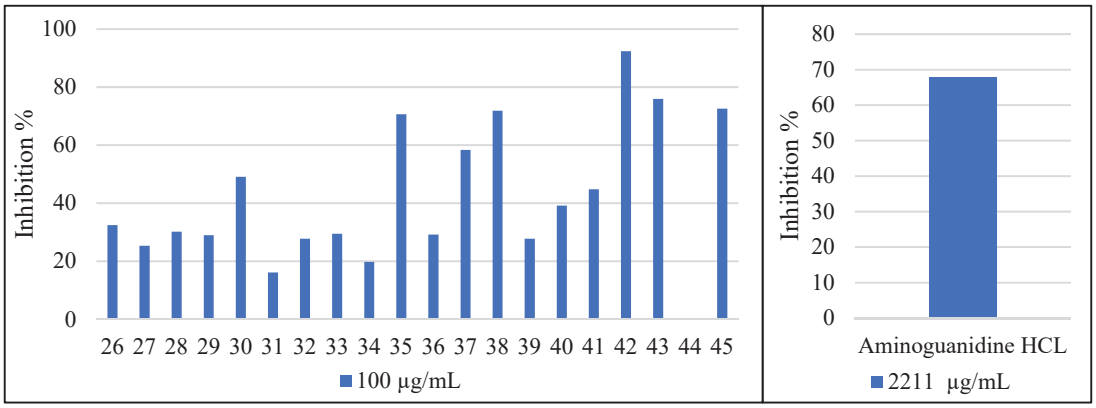


**Figure 45**. AGEs formation inhibitory activity of **26** – **45**

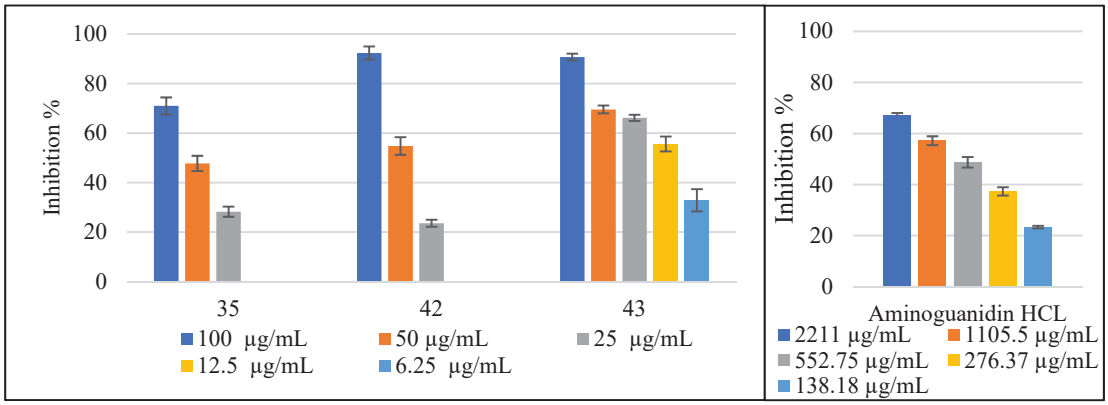


**Figure 46.** AGEs formation inhibitory activity of **35**, **42** and **43**

According to the previous studies that discussed the inhibitory effects of different flavonoids and phenolic compounds on AGEs formation, the results revealed that effects of flavonoids depend on their pattern of hydroxy group and their glyosidic nature. Moreover, it has been concluded that their effects against glycation, at least partly, due to their antioxidant properties [41, 74-77].

Inhibitory effects of isolated compounds (**26** – **45**) on AGEs formation were evaluated using a fluorescence method [78]. As shown in Table. 14 and Fig. 45 and 46, compound **35** ($IC_{50}$:

85.5±3.5 $\mu$M), **42** ($IC_{50}$: 96.5±1.8 $\mu$M) and **43** ($IC_{50}$: 34.9±1.2 $\mu$M) showed stronger inhibitory activity than that of a positive control aminoguanidine hydrochloride ($IC_{50}$: 7818±34.4 $\mu$M). The results revealed that the most inhibition effect was exhibited by myricetin (**43**). Comparison of $IC_{50}$ values of myricetin (**43**) and its 3-*O*-$\beta$-D-glucoside derivative (**42**) indicated that the presence of glucose moiety at C-3 of myricetin aglycone decrease the inhibition activity of AGEs formation. The other compounds did not show inhibitory activity.

### 2.4.3. Collagenase

Aging of skin is commonly associated with increased wrinkling, sagging, and increased laxity of skin [79]. The process of skin aging is induced by both intrinsic, and extrinsic factors, all leading to reduced structural integrity and loss of physiological function. Intrinsic aging is described as a natural consequence of physiological change over time affected by the genetic factors [80, 81]. On the other hand, extrinsic aging or premature aging, is an aging process caused by environmental influences (mainly from sun exposure) [82]. The mechanisms of intrinsic and extrinsic aging include the generation of reactive oxygen species (ROS) by oxidation metabolism and exposure to sun UV radiation (photoaging) [83, 84]. The degradation of the skin by UV radiation is accumulative process and the rate of degradation depends on the frequency, duration and intensity of solar exposure and natural protection by skin [85].

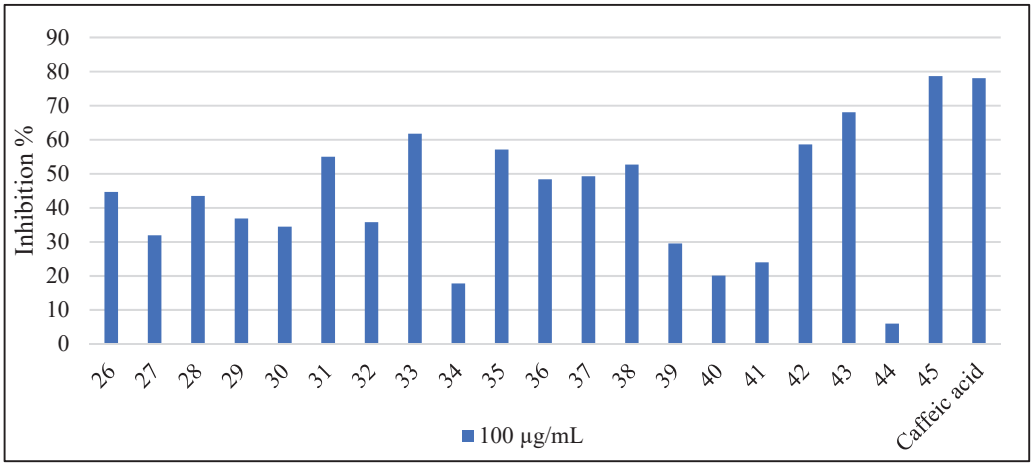


**Figure 47**. Collagenase inhibitory activity of **26** – **45**

UV exposure causes physical changes of skin through complex pathways and finally generates reactive oxygen species (ROS), matrix metalloproteinases (MMPs) and elastase secretion [86]. ROS directly affect skin lipids, protein and DNA leading to up-regulation of matrix metalloproteinases (MMPs) production, resulting in collagen breakdown [87]. MMPs are a family of transmembrane zinc-containing endoproteinases (including collagenase, gelatinase, stromelysins, membrane type MMPs and others) which characterized by their ability to degrade all components of the extracellular matrix (ECM) [88, 89]. Collagenase is responsible for ECM remodeling including collagen breakdown. Elastase, a serine proteinase, is primary responsible for the breakdown of elastin in ECM [89].

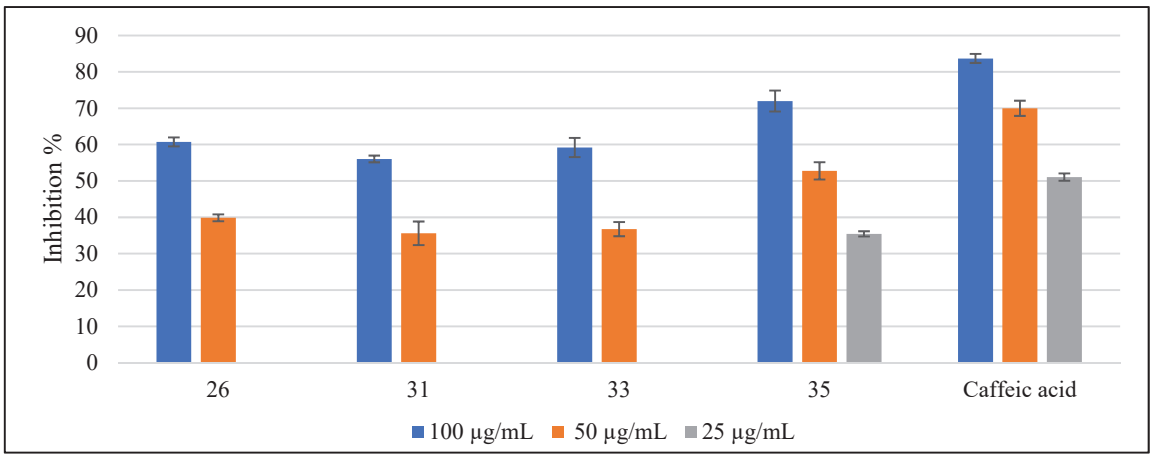


**Figure 48.** Collagenase inhibitory activity of **26**, **31**, **33**, **35**

An increase in MMPs expression in inflamed skin as well as in photoaged skin, leading to deterioration of collagen, elastin and other components of the dermal extracellular matrix result in wrinkle formation [90]. Therefore, search for anti-collagenase and/or anti-elastase agents may have beneficial effect for slow down skin aging.

Recently, many studied discussed the effect of flavonoids on MMPs. Most of them focused on their inhibitory activity against gelatinases (MMP-2 and MMP-9) [91-93]. Also, the direct modulatory effect of flavonoids on MMP-1 (mammalian collagenase-1) has been demonstrated [94-98]. The results found that the collagenase inhibitory activity of flavonoids depend on their hydroxy pattern and their concentration.

Therefore, we investigated the inhibitory effect of all isolated flavonoids and phenolic compounds against collagenase from *Clostridium histolyticum* to evaluate their therapeutic activity against ECM degradation and skin inflammation. This bacterial collagenase hydrolyses triple

helical collagen in both physiological and *in vitro* conditions using synthetic peptides as substrates. We found that kaempferol derivatives, demonstrated significant inhibition of collagenase.

Isolated compounds (**26** – **45**) were evaluated and showed to have, more or less, an inhibitory action on the collagenase obtained from *Clostridium histolyticum*. As shown in (Table.14) (Fig. 47 and 48), compounds (**26**, **31**, **33**) showed significant inhibition with $IC_{50}$ value ranging from 79.8 $\mu$M to 94.5 $\mu$M, while compound **35** exhibited $IC_{50}$ value of 64.0 $\mu$M which was more potent than that of positive control, caffeic acid (129±3.3 $\mu$M). The other compounds did not show inhibitory activity.

## 2.5. Experimental

### 2.5.1. General experimental procedures

IR spectra were recorded on Horiba FT-710 Fourier transform infrared (Horiba, Kyoto, japan), and UV spectra were obtained on Jasco V-520 UV/Vis spectrophotometers. Optical rotations data were measured on JASCO P-1030, while CD spectra were recorded on Jasco J-720 circular dichroism spectrometers (Jasco, Eston, MD). NMR experiments were measured on a Bruker avance 600 MHz and 700 MHz spectrometers, with tetramethylsilane (TMS) as an internal standard (Bruker, Biospin, Rheinstetten). Positive ion HR-ESI-MS spectra were recorded using a LTQ Orbitrap XL mass spectrometer (Thermo Fisher Scientific, Waltham, MA). Column chromatography (CC) was performed on Diaion HP-20 (Mitsubishi chemical Corp., Japan), silica gel 60 (230–400 mesh, Merck, Germany), and octadecyl silica (ODS) gel (Cosmosil 75$C_{18}$-OPN (Nacalai Tesque, Kyoto, Japan; $\Phi$ = 35 mm, $L$ = 350 mm), and TLC was performed on precoated silica gel plates 60 $GF_{254}$ (0.25 mm in thickness, Merck). HPLC was performed on ODS gel (Cosmosil 5$C_{18}$-AR, Nacalai Tesque, Kyoto, 10 mm, 250 mm, flow rate 2.5 mL/min) with a mixture of $H_2O$, acetone and MeOH, and the elute was monitored by refractive index and/or a UV detector. An amino column (Shodex Asahipak NH2P-50 4E (4.6 mm x 250 mm), $CH_3CN$-$H_2O$ (3:1) 1mL/min) together with a chiral detector (Jasco OR-2090*plus*) for HPLC analysis of sugars obtained after hydrolysis.

### 2.5.2. Plant material

Aerial part of *Cadaba rotundifolia* were collected from western region, near Makkah, Saudi Arabia, in April 2017. The collected plant was identified and classified by Nafee AlOthaiqi and Prof. Dr. Kadry AbdelKhalil, a plant taxonomist at Biology Department – Umm Al-Qura University, Makkah, Saudi Arabia. A voucher specimen (No. 15501) was deposited in the Herbarium of the Department of Pharmacognosy, Pharmacy college, King Saud University.

### 2.5.3. isolated compounds

*Kaempferol 3-O-[2-O-(trans-feruloyl)-3-O-β-D-glucopyranosyl]-β-D-glucopyranoside* (**26**)

Yellow amorphous powder $[\alpha]^{22}_{D}$ –79.0 (*c* 0.42, MeOH); HR-ESI-MS: *m/z*: 809.1888 $[M+Na]^+$ (calcd for $C_{37}H_{38}O_{19}Na$ 809.1899); UV $\lambda_{max}$ (MeOH) nm (log ε): 327 (4.21), 299 (4.12), 267 (4.13), 231 (4.23); IR (film) $\nu_{max}$: 3388, 2936, 1710, 1658, 1604, 1513, 1446, 1363, 1176, 1070, 1028 $cm^{-1}$; $^1H$ and $^{13}C$ data see Table 10.

*Kaempferol 3-O-β-neohesperidoside-7-O-[2-O-(cis-p-coumaroyl)-3-O-β-D-glucopyranosyl]-β-D-glucopyranoside* (**27**)

Yellow amorphous powder $[\alpha]^{22}_{D}$ +14.5 (*c* 0.60, MeOH); HR-ESI-MS: *m/z*: 1087.2875 $[M+Na]^+$ (calcd for $C_{48}H_{56}O_{27}Na$ 1087.2901); UV $\lambda_{max}$ (MeOH) nm (log ε): 351 (3.97), 316 (4.14), 267 (4.04), 229 (3.99); IR (film) $\nu_{max}$: 3397, 2924, 1721, 1657, 1603, 1512, 1442, 1367, 1157, 1072, 1024 $cm^{-1}$; $^1H$ and $^{13}C$ data see Tables 11.

*Kaempferol 3-O-[2,6-di-O-α-L--rhamnopyranosyl]-β-D-glucopyranoside-7-O-[6-O-(trans-feruloyl)]-β-D-glucopyranoside* (**28**)

Yellow amorphous powder $[\alpha]^{22}_{D}$ –82.5 (*c* 1.02, MeOH); HR-ESI-MS: *m/z*: 1101.3021 $[M+Na]^+$ (calcd for $C_{49}H_{58}O_{27}Na$ 1101.3058); UV $\lambda_{max}$ (MeOH) nm (log ε): 329 (4.17), 395 (4.00), 268 (4.05), 233 (4.11); IR (film) $\nu_{max}$: 3389, 2932, 1712, 1651, 1601, 1513, 1455, 1371, 1180, 1071, 1024 $cm^{-1}$; $^1H$ and $^{13}C$ data see Tables 12 and 13.

*kaempferol 3-O-[2,6-di-O-α-L-rhamnopyranosyl]-β-D-glucopyranoside-7-O-[6-O-(trans-p-coumaoyll)]-β-D-glucopyranoside* (**29**)

Yellow amorphous powder $[\alpha]^{22}_{D}$ –81.6 (*c* 0.36, MeOH); HR-ESI-MS: *m/z*: 1071.2925 $[M+Na]^+$ (calcd for $C_{48}H_{56}O_{26}Na$ 1071.2952); UV $\lambda_{max}$ (MeOH) nm (log ε): 348 (4.01), 317 (4.15), 267 (4.05), 228 (4.09); IR (film) $\nu_{max}$: 3379, 2912, 1721, 1660, 1601, 1499, 1445, 1372, 1172, 1074, 1034 $cm^{-1}$; $^1H$ and $^{13}C$ data see Tables 12 and 13.

*Kaempferol 3-O-[2-O-(trans-p-coumaroyl)-3-O-β-D-glucopyranosyl]-β-D-glucopyranoside* (**30**) [54]

Yellow amorphous powder, HR-ESI-MS: *m/z*: 779.1789 $[M+Na]^+$ (calcd for $C_{36}H_{36}O_{18}Na$ 779.1794); $^1H$ NMR ($CD_3OD$) $\delta$: 3.20 (1H, dd, $J$ = 8.5, 7.8 Hz, H-2‴), 3.29 (1H, t, $J$ = 8.5 Hz, H-4‴), 3.29 (1H, t, $J$ = 8.5 Hz, H-3‴), 3.34 (1H, m, H-5‴), 3.38 (1H, ddd, $J$ = 9.0, 6.0, 2.0 Hz, H-5″), 3.54 (1H, t, $J$ = 9.0 Hz, H-4″), 3.61 (1H, dd, $J$ = 12.0, 5.5 Hz, $H_1$-6‴), 3.64 (1H, dd, $J$ = 12.0, 6.0 Hz, $H_1$-6″), 3.81 (1H, dd, $J$ = 12.0, 2.0 Hz, $H_1$-6″), 3.88 (1H, dd, $J$ = 12.0, 2.0 Hz, $H_1$-6‴), 3.91 (1H, t, $J$ = 9.0 Hz, H-3″), 4.43 (1H, d, $J$ = 7.8 Hz, H-1‴), 5.22 (1H, dd, $J$ = 9.0, 8.0 Hz, H-2″), 5.74 (1H, d, $J$ = 8.0 Hz, H-1″), 6.17 (1H, d, $J$ = 2.0 Hz, H-6), 6.37 (1H, d, $J$ = 2.0 Hz, H-8), 6.37 (1H, br d, $J$ = 16.0 Hz, H-8‴), 6.82 (2H, d, $J$ = 8.5 Hz, H-3‴, 5‴), 6.91 (2H, d, $J$ = 8.5 Hz, H-3′, 5′), 7.48 (2H, d, $J$ = 8.5 Hz, H-2‴, 6‴), 7.68 (1H, br d, $J$ = 16.0 Hz, H-7‴), 8.01 (2H, d, $J$ = 8.5 Hz, H-2′, 6′).

*Kaempferol 3-O-β-neohesperidoside-7-O-[2-O-(trans-p-coumaroyl)-3-O-β-D-glucopyranosyl]-β-D-glucopyranoside* (**31**) [55]

Yellow amorphous powder, HR-ESI-MS: *m/z*: 1087.2875 $[M+Na]^+$ (calcd for $C_{48}H_{56}O_{27}Na$ 1087.2901); $^1H$ NMR ($CD_3OD$) $\delta$: 0.96 (3H, d, $J$ = 6.0 Hz, H-6 Rha), 3.22 (1H, dd, $J$ = 9.0, 8.0 Hz, H-2⁗), 3.25 (1H, ddd, $J$ = 9.0, 5.5, 1.5 Hz, H-5⁗), 3.27 (1H, m, H-4″), 3.29 (1H, m, H-4⁗), 3.31 (1H, m, H-3⁗), 3.31 (1H, m, H-5″), 3.35 (1H, m, H-4 Rha), 3.51 (1H, dd, $J$ = 12.0, 5.5 Hz, $H_1$-6″), 3.58 (1H, t, $J$ = 9.0 Hz, H-3″), 3.63 (1H, dd, $J$ = 9.0, 7.0 Hz, H-2″), 3.64 (1H, dd, $J$ = 12.0, 1.5 Hz, $H_1$-6⁗), 3.68 (1H, m, H-4‴), 3.70 (1H, m, H-5‴), 3.73 (1H, dd, $J$ = 12.0, 2.0 Hz, $H_1$-6″), 3.78 (1H, dd, $J$ = 12.0, 5.5 Hz, $H_1$-6⁗), 3.80 (1H, m, H-3 Rha), 3.92 (1H, dd, $J$ = 12.0, 2.0 Hz, $H_1$-6‴), 3.98 (1H, m, H-3‴), 3.99 (1H, m, $H_1$-6‴), 4.01 (1H, m, H-2 Rha), 4.02 (1H, m, H-5 Rha), 4.46 (1H, d, $J$ = 8.0 Hz, H-1⁗), 5.24 (1H, d, $J$ = 1.0 Hz, H-1 Rha), 5.29 (1H, dd, $J$ = 9.0, 8.0 Hz, H-2‴), 5.36 (1H, d, $J$ = 8.0 Hz, H-1‴), 5.75 (1H, d, $J$ = 7.0 Hz, H-1″), 6.37 (1H, d, $J$ = 2.0 Hz, H-6), 6.40 (1H, br d, $J$ = 16.0 Hz, H-8⁗), 6.67 (1H, d, $J$ = 2.0 Hz, H-8), 6.79 (2H, d, $J$ = 9.0 Hz, H-3⁗, 5⁗), 6.91 (2H, d, $J$ = 9.0 Hz, H-3′,5′), 7.47 (2H, d, $J$ = 9.0 Hz, H-2⁗, 6⁗), 7.70 (1H, br d, $J$ = 16.0 Hz, H-7⁗), 8.09 (2H, d, $J$ = 9.0 Hz, H-2′, 6′), and $^{13}C$ NMR ($CD_3OD$) $\delta$: 17.5 ($CH_3$-6 Rha), 62.3 ($CH_2$-6‴), 62.6 ($CH_2$-6″), 62.6 ($CH_2$-6⁗), 69.8 (CH-4‴), 69.9 (CH-5 Rha), 71.3 (CH-4⁗), 71.8 (CH-4″), 72.3 (CH-3 Rha), 72.4 (CH-2 Rha), 73.6 (CH-2‴), 74.0 (CH-4 Rha), 74.7 (CH-2⁗), 77.7 (CH-3⁗), 78.1 (CH-5⁗), 78.1 (CH-5‴), 78.3 (CH-5″), 78.9 (CH-3″), 80.0 (CH-2″), 84.7 (CH-3‴), 95.8 (CH-8), 99.6 (CH-1‴), 100.2 (CH-6), 100.2 (CH-1″), 102.6 (CH-1

Rha), 105.0 (CH-1′′′′), 107.9 (C-10), 114.9 (CH-8′′′), 116.2 (CH-3′,5′), 116.8 (CH-3′′′,5′′′), 122.9 (CH-1′), 127.2 (CH-1′′′), 131.4 (CH-2′′′,6′′′), 132.3 (CH-2′,6′), 134.7 (C-3), 147.5 (CH-7′′′), 157.8 (C-9), 159.2 (C-2), 161.4 (CH-4′′′), 161.5 (C-4′), 162.9 (C-5), 163.8 (C-7), 168.3 (C-9′′′), 179.5 (C-4).

*Kaempferol 3-O-β-neohesperidoside-7-O-[2-O-(trans-feruloyl)]-β-D-glucopyranoside* (**32**) [55]

Yellow amorphous powder, HR-ESI-MS: *m/z*: 955.2458 $[M+Na]^+$ (calcd for $C_{43}H_{48}O_{23}Na$ 955.2479); $^1H$ NMR ($CD_3OD$) *δ*: 0.96 (3H, d, *J* = 6.5 Hz, H-6 Rha), 3.24 (1H, ddd, *J* = 8.5, 6.0, 2.0 Hz, H-5′′), 3.29 (1H, t, *J* = 8.5 Hz, H-4′′), 3.37 (1H, m, H-4 Rha), 3.50 (1H, dd, *J* = 12.0, 6.0 Hz, H-6′′), 3.55 (1H, t, *J* = 9.0 Hz, H-4′′′), 3.59 (1H, t, *J* = 8.5 Hz, H-3′′), 3.63 (1H, dd, *J* = 8.5, 7.5 Hz, H-2′′), 3.64 (1H, m, H-5′′′), 3.73 (1H, dd, *J* = 12.0, 2.0 Hz, H-6′′), 3.77 (1H, m, H-6′′′), 3.78 (1H, m, H-3′′′), 3.79 (1H, m, H-3 Rha), 3.98 (1H, dd, *J* = 12.0, 1.5 Hz, H-6′′′), 4.01 (1H, m, H-2 Rha), 4.05 (1H, m, H-5 Rha), 5.14 (1H, dd, *J* = 9.0, 8.0 Hz, H-2′′′), 5.24 (1H, d, *J* = 1.0 Hz, H-1 Rha), 5.35 (1H, d, *J* = 8.0 Hz, H-1′′′), 5.75 (1H, d, *J* = 7.5 Hz, H-1′′), 6.38 (1H, d, *J* = 2.0 Hz, H-6), 6.43 (1H, br d, *J* = 16.0 Hz, H-8′′′′), 6.69 (1H, d, *J* = 2.0 Hz, H-8), 6.80 (1H, d, *J* = 8.0 Hz, H-5′′′′), 6.90 (2H, d, *J* = 9.0 Hz, H- H-3′, 5′), 6.07 (1H, dd, *J* = 8.0, 1.5 Hz, H-6′′′′), 7.19 (1H, d, *J* = 1.5 Hz, H-2′′′′), 7.70 (1H, br d, *J* = 16.0 Hz, H-7′′′), 8.07 (2H, d, *J* = 8.5, Hz, H-2′, 6′), and $^{13}C$ NMR ($CD_3OD$) *δ*: 17.5 ($CH_3$-6 Rha), 62.3 ($CH_2$-6′′′), 62.6 ($CH_2$-6′′), 69.9 (CH-5 Rha), 71.3 (CH-4′′′), 71.8 (CH-4′′), 72.3 (CH-3 Rha), 72.4 (CH-2 Rha), 74.0 (CH-4 Rha), 74.8 (CH-2′′′), 76.0 (CH-3′′′), 78.3 (CH-5′′′), 78.5 (CH-5′′), 78.9 (CH-3′′), 80.0 (CH-2′′), 95.7 (CH-8), 99.7 (CH-1′′′), 100.5 (CH-6), 102.6 (CH-1 Rha), 107.9 (C-10), 111.7 (CH-2′′′′), 115.5 (CH-8′′′′), 116.1 (CH-3′,5′), 116.4 (CH-5′′′′), 122.9 (CH-1′), 124.3 (CH-6′′′′), 127.8 (CH-1′′′′), 132.3 (CH-2′,6′), 134.7 (C-3), 147.5 (CH-7′′′′), 149.3 (CH-3′′′′), 150.6 (CH-4′′′′), 157.9 (C-9), 159.2 (C-2), 161.3 (CH-4′′′′), 161.5 (C-4′), 162.9 (C-5), 164.0 (C-7), 168.5 (C-9′′′′), 179.5 (C-4).

*Kaempferol 3-O-β-neohesperidoside-7-O-[2-O-(trans-p-coumaroyl)]-β-D-glucopyranoside* (**33**) [55]

Yellow amorphous powder, HR-ESI-MS: *m/z*: 925.2356 $[M+Na]^+$ (calcd for $C_{42}H_{46}O_{22}Na$ 925.2373); $^1H$ NMR ($CD_3OD$) *δ*: 0.96 (3H, d, *J* = 6.0 Hz, H-6 Rha), 3.23 (1H, ddd, *J* = 9.0, 5.5,

2.0 Hz, H-5″), 3.28 (1H, t, *J* = 9.0 Hz, H-4″), 3.37 (1H, m, H-4 Rha), 3.51 (1H, dd, *J* = 12.0, 5.5 Hz, H$_1$-6″), 3.55 (1H, t, *J* = 9.0 Hz, H-4‴), 3.58 (1H, t, *J* = 9.0 Hz, H-3″), 3.63 (1H, dd, *J* = 9.0, 7.5 Hz, H-2″), 3.64 (1H, m, H-5‴), 3.73 (1H, dd, *J* = 12.0, 2.0 Hz, H$_1$-6″), 3.76 (1H, m, H$_1$-6‴), 3.78 (1H, m, H-3‴), 3.79 (1H, m, H-3 Rha), 3.98 (1H, dd, *J* = 12.0, 1.5 Hz, H$_1$-6‴), 4.02 (1H, m, H-2 Rha), 4.05 (1H, m, H-5 Rha), 5.13 (1H, dd, *J* = 9.0, 8.0 Hz, H-2‴), 5.25 (1H, d, *J* = 1.0 Hz, H-1 Rha), 5.36 (1H, d, *J* = 8.0 Hz, H-1‴), 5.75 (1H, d, *J* = 7.5 Hz, H-1″), 6.38 (1H, d, *J* = 2.0 Hz, H-6), 6.40 (1H, br d, *J* = 16.0 Hz, H-8‴), 6.70 (1H, d, *J* = 2.0 Hz, H-8), 6.79 (2H, d, *J* = 8.5 Hz, H-3‴, 5‴), 6.90 (2H, d, *J* = 8.5 Hz, H-3′,5′), 7.46 (2H, d, *J* = 8.5 Hz, H-2‴, 6‴), 7.70 (1H, br d, *J* = 16.0 Hz, H-7‴), 8.08 (2H, d, *J* = 8.5 Hz, H-2′, 6′), and $^{13}$C NMR ($CD_3OD$) *δ*: 17.5 ($CH_3$-6 Rha), 62.3 ($CH_2$-6‴), 62.6 ($CH_2$-6″), 69.9 (CH-5 Rha), 71.3 (CH-4‴), 71.8 (CH-4″), 72.3 (CH-3 Rha), 72.4 (CH-2 Rha), 74.0 (CH-4 Rha), 74.8 (CH-2‴), 76.0 (CH-3‴), 78.3 (CH-5‴), 78.5 (CH-5″), 78.9 (CH-3″), 80.0 (CH-2″), 95.7 (CH-8), 99.7 (CH-1‴), 100.5 (CH-6), 102.6 (CH-1 Rha), 107.9 (C-10), 114.8 (CH-8‴), 116.1 (CH-3′,5′), 116.8 (CH-3‴,5‴), 122.9 (CH-1′), 127.1 (CH-1‴), 131.3 (CH-2‴,6‴), 132.3 (CH-2′,6′), 134.7 (C-3), 147.3 (CH-7‴), 157.9 (C-9), 159.2 (C-2), 161.3 (CH-4‴), 161.5 (C-4′), 162.9 (C-5), 164.0 (C-7), 168.3 (C-9‴), 179.5 (C-4).

*Kaempferol 3,4′-di-O-β-D-glucoside* (**34**) [99]

Yellow amorphous powder, HR-ESI-MS: *m/z*: 633.1427 $[M+Na]^+$ (calcd for $C_{27}H_{30}O_{16}Na$ 633.1426); $^1$H NMR ($CD_3OD$) *δ*: 3.21 (2H, m, H-5″, 5‴), 3.31 (1H, m, H-4″), 3.43 (1H, m, H-4‴), 3.43 (1H, m, H-3″), 3.45 (1H, m, H-2″), 3.53 (1H, m, H-3‴), 3.54 (1H, m, H-2‴), 3.54 (1H, m, H$_1$-6″), 3.71 (1H, m, H$_1$-6″, 6‴), 3.71 (1H, m, H$_1$-6‴),5.06 (1H, d, *J* = 7.0 Hz, H-1‴), 5.30 (1H, d, *J* = 7.5 Hz, H-1″), 6.24 (1H, d, *J* = 2.0 Hz, H-6), 6.34 (1H, d, *J* = 2.0 Hz, H-8), 7.22 (2H, d, *J* = 8.5 Hz, H-3′, 5′), 8.15 (2H, d, *J* = 8.5, Hz, H-2′, 6′), and $^{13}$C NMR ($CD_3OD$) *δ*: 62.5 ($CH_2$-6″), 62.6 ($CH_2$-6‴), 71.3 (CH-4″), 71.4 (CH-4‴), 74.9 (CH-2″), 75.7 (CH-2‴), 78.0 (CH-5″), 78.0 (CH-5‴), 78.3 (CH-3″), 78.3 (CH-3‴), 94.8 (CH-8), 100.0 (CH-6), 101.8 (CH-1‴), 104.0 (CH-1″), 105.9 (C-10), 117.2 (CH-3′,5′), 125.7 (CH-1′), 132.1 (CH-2′,6′), 135.9 (C-3), 158.5 (C-9), 158.6 (C-2), 161.1 (C-4′), 163.2 (C-5), 166.3 (C-7), 179.5 (C-4).

*Kaempferol 3-O-[2,6-di-O-α-L-rhamnopyranosyl]-β-D-glucoside* (**35**) [100]

Yellow amorphous powder, HR-ESI-MS: *m/z*: 763.1375 $[M+Na]^+$ (calcd for $C_{33}H_{40}O_{19}Na$ 763.2056); $^1H$ NMR ($CD_3OD$) $\delta$: 1.00 (3H, d, $J$ = 6.3 Hz, H-6 Rha I), 1.10 (3H, d, $J$ = 6.3 Hz, H-6 Rha II), 3.26 (1H, t, $J$ = 9.0 Hz , H-4 Rha II), 3.27 (1H, t, $J$ = 9.0 Hz , H-4″), 3.35 (1H, t, $J$ = 9.5 Hz , H-4 Rha I), 3.36 (1H, m, H-5″), 3.38 (1H, m, $H_1$-6″), 3.44 (1H, dq, $J$ = 9.0, 6.3 Hz, H-5 Rha II), 3.50 (1H, dd, $J$ = 9.0, 3.5 Hz, H-3 Rha II), 3.57 (1H, t, $J$ = 9.0 Hz, H-3″), 3.61 (1H, m, H-2 Rha II), 3.71 (1H, dd, $J$ = 9.0, 7.7 Hz, H-2″), 3.82 (1H, dd, $J$ = 9.0, 3.5 Hz, H-3 Rha I), 3.84 (1H, br d, $J$ = 12.0 Hz, $H_1$-6″), 4.02 (1H, m, H-2 Rha I), 4.08 (1H, dq, $J$ = 9.5, 6.3 Hz, H-5 Rha I), 4.52 (1H, d, $J$ = 1.0 Hz, H-1 Rha II), 5.24 (1H, d, $J$ = 1.0 Hz, H-1 Rha I), 5.62 (1H, d, $J$ = 7.7 Hz, H-1″), 6.20 (1H, d, $J$ = 2.0 Hz, H-6), 6.39 (1H, d, $J$ = 2.0 Hz, H-8), 6.91 (2H, d, $J$ = 9.0 Hz, H-3′,5′), 8.04 (2H, d, $J$ = 9.0 Hz, H-2′, 6′), and $^{13}C$ NMR ($CD_3OD$) $\delta$: 17.6 ($CH_3$-6 Rha I), 17.9 ($CH_3$-6 Rha II), 68.3 ($CH_2$-6″), 69.7 (CH-5 Rha I), 69.9 (CH-5 Rha II), 71.9 (CH-4″), 72.1 (CH-3 Rha II), 72.3 (CH-2 Rha II), 72.3 (CH-3 Rha I), 72.4 (CH-2 Rha I), 73.8 (CH-4 Rha II), 74.0 (CH-4 Rha I), 77.0 (CH-5″), 78.9 (CH-3″), 79.9 (CH-2″), 94.8 (CH-8), 99.8 (CH-6), 100.5 (CH-1″), 102.3 (CH-1 Rha II), 102.6 (CH-1 Rha I), 105.9 (C-10), 116.1 (CH-3′,5′), 123.1 (CH-1′), 132.2 (CH-2′,6′), 134.3 (C-3), 158.5 (C-9), 159.0 (C-4′), 161.5 (C-2), 163.1 (C-5), 165.7 (C-7), 179.3 (C-4).

*Kaempferol 3-O-β-neohesperidoside* (**36**) [100]

Yellow amorphous powder, HR-ESI-MS: *m/z*: 617.1477 $[M+Na]^+$ (calcd for $C_{27}H_{30}O_{15}Na$ 617.1477); $^1H$ NMR ($CD_3OD$) $\delta$: 0.98 (3H, d, $J$ = 6.5 Hz, H-6 Rha), 3.26 (1H, ddd, $J$ = 9.0, 5.5. 2.0 Hz, H-5″), 3.30 (1H, m , H-4″), 3.37 (1H, t, $J$ = 9.0 Hz , H-4 Rha), 3.53 (1H, dd, $J$ = 12.0, 5.5 Hz, $H_1$-6″), 3.59 (1H, t, $J$ = 9.0 Hz, H-3″), 3.64 (1H, dd, $J$ = 9.0, 7.5 Hz, H-2″), 3.76 (1H, dd, $J$ = 12.0, 2.0 Hz, $H_1$-6″), 3.81 (1H, dd, $J$ = 9.0, 3.5 Hz, H-3 Rha), 4.03 (1H, dd, $J$ = 3.5, 1.5 Hz , H-2 Rha), 4.06 (1H, dq, $J$ = 9.0, 6.5 Hz, H-5 Rha), 5.24 (1H, d, $J$ = 1.5 Hz, H-1 Rha), 5.76 (1H, d, $J$ = 7.5 Hz, H-1″), 6.19 (1H, d, $J$ = 1.5 Hz, H-6), 6.39 (1H, d, $J$ = 1.5 Hz, H-8), 6.91 (2H, d, $J$ = 9.0 Hz, H-3′,5′), 8.06 (2H, d, $J$ = 9.0 Hz, H-2′, 6′), and $^{13}C$ NMR ($CD_3OD$) $\delta$: 17.5 ($CH_3$-6 Rha), 62.6 ($CH_2$-6″), 69.9 (CH-5 Rha), 71.8 (CH-4″), 72.2 (CH-3 Rha), 72.4 (CH-2 Rha), 74.0 (CH-4 Rha), 78.3 (CH-5″), 78.9 (CH-3″), 80.0 (CH-2″), 94.6 (CH-8), 99.7 (CH-6), 100.2 (CH-1″), 102.6 (CH-1 Rha), 105.9 (C-10), 116.1 (CH-3′,5′), 123.0 (CH-1′), 132.1 (CH-2′,6′), 134.4 (C-3), 158.4 (C-9), 158.5 (C-4′), 161.3 (C-2), 163.1 (C-5), 165.6 (C-7), 179.3 (C-4).

*Kaempferol 3-O-β-rutinoside* (**37**) [100]

Yellow amorphous powder, HR-ESI-MS: *m/z*: 617.1477 $[M+Na]^+$ (calcd for $C_{27}H_{30}O_{15}Na$ 617.1477); $^1H$ NMR ($CD_3OD$) $\delta$: 1.11 (3H, d, $J$ = 6.5 Hz, H-6 Rha), 3.23 (1H, t, $J$ = 9.0 Hz , H-4″), 3.27 (1H, t, $J$ = 9.5 Hz , H-4 Rha), 3.30 (1H, m, H-5″), 3.37 (1H, dd, $J$ = 12.0, 6.5 Hz,, $H_1$-6″), 3.40 (1H, t, $J$ = 9.0 Hz, H-3″), 3.43 (1H, dd, $J$ = 9.0, 7.5 Hz, H-2″), 3.44 (1H, m, H-5 Rha),3.51 (1H, dd, $J$ = 9.5, 3.5 Hz, H-3 Rha), 3.62 (1H, dd, $J$ = 3.5, 1.5 Hz, H-2 Rha), 3.79 (1H, br d, $J$ = 12.0, 2.0 Hz, $H_1$-6″), 4.5 (1H, d, $J$ = 1.0 Hz, H-1 Rha), 5.12 (1H, d, $J$ = 7.5 Hz, H-1″), 6.20 (1H, d, $J$ = 2.0 Hz, H-6), 6.40 (1H, d, $J$ = 2.0 Hz, H-8), 6.88 (2H, d, $J$ = 9.0 Hz, H-3′,5′), 8.05 (2H, d, $J$ = 9.0 Hz, H-2′, 6′), and $^{13}C$ NMR ($CD_3OD$) $\delta$: 17.9 ($CH_3$-6 Rha), 68.6 ($CH_2$-6″), 69.8 (CH-5 Rha), 71.4 (CH-4″), 72.1 (CH-2 Rha), 72.3 (CH-3 Rha), 73.9 (CH-4 Rha II), 75.8 (CH-2″),77.2 (CH-5″), 78.1 (CH-3″), 94.9 (CH-8), 100.0 (CH-6), 104.6 (CH-1″), 102.4 (CH-1 Rha II), 105.7 (C-10), 116.2 (CH-3′,5′), 122.8 (CH-1′), 132.4 (CH-2′,6′), 135.5 (C-3), 158.6 (C-9), 159.4 (C-4′), 161.5 (C-2), 163.0 (C-5), 166.1 (C-7), 179.4 (C-4).

*Kaempferol 3-O-β-D-glucoside* (**38**) [100]

Yellow amorphous powder, HR-ESI-MS: *m/z*: 471.0896 $[M+Na]^+$ (calcd for $C_{21}H_{20}O_{11}Na$ 471.0896); $^1H$ NMR (DMSO) $\delta$: 3.19 (1H, ddd, $J$ = 9.0, 6.0, 2.0 Hz, H-5″), 3.32 (1H, t, $J$ = 9.0 Hz , H-4″), 3.41 (1H, t, $J$ = 9.0 Hz, H-3″), 3.44 (1H, dd, $J$ = 9.0, 8.0 Hz, H-2″), 3.52 (1H, dd, $J$ = 12.0, 6.0 Hz, $H_1$-6″), 3.68 (1H, dd, $J$ = 12.0, 2.0 Hz, $H_1$-6″), 5.26 (1H, d, $J$ = 7.5 Hz, H-1″), 6.21 (1H, d, $J$ = 2.0 Hz, H-6), 6.40 (1H, d, $J$ = 2.0 Hz, H-8), 6.90 (2H, d, $J$ = 9.0 Hz, H-3′,5′), 8.06 (2H, d, $J$ = 9.0 Hz, H-2′, 6′), and $^{13}C$ NMR (DMSO) $\delta$: 61.0 ($CH_2$-6″), 70.0 (CH-4″), 74.4 (CH-2″), 76.6 (CH-5″), 77.7 (CH-3″), 93.8 (CH-8), 98.8 (CH-6), 101.0 (CH-1″), 104.1 (C-10), 115.3 (CH-3′,5′), 121.0 (CH-1′), 131.0 (CH-2′,6′), 133.3 (C-3), 156.4 (C-2), 156.5 (C-9), 160.1 (C-4′), 161.4 (C-5), 164.3 (C-7), 177.6 (C-4).

*Rhamnocitrin 3-O-β-neohesperidoside* (**39**) [101]

Yellow amorphous powder, HR-ESI-MS: *m/z*: 631.1631 $[M+Na]^+$ (calcd for $C_{28}H_{32}O_{15}Na$ 631.1631); $^1H$ NMR ($CD_3OD$) $\delta$: 0.94 (3H, d, $J$ = 6.0 Hz, H-6 Rha), 3.22 (1H, ddd, $J$ = 9.0, 5.5. 2.0 Hz, H-5″), 3.26 (1H, m , H-4″), 3.33 (1H, t, $J$ = 9.5 Hz , H-4 Rha), 3.49 (1H, dd, $J$ = 12.0, 5.5 Hz, $H_1$-6″), 3.54 (1H, t, $J$ = 9.0 Hz, H-3″), 3.61 (1H, dd, $J$ = 9.0, 7.5 Hz, H-2″), 3.72 (1H, dd, $J$ =

12.0, 2.0 Hz, $H_1$-6″), 3.76 (1H, dd, *J* = 9.5, 3.5 Hz, H-3 Rha), 3.99 (1H, dd, *J* = 3.5, 1.0 Hz , H-2 Rha), 4.01 (1H, dq, *J* = 9.5, 6.0 Hz, H-5 Rha), 5.21 (1H, d, *J* = 1.0 Hz, H-1 Rha), 5.75 (1H, d, *J* = 7.5 Hz, H-1″), 6.31 (1H, d, *J* = 1.5 Hz, H-6), 6.58 (1H, d, *J* = 1.5 Hz, H-8), 6.88 (2H, d, *J* = 9.0 Hz, H-3′,5′), 8.07 (2H, d, *J* = 9.0 Hz, H-2′, 6′), and $^{13}$C NMR ($CD_3OD$) *δ*: 17.8 ($CH_3$-6 Rha), 56.7 ($OCH_3$), 62.9 ($CH_2$-6″), 70.2 (CH-5 Rha), 72.1 (CH-4″), 72.6 (CH-3 Rha), 72.7 (CH-2 Rha), 74.3 (CH-4 Rha), 78.6 (CH-5″), 79.2 (CH-3″), 80.4 (CH-2″), 93.2 (CH-8), 99.1 (CH-6), 100.5 (CH-1″), 102.9 (CH-1 Rha), 107.1 (C-10), 116.4 (CH-3′,5′), 123.3 (CH-1′), 132.5 (CH-2′,6′), 134.9 (C-3), 158.6 (C-9), 160.1 (C-4′), 161.7 (C-2), 163.2 (C-5), 167.3 (C-7), 179.7 (C-4).

*Myricetin 3-O-[2,6-di-O-α-L-rhamnopyranosyl]-β-glucoside* (**40**) [100]

Yellow amorphous powder, HR-ESI-MS: *m/z*: 795.1944 $[M+Na]^+$ (calcd for $C_{33}H_{40}O_{21}Na$ 795.1954); $^1$H NMR ($CD_3OD$) *δ*: 1.00 (3H, d, *J* = 6.0 Hz, H-6 Rha I), 1.10 (3H, d, *J* = 6.0 Hz, H-6 Rha II), 3.25 (1H, t, *J* = 9.5 Hz , H-4 Rha II), 3.25 (1H, t, *J* = 9.0 Hz , H-4″), 3.38 (1H, t, *J* = 9.5 Hz , H-4 Rha I), 3.39 (1H, m, H-5″), 3.41 (1H, m, $H_1$-6″), 3.45 (1H, dq, *J* = 9.5, 6.0 Hz, H-5 Rha II), 3.52 (1H, dd, *J* = 9.0, 3.5 Hz, H-3 Rha II), 3.55 (1H, t, *J* = 9.0 Hz, H-3″), 3.60 (1H, dd, *J* = 3.5, 1.0 Hz, H-2 Rha II), 3.71 (1H, dd, *J* = 9.0, 8.0 Hz, H-2″), 3.82 (1H, dd, *J* = 9.0, 3.5 Hz, H-3 Rha I), 3.84 (1H, br d, *J* = 12.0 Hz, $H_1$-6″), 4.03 (1H, dd, *J* = 3.5, 1.0 Hz, H-2 Rha I), 4.13 (1H, dq, *J* = 9.5, 6.0 Hz, H-5 Rha I), 4.53 (1H, d, *J* = 1.0 Hz, H-1 Rha II), 5.23 (1H, d, *J* = 1.0 Hz, H-1 Rha I), 5.58 (1H, d, *J* = 8.0 Hz, H-1″), 6.20 (1H, d, *J* = 2.0 Hz, H-6), 6.38 (1H, d, *J* = 2.0 Hz, H-8), 7.26 (2H, s, H-2′, 6′), and $^{13}$C NMR ($CD_3OD$) *δ*: 17.5 ($CH_3$-6 Rha I), 17.8 ($CH_3$-6 Rha II), 68.3 ($CH_2$-6″), 69.7 (CH-5 Rha I), 70.1 (CH-5 Rha II), 71.8 (CH-4″), 72.2 (CH-3 Rha II), 72.3 (CH-2 Rha II), 72.3 (CH-3 Rha I), 72.4 (CH-2 Rha I), 73.9 (CH-4 Rha II), 74.1 (CH-4 Rha I), 77.0 (CH-5″), 78.8 (CH-3″), 80.3 (CH-2″), 94.7 (CH-8), 99.7 (CH-6), 100.6 (CH-1″), 102.3 (CH-1 Rha II), 102.8 (CH-1 Rha I), 105.9 (C-10), 110.2 (CH-2′,6′), 122.5 (CH-1′), 134.6 (C-3), 137.9 (C-4′), 146.4 (CH-3′,5′), 158.5 (C-9), 159.0 (C-2), 163.2 (C-5), 165.7 (C-7), 179.3 (C-4).

*Myricetin 3-O-β-neohesperidoside* (**41**) [100]

Yellow amorphous powder, HR-ESI-MS: *m/z*: 649.1375 $[M+Na]^+$ (calcd for $C_{27}H_{30}O_{17}Na$ 649.1375); $^1$H NMR ($CD_3OD$) *δ*: 1.00 (3H, d, *J* = 6.0 Hz, H-6 Rha), 3.24 (1H, ddd, *J* = 9.0, 5.5.

2.0 Hz, H-5″), 3.35 (1H, t, *J* = 9.0 Hz , H-4″), 3.38 (1H, t, *J* = 9.5 Hz , H-4 Rha), 3.58 (1H, t, *J* = 9.0 Hz, H-3″), 3.60 (1H, dd, *J* = 12.0, 5.0 Hz, $H_1$-6″), 3.72 (1H, dd, *J* = 9.0, 7.5 Hz, H-2″), 3.76 (1H, dd, *J* = 12.0, 2.0 Hz, $H_1$-6″), 3.79 (1H, dd, *J* = 9.5, 3.5 Hz, H-3 Rha), 4.03 (1H, dd, *J* = 3.5, 1.0 Hz , H-2 Rha), 4.07 (1H, dq, *J* = 9.5, 6.0 Hz, H-5 Rha), 5.23 (1H, d, *J* = 1.0 Hz, H-1 Rha), 5.78 (1H, d, *J* = 7.5 Hz, H-1″), 6.19 (1H, d, *J* = 2.0 Hz, H-6), 6.38 (1H, d, *J* = 2.0 Hz, H-8), 7.26 (2H, d, s, H-2′, 6′), and $^{13}$C NMR ($CD_3OD$) *δ*: 17.4 ($CH_3$-6 Rha), 62.5 ($CH_2$-6″), 70.0 (CH-5 Rha), 71.8 (CH-4″), 72.2 (CH-3 Rha), 72.4 (CH-2 Rha), 74.0 (CH-4 Rha), 78.2 (CH-5″), 78.9 (CH-3″), 80.2 (CH-2″), 94.4 (CH-8), 99.5 (CH-6), 100.0 (CH-1″), 102.7 (CH-1 Rha), 105.8 (C-10), 109.8 (CH-2′,6′), 122.3 (CH-1′), 134.6 (C-3), 137.7 (C-4′), 146.4 (CH-3′,5′), 158.3 (C-9), 158.4 (C-2), 163.8 (C-5), 165.6 (C-7), 179.3 (C-4).

*Myricetin 3-O-β-D-glucoside* (**42**) [100]

Yellow amorphous powder, HR-ESI-MS: *m/z*: 503.0796 $[M+Na]^+$ (calcd for $C_{21}H_{20}O_{13}Na$ 503.0796); $^1$H NMR (DMSO) *δ*: 3.22 (1H, ddd, *J* = 9.0, 5.4, 2.0 Hz, H-5″), 3.31 (1H, t, *J* = 9.0 Hz , H-4″), 3.45 (1H, t, *J* = 9.0 Hz, H-3″), 3.46 (1H, dd, *J* = 9.0, 7.7 Hz, H-2″), 3.60 (1H, dd, *J* = 12.0, 5.4 Hz, $H_1$-6″), 3.60 (1H, dd, *J* = 12.0, 2.0 Hz, $H_1$-6″), 5.47 (1H, d, *J* = 7.7 Hz, H-1″), 6.20 (1H, d, *J* = 2.0 Hz, H-6), 6.38 (1H, d, *J* = 2.0 Hz, H-8), 7.19 (2H, s, H-2′, 6′), and $^{13}$C NMR (DMSO) *δ*: 61.5 ($CH_2$-6″), 70.3 (CH-4″), 74.3 (CH-2″), 77.0 (CH-5″), 78.1 (CH-3″), 93.7 (CH-8), 99.0 (CH-6), 101.2 (CH-1″), 104.4 (C-10), 108.9 (CH-2′,6′), 120.4 (CH-1′), 133.9 (C-3), 137.1 (C-4′), 145.8 (CH-3′,5′), 156.9 (C-9), 156.7 (C-2), 161.7 (C-5), 164.5 (C-7), 177.8 (C-4).

*Myricetin* (**43**) [102]

Yellow amorphous powder, HR-ESI-MS: *m/z*: 317.0986 $[M–H]^-$ (calcd for $C_{15}H_9O_8$ 317.0268); $^1$H NMR (DMSO) *δ*: 6.20 (1H, d, *J* = 1.5 Hz, H-6), 6.38 (1H, d, *J* = 1.5 Hz, H-8), 7.24 (2H, s, H-2′, 6′), and $^{13}$C NMR (DMSO) *δ*: 93.6 (CH-8), 98.6 (CH-6), 103.4 (C-10), 107.6 (CH-2′,6′), 121.3 (CH-1′), 136.3 (C-3), 146.1 (CH-3′,5′), 147.2 (C-4′), 156.5 (C-9), 156.5 (C-2), 161.7 (C-5), 164.3 (C-7), 176.2 (C-4).

*Beitingxinhuagtong C* (**44**) [103]

Yellow amorphous powder, HR-ESI-MS: *m/z*: 621.1788 $[M+Na]^+$ (calcd for $C_{27}H_{34}O_{15}Na$ 621.1790); $^1H$ NMR ($CD_3OD$) $\delta$: 2.90 (2H, t, $J$ = 7.5 Hz, H-9), 3.31 (2H, m, H-4″, H-4‴), 3.45 (1H, m, H-2″), 3.47 (2H, m, H-8), 3.49 (2H, m, H-3″, 3‴), 3.54 (1H, m, H-2‴), 3.63 (2H, m, H-5″, 5‴), 3.68 (1H, m, $H_1$-6″, 6‴), 3.95 (1H, d, $J$ = 12.0 Hz, $H_1$-6″, 6‴), 5.04 (1H, d, $J$ = 7.0 Hz, H-1‴), 5.13 (1H, d, $J$ = 7.5 Hz, H-1″), 6.24 (1H, d, $J$ = 2.0 Hz, H-3), 6.49 (1H, d, $J$ = 2.0 Hz, H-5), 6.70 (2H, d, $J$ = 8.5 Hz, H-3′, 5′), 7.07 (2H, d, $J$ = 8.5, Hz, H-2′, 6′), and $^{13}C$ NMR ($CD_3OD$) $\delta$: 30.7 ($CH_2$-9), 47.3 ($CH_2$-8), 62.8 ($CH_2$-6″), 62.8 ($CH_2$-6‴), 71.5 (CH-4″), 71.6 (CH-4‴), 74.7 (CH-2″), 74.7 (CH-2‴), 77.8 (CH-3″), 78.4 (CH-3‴), 78.5 (CH-5″), 78.5 (CH-5‴), 95.5 (CH-5), 99.7 (CH-3), 101.0 (CH-1″), 101.8 (CH-1‴), 108.4 (CH-1), 116.1 (CH-3′, 5′), 130.4 (CH-2′,6′), 133.7 (C-1′), 156.4 (C-4′), 161.7 (C-4), 164.6 (C-2), 166.5 (C-6), 207.1 (C-7).

*Phloretin* (**45**) [104]

Yellow amorphous powder, HR-ESI-MS: *m/z*: 297.0733 $[M+Na]^+$ (calcd for $C_{15}H_{14}O_5Na$ 297.0733); $^1H$ NMR ($CD_3OD$) $\delta$: 2.85 (2H, t, $J$ = 7.5 Hz, H-9), 3.27 (2H, t, $J$ = 7.5 Hz, H-8), 5.85 (2H, d, $J$ = 2.0 Hz, H-3, 5), 6.72 (2H, d, $J$ = 8.5 Hz, H-3′, 5′), 7.05 (2H, d, $J$ = 8.5, Hz, H-2′, 6′), and $^{13}C$ NMR ($CD_3OD$) $\delta$: 31.4 ($CH_2$-9), 47.2 ($CH_2$-8), 95.8 (CH-3, 5), 105.3 (CH-1), 116.1 (CH-3′, 5′), 130.3 (CH-2′,6′), 134.0 (C-1′), 156.2 (C-4′), 165.7 (C-4), 166.0 (C-2), 166.0 (C-6), 206.5 (C-7).

2.5.4. Acid hydrolysis of **26** – **29**

The isolated compounds **26** – **29** (1.0 mg each) were hydrolyzed with 1 M HCl (1.0 mL) at 80 ºC for 3hr. After cooling, the reaction mixtures were neutralized with Amberlite IRA96SB ($OH^-$ form), and the resin was removed by filtration. Then, the filtrates were extracted with EtOAc. The aqueous layers were analyzed by HPLC with an amino column [Asahipak NH2P-50 4E, $CH_3CN$-$H_2O$ (3:1), 1mL/min] and a chiral detector (JASCO OR-2090plus) in comparison with D-glucose as authentic standard. The aqueous layers of hydrolyzed compounds showed peak at $t_R$ 8.1 min which coincided with that of D-glucose (positive optical rotation). The $t_R$ of the L-rhamnose (negative optical rotation) was 6.5 min [46].

2.5.5. Alkaline hydrolysis of **26** – **28**

Compounds **26** – **28** (3.0 mg each) were prepared as solutions in 50% aqueous 1,4-dioxane (0.5 mL). These solutions were treated with 10% aqueous KOH (0.5 mL) and stirred at 37 ºC 1 h. The reaction mixtures were neutralized with an ion-exchange resin Amberlite IR-120B ($H^+$-form), then filtrated and evaporated. The residues were dissolved in EtOAc and subjected to HPLC analysis [Cosmosil C18-PAQ, MeOH-$H_2O$ (45:50), 1mL/min)] with UV (254 nm) detector to identify the ferulic acid ($t_R$ 16.7 min) from **26** and **28**, and *cis*-*p*-coumaric acid ($t_R$ 15.1 min) from **27** [47]. The authentic *cis*-*p*-coumaric acid was prepared according to the literature [105].

2.5.6. DPPH radical scavenging activity

Free radical scavenging activity were evaluated by using a quantitative DPPH assay. The absorbance of various concentrations of test compounds dissolved in 100 $\mu$L of MeOH in 96-well microtiter plate were measured at 515 nm as ($A_{blank}$). Then, a 100 $\mu$L of DPPH solution (200 $\mu$M) was added to each well. The plate was incubated in dark chamber at room temperature for 30 min before measuring the absorbance ($A_{sample}$) again. The following equation was used to calculate % inhibition of free radicals:

$$\% \text{ Inhibition} = [1 - (A_{sample} - A_{blank})/ (A_{control} - A_{blank})] \times 100$$

where $A_{control}$ is the absorbance of control (DMSO and all reagents, except test compound). Their $IC_{50}$ values were determined based on three independent experiments [48].

2.5.7. Collagenase inhibition assay

Collagenase inhibitory activity was examined using the modified method described by Teramachi *et*. *al*. (2005). Briefly, the test compounds, enzyme solution (final concentrations of collagenase: 10 µg/mL) and 50 mM Tricine buffer (pH 7.5) were added to 96-well microtiter plate, and preincubated for 10 min at 37 °C. Afterwards, the substrate solution ((7-methoxycoumarin-4-yl) acetyl-L-prolyl-L-leucyl-[$N^{\beta}$-(2,4-dinitrophenyl)-L-2,3-diaminopropionyl]-L-alanyl-L-arginine amide) at final concentration of 10 µM was added to initiate the reaction. The fluorescence values were measured at an excitation of 320 nm and emission of 405 nm after 0 min and 30 min

incubation at 37 °C using a fluorescence plate reader (EnSpire, PerkinElmer Japan). These assays were performed in triplicate using caffeic acid as a positive control and the concentrations required for 50% inhibition ($IC_{50}$) of the intensity of fluorescence were determined graphically [106].

2.5.8. Determination of AGEs formation in vitro

The reaction mixture, 10 mg/mL of bovine serum albumin in 50 mM phosphate buffer (pH 7.4) containing 0.02% sodium azide, was added to a 0.5 M ribose solution. The reaction mixture was then mixed with the test compounds. After incubation at 37°C for 24 h, the fluorescent reaction products were assayed with a spectrofluorometric detector (EnSpire, PerKinElmer, Inc., Japan; Ex: 370 nm, Em: 440 nm). Measurements were performed in triplicate and $IC_{50}$ of the intensity of fluorescent were determined graphically. [78].

## CONCLUSIONS

Chemical investigation of EtOAc and 1-BuOH fractions of the methanolic extract of *Lasianthus verticillatus* leaves afforded twenty-five compounds (**1** – **25**) that revealed diverse chemical structural type of iridoids including asperuloside and Lasianol and their glycosides and acylated glycosides derivatives together with bis-iridoid glycosides, in addition to lignans and megastigmanes. The isolated compounds were identified as two new iridoids (**1** – **2**), three new iridoid glycosides (**3**, **4** and **8**), four new acylated iridoid glycosides (**5** – **7** and **9**), three new bis-iridoid glycosides (**10** – **12**) and new tetrahydrofuran lignan glucoside (**13**) together with twelve known compounds (**14** – **25**). All compounds were evaluated for their free radical scavenging properties by DPPH radical scavenging assay. Potent free scavenging activity were exhibited by a new compound (**9**), together with secoisolariciresinol diglucoside (**23**) and huazhongilexin (**25**), while new compounds lasianosides C and D (**5** and **6**) together with 8,8′-bisdihydrosiringenin glucoside (**24**) displayed significant scavenging activity. According to the above results, *L. verticillatus* leaves considered as a good source for antioxidant compounds.

Chemical investigation of 1-BuOH fractions of the methanolic extract of *Cadaba rotundifolia* aerial parts led to isolation of twenty phenolic compounds (**26** – **45**) including flavonols and dihydrochalcone derivatives. The structures of isolated compounds were elucidated as kaempferol glycosides and acylated glycosides (**26** – **38**), rhamnocitrin glycoside (**39**), myricetin and its glycosides (**40** – **43**), together with dihydrochalcone compound and its glycoside derivative (**44** and **45**). These isolated compounds were examined for their DPPH radical scavenging assay, AGEs formation and collagenase. Myricetin and its glycosides derivatives exhibited potent free radical scavenging activity (**40** – **43**), while myricetin and its 3-*O*-*β*-D-glucoside (**42** – **43**) together with kaempferol 3-*O*-[2,6-di-*O*-*α*-L-rhamnopyranosyl]-*β*-D-glucoside (**35**) showed stronger AGEs formation inhibition. kaempferol 3-*O*-[2,6-di-*O*-*α*-L-rhamnopyranosyl]-*β*-D-glucoside (**35**) exhibited the stronger inhibition of collagenase with other kaempferol acylated glycosides derivatives (**26**, **31**, **33**). This work indicated that these active constituents and crude extract of *C. rotundifolia* aerial parts may become a useful remedy for the AGEs associated diseases.

**ACKNOWLEDGMENT**

The measurements of HR-ESI-MS were performed with LTQ Orbitrap XL spectrometer at the Natural Science Center for Basic Research and Development (N-BARD), Hiroshima University. This work was supported in part by King Saud University External Joint Supervision Program (EJSP), Kingdom of Saudi Arabia, and by Grants-in-Aid from the Ministry of Education, Culture, Sports, Science and Technology of Japan, and the Japan Society for the Promotion of Science (Nos., 15H04651 and 17K15465, 17K08336 and 18K06740).

## References


1. Robbrecht E., Manen J. F., The major evolutionary lineages of the coffee family (Rubiaceae, angiosperms). Combined analysis (nDNA and cpDNA) to infer the position of Coptosapelta and Luculia, and supertree construction based on *rbcL*, *rps*16, *trnLtrnF* and *atpB-rbcL* data. A new classification in two subfamilies, Cinchonoideae and Rubioideae. *Syst & Geogr Pl*, **76**, 85-46 (2006).
2. Briggs L. H., Nicholls G. A., Chemistry of the coprosma genus VIII. The occurrence of asperuloside. *J. Chem. Soc*., **1954**, 3940-3943 (1954).
3. Kooiman P., The occurrence of asperulosidic glycosides in the Rubiaceae. *Acta Bot Neerl*, **18**, 124-137 (1969).
4. Inouye H., Takeda Y., Nishimura H., Kanomi A., Okuda T., Puff C., Chemotaxonomic studies of Rubiaceous plant containing iridoid glycosides. *Phytochemistry*, **27**, 2591-2598 (1988).
5. Robbrecht E., Tropical woody Rubiaceae. Opera Botanica Belgica., **1**, 132 (1988).
6. Zhu H., Two new subspecies of *Lasianthus inodorus* (Rubiaceae) from Kinabalu, Borneo, and their biogeographical implication, *Blumea*, **46**, 447-455 (2001).
7. Wiart C., Medicinal plants of the Asia – Pacific: drugs for the future?. World Scintific Publishing Co. Pte. Ltd, Singapore, pp. 588 (2006).
8. Napiroon T., Balslev H., Duangjai S., Sookchaloem D., Chayamarit K., Santimaleeworagun W., Vajrodaya S., Antibacterial property testing of two species of tropical plant *Lasianthus* (Rubiaceae). *Southeast Asian J. Trop. Med. Public Health*, **48**, 117-123 (2017).
9. Li B., Zhang D.M., Luo Y.M., A new sesquiterpenes lactone from the roots of *Lasianthus acuminatissimus*. *Yao Xue Xue Bao*, **41**, 426-430 (2006).
10. Thai Forest Bulletin, Botany, Forest Herbarium (BKF) Department of National Parks, *Wildlife and Plant Conservation*, **31**, pp. 88 (2001).
11. Yang D, Zhang C., Liu X, Zhang Y, Wang K, Ceng Z., Chemical constituents and antioxidant activity of *Lasianthus hartii*. *Chem Nat Compd*, **53**, 390-393 (2017).
12. Takeda Y., Shimidzu H., Mizuno K., Inouchi S., Masuda T., Hirata E., Shinzato T., Aramoto M., Otsuka H., An iridoid glucoside dimer and a non-glycosidic iridoid from the leaves of *Lasianthus wallichii*. *Chem. Pharm. Bull*., **50**, 1395-1397 (2002).

13. Takeda Y., Shimizu H., Masuda T., Hirata E., Shinzato T., Bando M., Otsuka H., Lasianthionosides A–C, megastigmane glucosides from leaves of *Lasianthus fordii*. *Phytochemistry*, **65**, 485-489 (2004).
14. Li B., Lai X. W., Xu X. H., Yu B. W., Zhu Y., A new anthraquinone from the root of *Lasianthus acuminatissimus*. *Yao Xue Xue Bao*, **42**, 502-504 (2007).
15. Li B., Zhang D. M., Luo Y. M., Chen X., Three new antitumor anthraquinone glycosides from *Lasianthus acuminatissimus* Merr. *Chem*. *Pharm*. *Bull*., **54**, 297-300 (2006).
16. Li B., Zhang D. M., Luo Y. M., Chemical constituents from root of *Lasianthus acuminatissimus* I. *Zhongguo Zhong Yao Za Zhi*, **31**,133-135 (2006).
17. Dallavalle S., Jayasinghe L., Kumarihamy B. M. M., Merlini L., Musso L., Scaglioni L., A new 3,4-*seco*-lupane derivative from *Lasianthus gardneri*. *J*. *Nat*. *Prod*., **67**, 911-913 (2004).
18. Zhu H., Roos M. C., Ridsdale C. E., A taxonomic revision of the Malasian species of *Lasianthus* (Rubiaceae). *Blumea*, **57**, 1-102 (2012).
19. http://mikawanoyasou.org/data/ruriminoki.htm
20. Otsuka H., Yoshimura K., Yamasaki K., Cantoria M. C., Isolation of 10-*O*-Acyl Iridoid glucosides from a Philippine medicinal plant, *Oldenlandia corymbose* L. (Rubiaceae). *Chem*. *Pharm*. *Bull*. **39**, 2049–2052 (1991).
21. Demirezer L. O., Gurbuz F., Guvenlap Z., Stroch K., Zeeck A., Iridoid, flavonoids and monoterpene glycosides from *Galium verum* subsp. *Verum*. *Turk*. *J*. *Chem*. **30**, 525-534 (2006).
22. Kamiya K., Hamabe W., Harad S., Murakami R., Tokuyama S, Satake T., Chemical constituents of *Morinda citrifolia* roots exhibited hypoglycemic effects in streptozotocin-induced diabetic mice. *Biol*. *Pharm*. *Bull*., **31**, 935-938 (2008).
23. Podanyi B., Kocsis A., Szabo L., Reid R. S., An NMR study of the solution conformation of two asperuloside derivatives. *Phytochemistry*, **29**, 861–866 (1990).
24. Ma J., Dey M., Yang H., Poulev A., Poleva R., Dorn R., Lipsky P. E., Kennelly E. J., Raskin I., Anti-inflammatory and immunosuppressive compounds from *Tripterygium wilfordii*. *Phytochemistry*, **68**, 1172–1178 (2007).
25. Nithiya T., Udayakumar R., *In vitro* antioxidant properties of phloretin–An important phytocompound. *J*. *Biosci*. *Med*., **4**, 85-94 (2016).
26. Aruoma O. I., Free radicals, Oxidative stress and antioxidants in human health and disease. *J*. *Am*. *Oil*. *Chem*. *Soc*., **75**,199-212 (1998).

27. Ames B. N., Dietary carcinogens and anticarcinogens. Oxygen radicals and degenerative diseases. *Science*, **221**, 1256-1264 (1983).
28. Scherer R., Godoy H. T., Antioxidant activity index (AAI) by the 2,2-diphenyl-1-picrylhydrazyl method. *Food Chem*., **112**, 654-658 (2009).
29. Ito N., Hirose M., Fukushima S., Tsuda H., Shirai T., Tatematsu M., Studies on antioxidants: Their carcinogenic and modifying effect on chemical carcinogenesis. *Food Chem*. *Toxicol*., **24**, 1099-1102 (1986).
30. Whysner L., Wang C. X., Zang E., Iatropoulos M. J., Williams G. M., Dose response of promotion by Butylated hydroxyanisole in chemically initiated tumors of the rat forestomach. *Food Chem*. *Toxicol*., **32**, 215-222 (1994).
31. Masek A., Chrzescijanska E., Latos M., Determination of antioxidant of caffeic acid and *p*-coumaric acid by using electrochemical and spectrophotometric assays. Int. *J. Electrochem*. *Sci*., **11**, 10644-10658 (2016).
32. Moon J., Terano J., Antioxidant activity of caffeic acid and dihydrocaffeic acid in lard and human low-density lipoprotine. *J. Agric*. *Food Chem*., **46**, 5062-5065 (1998).
33. Peng J., Feng X. Z., Li G. Y., Liang X. T., Chemical investigation of genus *Hedyotis* II. Isolation and identification of iridoids from *Hedyotis chrysotricha*. *Acta Pharmaceutica Sinica*, **32**, 908-913 (1998).
34. Taskova R. M., Gotfredsen C. H., Jensen S. R., Chemotaxonomy of Veroniceae and its allies in the Plantaginaceae. *Phytochemistry*, **67**, 286–301 (2006).
35. Hashimoto T., Tori M., Askawa Y., Piscicidal sterol acylglucosides from *Edgeworthia chrysantha*. *Phytochemistry*, **30**, 2927–2931 (1991).
36. Marino S., Borbon N., Zollo F., Ianaro A., Meglio P., Iorizzi M., Magastigmane and phenolic components from *Laurus nobilis* L. leaves and their inhibitory effects on nitric oxide production. *J. Agric. Food. Chem.*, **52**, 7525-7531 (2004).
37. Matsunami K., Otsuka H., Takeda Y., Structural Revisions of Blumenol C Glucoside and Byzantionoside B. *Chem*. *Pharm*. *Bull*., **58**, 438-441(2010).
38. Zhang W., Xu S., Purification of secoisolariciresinol diglucoside with column chromatography in sephadex LH-20. *J Chromatogr Sci*, **45**, 177–182 (2007).
39. Abe F., Yamauchi T., Lignans from *Trachelospermum asiaticum* (Tracheolospermum. II). *Chem*. *Pharm*. *Bull*., **43**, 4340–4345 (1986).

40. Lin L. D., Qin G. W., Xu R. S., Tian Z. Y., Lu Y., Zheng Q. T., Studies on chemical constituents of *Ilex centrochinensis*. *Acta Chim*. *Sinica*, **53**, 98–101 (1995).
41. Sugimoto S., Wanas A. S., Mizuta T., Matsunami K., Kamel M. S., Otsuka H., Structure elucidation of secondary metabolites isolated from the leaves of *lxora undulate* and their inhibitory activity toward advanced glycation end-products formation. *Phytochemistry*, **108**, 189-195 (2014).
42. Yoshikawa M., Sugimoto S., Nakamura S., Matsuda H., Medicinal flowers. XXII structures of chakasaponins V and VI, chakanoside I, and chakaflavonoside A from flower buds of Chinese tea plant (*Camellia sinensis*). *Chem*. *Pharm*. *Bull*., **56**, 1297-1303 (2008).
43. Matsunami K., Takamori I., Shinzato T., Aramoto M., Kondo K., Otsuka K., Takeda Y., Radical-scavenging activities of new megastimane glucosides from *Macaranga tanarius* (L.) MULL.-ARG. *Chem*. *Pharm*. *Bull*., **54**, 1403-1407 (2006).
44. Kamel W. M., El-Ghani M. M., El-Bous M. M., Taxonomic study of Capparaceae from Egypt: Revisited. *AJPSB*, **3**, 27-35 (2009).
45. Hosni H. A., Hejazy A. K., Contribution to the flora of Asir, Saudi Arabia. *Candollea*, **51**, 169-202 (1996).
46. Yousif G., Iskander G. M. and Eisa E., Alkaloid components in the Sudan flora. Part II. Alkaloid of *Cadaba farinose* and *C. rotundifolia*. *Fitoterapia*, **55**, 117-118 (1986).
47. Ahmad V., Amber A., Arif S., Chen M. H. M, Clardy J., Cadabicine, an alkaloid from Cadaba farinose. *Phytochemistry*, **24**, 2709-2711 (1985).
48. Al-Musayeib N. M., Mohamed G. A., Ibrahim S. R. M., Ross S. A., Lupeol-3-O-decanoate, a new triterpene ester from Cadaba farinose Frossk. Growing in Saudi Arabia. *Med*. *Chem*. *Res*., **22**, 5297-5302 (2013).
49. Mohamed G. A, Ibrahim S. R. M., Al-Musayeib N.M, Ross S. A., New anti-inflammatory flavonoids from Cadaba glandulosa Frossk. *Arch*. *Pharm*. *Res*., **37**, 459-466 (2014).
50. Velmurugan P. Kamaraj M., Prema D., Phytochemical constituents of *cadaba trifoliata* Roxb. root extract. *International Journal of Phytomedicine*, **2**, 379-384 (2010).
51. Alothyqi N., Almalki M., Albaqa'ai M., Alsamiri H., Alrashdi S.M., Ibraheem F., Osman G. H. E., In vitro antibacterial activity of four Saudi medicinal plants. *J Microb Biochem Technol*, **8**, 83-89 (2016).

52. Harbaum B., Hubbermann E. M., Wolf C., Herges R., Zhu Z., Schwarz K., Identification of flavonoids and hydroxycinnamic acid in pak choi varieties (*Brassica campestris* L. ssp. *chinesis* var. *communis*) by HPLC-ESI-MS $^{n}$ and NMR and their quantification by HPLC-DAD. *J. Agric. Food Chem.*, **3**, 8251-8260 (2007).
53. Gossan D. P. A., Alabdul Majed A., Yao-Kouassi P. A., Coffy A. A., Harakat D., Voutaquenne-Nazabadioko L., New acylated flavonol glycosides from the aerial parts of *Gouania longipetala*. *Phytochem. Lett.*, **11**, 306-310 (2015).
54. Corea G., Fattorusso E., Lanzotti V., Saponins and flavonoids of *Allium triquetrum*. *J. Nat. Prod.*, **66**, 1405-1411 (2003).
55. Carotenuto A., Feo V. D., Fattorusso E., Lanzotti V., Magnot S., Cicala C., The flavonoids of *Alliun ursinum*. *Phytochemistry*, **41**, 531-536 (1996).
56. Choudhury K. D., Choudhury M. D., Paul S. B., Antioxidant activity of leaf extracts od *Lasianthus lucidus* BLUM. *Int. J Pharm Pharm Sci.*, **4**, 533-535 (2012).
57. Chaabi M., Beghidja N., Benayache S., Lobstein A., Activity-guided isolation of antioxidant princioles from *Limoniastrum feei* (Girard) Batt. *Z. Naturforsch.*, **63c**, 801-807, (2008).
58. Jin SL., Yin YG., In vivo antioxidant activity of total flavonoids from indocalamus leaves in aging mice caused by D-galactose. *Food Chem. Toxicol.*, **50**, 3814-3818 (2012).
59. Li P., Jia J., Zhang D., Xie J., Xu X., Wei D., *In vitro* and *in vivo* antioxidant activities of a flavonoid isolated from celery (*Apium graveolens* L. var. dulce). *Food Funct.*, **5**, 50-56 (2014).
60. Majewska M., Skrzycki M., Podsiad M., Czeczot H., Evaluation of antioxidant potential of flavonoids: an *in vitro* study. *Acta Pol Pharm*, **68**, 611-615 (2011).
61. Martino L. D., Mencherini T., Mancini E., Aquino R.P., Almeida L. F., Feo V. D., *In vitro* phytotoxicity and antioxidant activity of selected flavonoids. *Int. J. Mol. Sci.*, **13**, 5406-5419 (2012).
62. Ani V., Varadaraj M. C., Naidu K. A., Antioxidant and antibacterial activities of polyphenolic compounds from bitter cumin (*Cuminum nigrum* L.). *Eur Food Res Technol*, **224**, 109-115 (2006).
63. Kehrer J. P., Klotz L., Free radicals and related reactive species as mediators of tissue injury and disease: implications for health. *Crit. Rev. Toxicol.*, **45**, 765-798 (2015).

64. Sharma P., Jha A. B., Dubey R. S., Pessarakli M., Reactive oxygen species, oxidative damage, and antioxidative defense mechanism in plants under stressful conditions. *J. Bot*., **2012**, 26 pages (2012)
65. Ramasamy R., Bucciarelli L. G., Yan S. F., Schmidt A. M., Advanced glycation end products, RAGE, and aging. In: *Aging and age-related disorder*. Bondy S., Maiese K. (Eds.). Springer, New York, **8**, pp. 2183-2187 (2012).
66. Maillard L. C, The action of amino acids on sugars; the formation of melanoidin by methodic route. *Cr*. *Hebd*. *Acad*. *Sci*., **154**, 66-68 (1912).
67. Reddy V. P., Beyaz A., Inhibitor of Maillard reaction and AGE breakers as therapeutics for multiple diseases. *Drug Discov*. *Today*, **11**, 646-654 (2006).
68. Peyroux J., Sternberg M., Advanced glycation endproducts (AGEs): Pharmacological inhibition in diabetes. *Pathol*. *Biol*., **45**, 405-419 (2006).
69. Ahmed N., Advanced glycation endproducts–Role in pathology of diabetic complications. *Diabetes Res*. *Clin*. *Pract*., **67**, 3-21 (2005).
70. Goldberg T., Cai W. J., Peppa M., Dardaine V., Balgia B. S., Uribarri J., Vlassara H., advanced glycoxidation end products in commonly consumed food. *J*. *Am*. *Diet*. *Assoc*., **104**, 1287-1291 (2004).
71. Sajithlal G.B., Chithra P., Chandrakasan G., Advanced glycation end products induce crosslinking of collagen *in vitro*. *Biochem*. *Biophys*. *Acta Mol*. *Basis Dis*., **1407**, 215-224 (1998).
72. Lohwasser C., Neureiter D., Weigle B., Kirchner T., Schuppan D., The receptor of advanced glycation end products is highly expressed in the skin and upregulated by advanced glycation end products and tumor necrosis factor-alpha. *J*. *Investig*. *Dermatol*., **126**, 291-299 (2006).
73. Lee K. H., Whang W. K., Inhibitory effects of bioassay-guided isolation of anti-glycation components from *Taraxacum coreanum* and simultaneous quantification. *Molecules*, **23**, 14 pages (2018).
74. Yang R., Wang W., Chen H., He Z., Jia A., The inhibition of advanced glycation end-products by five fractions and three main flavonoids from *Camellia nitidissima* Chi flowers. *J Food Drug Anal*, **26**, 252-259 (2018).
75. Wu C., Yen G., Inhibitory effect of naturally occurring flavonoids on the formation of advanced glycation endproducts. *J*. *Agric*. *Food*. *Chem*., **53**, 3167-3173 (2005).

76. Alam Md. M., Ahmed I., Naseem I., Inhibitory effect of quercetin in the formation of advance glycation end products of human serum albumin: An *in vitro* and molecular interaction study. *Int*. *J*. *Biol*. *Macromol*., **79**, 336-343 (2015).
77. Sasaki K., Chiba S., Yohizaki F., Effect of natural flavonoids, stilbenes and caffeic acid oligomers on protein glycation. *Biomed Rep*, **2**, 628-632 (2014).
78. Séro L., Sanguinet L., Blanchard P., Dang B. T., Morel S., Richomme P., Séraphin D., Séverine D., Tuning a 96-well microtiter plate fluorescence-based assay to identify AGE inhibitors in crude plant extracts. *Molecules*, **18**, 14320-14339 (2013).
79. Jenkins G., Molecular mechanism of skin ageing. *Mech*. *Ageing Dev*., **123**, 801-810 (2002).
80. Landau M., Exogenous factors in skin aging. *Curr*. *Prob*. *Dermatol*., **35**, 1-3 (2007).
81. Farage M. A., Miller K. W., Elsner P., Maibach H. I., Intrinsic and extrinsic factors in skin ageing: a review. *Int*. *J*. *Cosmet*. *Sci*., **30**, 87-95 (2008).
82. Kusumawati I., Indrayanto G., Natural antioxidant in cosmetics. In: *Studies in natural product chemistry*, Atta-urahman F., (Eds.). Elsevier B. V., Amesterdam, pp. 485-505 (2013).
83. Gonzaga E. R., Role of UV light in photoaging, skin aging, and skin cancer. *Am*. *J*. *Clin*. *Dermatol*., **10**, 19-24 (2009).
84. Kammeyer A., Luiten R. M., Oxidative events and skin aging. *Aging Res*. *Rev*., **21**, 16-29 (2015).
85. Ortonne J. P., Photoprotective properties of skin melanin. *Br*. *J*. *Dermatol*., **146**, 7-10 (2002).
86. Demeule M., Brossard M., Pagé M., Gingras D., Béliveau R., Matrix metalloproteinase inhibition by green tea catechins. *Biochim*. *Biophys*. *Acta*., **1487**, 51-60 (2000).
87. Rabe J. H., Mamelak A. J., McElgunn P. J., Morison W. L., Sauder D. N., Photoaging: Mechanisms and repair. *J*. *Am*. *Acad*. *Dermatol*., **55**, 1-19 (2006).
88. Mandrone M., Lorenzi B., Venditti A., Guarcini L., Bianco A., Sanna C., Ballero M., Poli F., Antognoni F., Antioxidant and anti-collagenase activity of *Hypericum hircinum* L. *Ind Crops Prod*, **76**, 402-408 (2015).
89. Pientaweeratch S., Panapisal V., Tansirikongkol A., Antioxidant, anti-collagenase and anti-elastase activities of *Phyllanthus emblica*, *Manilkara zapota* and silymarin: an *in vitro* comparative study for anti-aging applications. *Pharm Biol*., **54**, 1865-1872 (2016).
90. Fisher G. J., Voorhees J., Molecular mechanisms of photoaging and its prevention by retinoic acid: Ultraviolet irradiation induces MAP kinase signal transduction cascades that induce Ap-

1-regulated matrix metalloproteinases that degrade human skin *in vivo*. *J*. *Investig*. *Dermatol*. *Symp*. *Proc*., **3**, 61-68 (1998).

91. Saragusti A. C., Ortega M. G., Cabrera J. S., Estrin D. A., Marti M. A., Chiabrando G. A., Inhibitory effect of quercetin on matrix metalloproteinase 9 activity molecular mechanism and structure-activity relationship of the flavonoid-enzyme interaction. *Eur*. *J*. *Pharmacol*., **644**, 138-145 (2010).
92. Lee H. J., Im AR., Kim S.M., Kang H. S., Lee J. D., Chae S., The flavonoid hesperdin exerts anti-photoaging effect by down regulating matrix metalloproteinase (MMP)-9 expression via mitogen activated protein kinase (MAPK)-dependent signaling pathways. *BMC Complement Altern Med*, **18**, 9 pages (2018).
93. Ende C., Gebhartd R., Inhibition of matrix metalloproteinase-2 and -9 Activities by selected flavonoids. *Planta Med*., **70**, 1006-1008 (2004).
94. Lim H., Kim H. P., Inhibition of mammalian collagenase, matrix metalloproteinase-1, by naturally occurring flavonoids. *Planta Med*., **73**, 1267-1274 (2007).
95. Sin Y., Kim H. P., Inhibition of collagenase by naturally-occurring flavonoids. *Arch*. *Pharm*. *Res*., **28**, 1152-1155 (2005).
96. Nguyen T. T., Moon YH., Ryu YB., Kim YM., Nam SH., Kim MS., Kimura A., Ki, D., The influence of flavonoid compounds on the *in vitro* inhibition study of human fibroblast collagenase catalytic domain expressed in *E*. *coli*. *Enzyme Microb*. *Technol*., **52**, 26-31 (2013).
97. Kim H., Jeong YU., Kim JH., Park YJ., 3, 5, 6, 7, 8, 3′, 4′-Heptamethoxyflavone, a citrus flavonoid, inhibits collagenase activity and induces type I procollagen synthesis in HDFn cells. *Int J Mol Sci*, **19**, 12 pages (2018).
98. Widywati R., Sugimoto S., Yamano Y., Sukardiman, Otsuka H., Matsunami K., New isolinariins C, D and E, flavonoid glycosides from *Linaria Jopanica*. *Chem*. *Pharm*. *Bull*., **64**, 517-521 (2016).
99. Lee K. T., Choi J. H., Kim D. H., Son K. H., Kim W. B., Kown S. H., Park H. J., Constituents and antitumor principle of *Allium victorialis* var. *platyphyllum*. *Archives of pharmacal Research*, **24**, 44-50 (2001).
100. Kazuma K., Noda N., Suzuki M., Malonylated flavonol glycosides from the petals of *Clitoria ternatea*. *Phytochemistry*, **62**, 229-237 (2003).

101. Walter A., Sequin U., Flavonoids from the leaves of *Boscia salicifolia*. *Phytochemistry*, **29**, 2561-2563(1990).
102. Mabry T. J., Markham K. R., Thomas M. B., The systematic identification of flavonoids. *Springer Verlag*., New York. Pp. 2204 (1970).
103. Zheng X., Li M., Zeng M., Zhang J., Zhao X., Lv J., Zhang Z., Feng W., Extraction method of beitingxinhuangtong C from *Lipidium apetalum* and its applicayion in preparing estrogenic drug. *From Faming Zhuanli Shenging Gongkai Shoumingshu*, CN 1076024640 A 201180119 (2018).
104. Qin X., Xing Y. F., Zhou Z., Yao Y., Dihydrochalcone compounds isolated from Crabapple leaves showed anticancer effects on human cancer cell line. *Molecules*, **20**, 21193-21230 (2015).
105. Mitani T., Mimura H., Ikeda K., Nishide M., Yamaguchi M., Koyama H., Hayashi, Y., Sakamoto H. Process for the purification of *cis-p*-coumaric acid by cellulose column chromatography after the treatment of the *trans* isomer with ultraviolet irradiation. *Anal. Sci.*, **34**, 1195-1199 (2018).
106. Teramachi F., Koyano T., Kowthayakorn T., Hayashi M., Komiyama K., Ishibashi M., Collagenase inhibitory quinic acid esters from *Ipomoea pes-caprae*. *J. Nat. Prod*., **86**, 794-796 (2005).